1987

Induction motor analyses including non-sinusoidal excitation

Mohammad El-Hosainy Ismaeel
Iowa State University

Order Number 8805087

Induction motor analyses including non-sinusoidal excitation

Ismaeel, Mohammad El-Hosainy, Ph.D.

Iowa State University, 1987

U·M·I
300 N. Zeeb Rd.
Ann Arbor, MI 48106

PLEASE NOTE:

In all cases this material has been filmed in the best possible way from the available copy. Problems encountered with this document have been identified here with a check mark __√__.

1. Glossy photographs or pages _____
2. Colored illustrations, paper or print _____
3. Photographs with dark background _____
4. Illustrations are poor copy _____
5. Pages with black marks, not original copy _____
6. Print shows through as there is text on both sides of page _____
7. Indistinct, broken or small print on several pages __√__
8. Print exceeds margin requirements _____
9. Tightly bound copy with print lost in spine _____
10. Computer printout pages with indistinct print _____
11. Page(s) _____ lacking when material received, and not available from school or author.
12. Page(s) _____ seem to be missing in numbering only as text follows.
13. Two pages numbered _____. Text follows.
14. Curling and wrinkled pages _____
15. Dissertation contains pages with print at a slant, filmed as received __√__
16. Other _____

_____

_____

Induction motor analyses
including non-sinusoidal excitation

by

Mohammad El-Hosainy Ismaeel

A Dissertation Submitted to the
Graduate Faculty in Partial Fulfillment of the
Requirements for the Degree of
DOCTOR OF PHILOSOPHY

Department: Electrical Engineering and Computer Engineering
Major: Electrical Engineering (Electric Power)

Approved:

Signature was redacted for privacy.

Signature was redacted for privacy.

In Charge of Major Work

Signature was redacted for privacy.

For the Major Department

Signature was redacted for privacy.

For the Graduate College

Iowa State University
Ames, Iowa

1987

TABLE OF CONTENTS

LIST OF FIGURES

LIST OF TABLES

I. INTRODUCTION

A. Historical Background

The history of the induction motor extends as far back as the 19th century. It started in 1824 with the discovery made by Gambey [from Ref. 79], the instrument-maker of Paris, that a compass needle, when disturbed and set oscillating, comes to rest more quickly when it is in the vicinity of copper than when wood is near it. At that time also, Barlow and Marsh, at Woolwich, had observed the effect on a magnetic needle of rotating it near a sphere of iron [from Ref. 79]. Arago published an account of an experiment with a compass needle within rings of different materials in the 1890s [from Ref. 79]. In this experiment, he pushed the needle aside to about 45° and counted the number of oscillations made by the needle before the swing decreased to 10°. With a ring of wood, the number of oscillations was 145, with a copper ring 66, and with stout copper ring only 33. In 1825, he suspended a compass needle over a rotating copper disc and found that by turning the disc slowly, the needle is deviated out of the magnetic meridian. By rotating the disc fast enough, he found that continuous rotation of the needle could be produced.

The brilliant discovery by Faraday, in 1831, of electromagnetic induction provided the solution to the question of the origin of the forces present in the above experiments of Gambey, Barlow and Marsh, and Arago. Faraday showed that the rotation of the Arago disc was due to induced currents, set up in the disc by the relative motion of the

disc and the compass needle. The magnetic field caused by those induced currents, in turn, interacted with the magnetic needle and caused its motion. From 1831 to 1879, this valuable discovery produced no further results. In June 1879, Walter Baily read a paper [from Ref. 79] before the Physical Society of London on "A Mode of Producing Arago's Rotations." Baily used a fixed electromagnet with four magnet cores joined to a yoke.

The four magnet cores were about four inches long and each was wound with about 150 turns of insulated copper of 2.5 mm diameter. The coils were connected two and two in series, similar to two independent horseshoe magnets, and were diagonally across from one another.

The two circuits were connected separately to a revolving commutator, built from a simple arrangement of springs and contact strips mounted on a piece of wood, with a wire handle by which it was turned. By rotation, the current from two batteries was caused to be reversed alternately in the two circuits, and this gave rise to the following changes in polarity of the four poles.

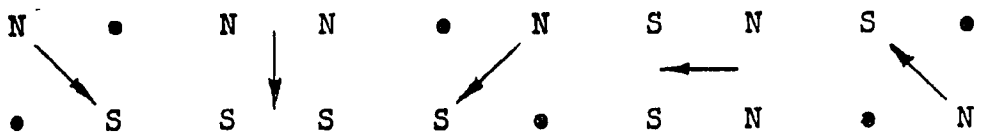

In this rotating magnetic field, a copper disc was suspended. Baily stated: "The rotation of the disc is due to that of the magnetic field in which it is suspended, and we should expect that if a similar motion

of the field could be produced by any other means, the result would be a similar motion of the disc" [from Ref. 79]. Baily also suggested that if a whole circle of poles was arranged under the disc, successively excited in opposite pairs, the series of impulses would all tend to make the disc revolve in one direction around the axis, and added, "In one extreme case, when the number of electromagnets is infinite, we have the case of a uniform rotation of the magnetic field, such as we obtain by rotating permanent magnets" [from Ref. 79]. It is clear that Baily had grasped the fundamental principle of action of the induction motor, and the motor he exhibited before the Physical Society in 1879 was the first induction motor. But, it needed later important discoveries of methods for producing the revolving field by means of alternating currents to make it the useful machine that it is today.

The next discovery was made by Marcel Deprez in 1883 [from Ref. 79]. He fed alternating current to a coil, which produced an alternating or oscillating field along the OX axis. He supplied another coil, whose magnetic axis made an angle of 90° with the OX axis, with alternating current, whose phase difference was 90° in time from the current in the first coil, and showed that a revolving field of constant amplitude could be produced. The frequency of the two currents was the same. He also showed that if the two currents were of equal frequency, but not of equal amplitude, an elliptically rotating field was produced. The number of turns in each coil was the same.

Professor Ferraris [from Ref. 79] arrived at the same conditions as Baily and Deprez in 1885, and apparently without knowing of the work of either. His paper on "Electrodynamic Rotations Produced by Means of Alternating Currents" was published in 1888. He suggested the method of obtaining currents, differing in phase by nearly 90°, by inserting a resistance in one winding and inductance in the other, thus making the ratio (reactance/resistance) small in one winding and large in the other. This method is largely used for starting single-phase motors.

Next followed the great work of Nicola Tesla between 1887 and 1891 [from Ref. 79]. His research placed the induction motor on a sound foundation. His patents were sold to the Westinghouse Company of America, whose pioneer efforts in this field must be recognized. In that period, however, the only ac supply circuits were single phase, and the frequencies were 133 and 125 Hz. These supply frequencies were obviously unsuitable for the development of the motor.

In 1891, the Electrotechnical Exhibition was held at Frankfort and the three-phase transmission of power was demonstrated. Two turbine-driven three-phase generators were installed at Lauffen, Germany, generating 1400 A at 55 V. The frequency was 40 Hz. Three-phase transformers were installed at each end of the line to raise the voltage to 8000 V at Lauffen, and to reduce it to 65 V at Frankfort. The distance of transmission was 110 miles. This bold experiment demonstrated the feasibility of three-phase transmission of energy.

The load consisted of a 100 hp three-phase motor and also lamps. Several German firms exhibited different types of three-phase induction motors at the Exhibition. One three-phase, 3 bhp motor had the three-phase supply brought into the rotor by three slip-rings, the secondary circuit, being the stator winding, consisted of a closed-circuit winding. Several motors, built by the Oerlikon Company and designed by C. E. L. Brown, were shown. One such motor was a three-phase, 20 bhp motor. It had a distributed stator winding and a squirrel-cage rotor and a small air-gap. The squirrel-cage rotor was the invention of Dolivo-Dobrowolsky, who cooperated with C. E. L. Brown in the design of these motors. This motor of Brown's closely resembled in construction the induction motor of today. From the short account given, it will be realized that much progress was made purely as the result of experiment, and that much theoretical investigation was needed to explain the reactions taking place in the motor, and to show how it could be designed to give the characteristics desired.

To that end, it was necessary to give a lucid theory of alternating currents. Thomas H. Blakesley gave a series of ten brilliant papers in Electrician in 1885 [from Ref. 79]. He discussed, for the first time, alternating current phenomena by means of polar diagrams.

In 1892, F. Bedell and A. C. Crehore [from Ref. 79] published their book, Alternating Currents, in which the polar diagrams were used and applied to the theory of the transformer and the locus of the primary e.m.f. of the current transformer was shown to be a circle. In 1894, Kapp [from Ref. 79] gave a very lucid elementary account of the

phenomena in induction motors. The polar diagram was developed and included the primary resistance and leakage flux.

In 1895, Blondel [from Ref. 79] gave his papers on "Some General Properties of Revolving Magnetic Fields." In these papers, published in EcLairge Electrique, he unfolded the theory of the composition of magnetic fluxes, including leakage fluxes. In 1895, B. A. Behrend [8] also proved that the locus of the primary current of the alternating-current transformer is a circle in the polar diagrams, provided the primary resultant magnetic field is constant. The circle locus of the induction motor was also shown by A. Heyland in 1894 [8]. There has been much controversy about priority in this discovery.

The circle diagram in use today is undoubtedly due to Behrend. Details are described in Behrend's book, the first edition of which was published in 1901 [8]. The second edition was published in 1921 [8]. At that time, the general outline was clearly seen, but there remained many important questions to be answered. The circle diagram clearly demonstrated the need for a small air-gap length, for high power factor, and for a large ideal short-circuit current. All the main characteristics, such as torque, power, current, slip and efficiency are readily determined from the Behrend circle diagram.

Although the relation of dimensions to characteristics was known by about 1900 or so, it remained to determine the effect of harmonics from the distribution of the winding, and from the slots on the performance of the motor. Such harmonics produce noise and vibration and may, by producing saddle backs in the torque

curve, make the machine crawl and prevent it from accelerating to full speed. The question of noise has been investigated by H. Fritz, Kron and Chapman. A large number of papers has been written on this subject [55, 56, 79].

The question of improved efficiency has resulted in improvements in the manufacture of steel laminations, such as through the introduction of silicon into the steel. Brands known as stalloy and super-stalloy have been introduced, and are used in those cases where it is necessary to keep down the iron losses, e.g., in totally enclosed machines, and especially in machines for 400 Hz, such as those used in the automatic pilots in aircraft. The effects of various forms of unbalance, either from unbalanced applied voltage or from the dissymmetry in the rotor circuit, have been studied through the concept of the symmetrical components. This work started by Fortiscue in 1918 [35], and was followed by others.

From time to time, attempts have been made to adapt Maxwell's equations to electrical machines. Perhaps the earliest definitive paper was published by Creedy [25] in 1917, although in earlier papers, Carter [15], Cullen and Barton [26] and Douglas [32] had shown the importance of the applications of the field concept. The next significant contribution was made by Hague, who published a series of papers between 1917 and 1926. These are now available in book form [46]. These authors indicate that the solution to an electrical-machine problem can be obtained by determining the electromagnetic fields in the various regions of the machine.

The contributions from 1899 to the present day are well spread over this entire period. A survey of the literature shows that the field-theory methods of predetermining the performance characteristics of electrical machines can be broadly classified as (a) energy-storage methods, (b) energy-transfer methods, (c) methods derived from analogies between the field theory and circuit theory, and (d) certain special techniques, such as the method of images, conformal transformation and graphical techniques.

The development of static switching devices with high power ratings is leading to their increasing application in the control of electrical machines. Two important applications of this type are in static frequency converters and voltage controllers, both of which are utilized to provide control of the torque and speed characteristics of ac machines. In particular, they are now being used to obtain flexible performance characteristics from robust, but inherently constant-speed cage induction motors. In many of these systems, the output voltage and current waveforms of the static converters are rich in harmonics. These harmonics have detrimental effects on motor performance.

The orders and magnitudes of the current harmonics which are present in the converter output depend on the design of the static converter, and, to a lesser extent, on the type of load. The converter output is usually amenable to analysis by Fourier series.

Some earlier publications [52, 53] on this topic have considered the losses and torques produced in cage induction motors from

distorted supply waveforms. Each of these has indicated, in some detail, that the resultant additional steady-state torque is negligible, although Jain [52] omitted the skin effect in his calculations. In some cases [18, 52, 53], the additional losses have been found to be small, but it has also been shown [19, 20] that if the input waveforms have a high harmonic content, the additional losses may be as high as the losses contributed by the fundamental voltages and currents. This result highlights the need for an accurate assessment of the time-harmonic losses. Fluxes and currents resulting from the input harmonics occur at relatively high frequencies, which means that the skin effect should be included in the I^2R calculations. Core losses due to harmonic main fluxes occur at high frequencies, but the fluxes are highly damped by induced secondary currents. The methods used are based on the conventional induction motor equivalent circuit, but includes modifications to the conventional theory necessary to account for the time harmonic effects [18-20, 52, 53].

Very recently, the problem of harmonic pollution on power systems has led to the detriment of electrical appliances to harmonics, as well as their aging due to harmonics of the power system's voltage [41, 42, 78]. This problem is also treated by using the conventional equivalent circuit of the induction machines.

B. Problem Formulation

The literature search reveals that most of the work in the induction machine theory depends mainly on circuit theory, and field

theory is just used as an aid in obtaining the numbers to go in the lumped circuits. For a long time, generalized machine theory, with its emphasis on circuit ideas, has pushed field theory into the background. The result has been to produce young engineers who are adept at formulation and manipulation of matrix equations, but who have little idea of the physical significance of the circuit parameters [28]. Also, the teaching of electrical machines has emphasized detailed practice. The reaction to this teaching is a feeling that textbook machines are 'energy transducers' bearing no relation to useful machines [28]. It is generally recognized that for a number of the outstanding problems on electrical machines, the solution can only be achieved by field methods. It would be appropriate to adopt field methods to solve the field problem of electrical machines as a boundary value problem. This would give a more exact solution, on one hand, and a deeper insight into the phenomena taking place in these kinds of machines, on the other hand. The development of field techniques for induction motor analysis is one of the objectives of this dissertation.

C. Research Objectives

The purpose of this study is to provide a general analysis for the field problem in induction machines, based on the solution of Maxwell's field equations. The specific objectives of this research work may be summarized as follows:

1. Modeling the electric machine by an appropriate mathematical model, that will accurately represent the actual machine, with the relative ease of applying Maxwell's field equations to it.
2. Formulation of the boundary value problem of the induction machine, and its necessary boundary conditions. The formulation may be in its most general form to permit individual primary loading and to derive balanced loading from it as a special case.
3. Solution of the field equations taking into account both the space and time spectrums that may arise from the machine winding and the electric loading.
4. Development of a simple approach for handling the field problem, as stated above, without sacrificing the modeling implementations of the problem.
5. Illustrate the theory by studying a specific example, using a digital computer, to predict the machine performance under different electric loadings.

D. Research Outline

To achieve the above objectives, this research work has been divided into six chapters and an appendix. The first chapter starts with a brief historical survey to the subject, showing the importance

of using the field analysis for solving the machine problems, as well as getting a reasonable interpretation for the phenomena taking place in the electric machines.

Chapter II is devoted to the development of an electromagnetic theory for the induction motor. The theory is based on a five-region model. The basic field equations in each region have been derived from Maxwell's field equations. The additional constraint field equations that arise from the machine configurations have also been derived. The resulting field equations constitute a system of elliptic partial differential equations. This system, together with its relevant boundary conditions, has been solved from a very general approach, including both the whole space and time spectrums (harmonics). The expressions of force and power are also developed to permit the prediction of motor performance.

Chapter III deals with the development of a simplified field analysis for the induction motor. This analysis is based on the wave impedance concept, analogous to the impedance concept found in the familiar transmission-line theory. To widen the scope of this chapter, a different mathematical model has been chosen to develop this field analysis. The space and time spectrums (harmonics) are also kept during the development. The analysis presented in this chapter represents a generalization and extension to the work of Cullen and Barton [26], Freeman [37, 38], Freeman and Smith [40] and Greig and Freeman [45]. The analysis establishes a general approach capable of

describing any arbitrary electric or magnetic loading, as well as a general method for calculating the machine currents and equivalent impedances. The method given can also be extended to the fault conditions, as well as to single-phase machines.

Chapter IV is devoted to the extension of the solution of the general field problem given in Chapter II, to mathematical models consisting of more regions than those given before. The analysis of this chapter is introduced in a different procedure from that given in Chapter II. It permits a systematic handling of multi-region mathematical models. The purpose of this chapter is to study the influence of these additional regions on the machine performance.

Chapter V presents the results obtained from the application of the theories presented, in the previous chapters, to a specific theoretical induction motor. The computer programs, according to the theories developed, have been coded for this motor. The performance characteristics, as well as the effect of design parameters on the motor performance, have been studied.

Chapter VI is devoted to the conclusions, as well as the basic contribution of this research.

II. QUASI-THREE-DIMENSIONAL ANALYSIS OF INDUCTION MOTORS

A. Introduction

Analysis of electromagnetic machines may be performed by using either the circuit or field approach. The circuit approach when applied directly involves lumped parameter representation, in one form or another. These parameters can be evaluated theoretically by individual field calculations, usually of an approximate character. The electric equivalent circuit has proved to be very useful as a representation for electrical machines in general. However, the field approach is preferable to the circuit approach because it allows more information about conditions in the material that may be subject to electric and magnetic stresses and accompanying nonlinearities. It would be preferable when dealing with rotating machines, in general, to solve the electromagnetic field equations, given the boundary conditions, to obtain the values of electric and magnetic flux densities at all points. This would eliminate many of the approximations found in the electric circuit approach.

Due to the complicated nature of the structure of the induction motor, a direct application of Maxwell's field equations to the different regions of the motor is quite impractical.

A machine model is chosen which substitutes the alternating tooth/slot structure by an anisotropic magnetic mass with equivalent permeabilities. The model, while sacrificing the finer details of construction, yields a faithful global representation of the field

quantities, and permits a thorough direct integration of Maxwell's field equations.

B. Mathematical Model

Figure 2.1a shows part of a developed machine, and Figure 2.1b shows its equivalent anisotropic magnetic regions. An orthogonal stationary system of coordinates is used whereby the x-axis coincides with the lower surface of the secondary slot region, the y-axis points towards the primary region, and the z-axis is parallel to the machine's shaft. This coordinate system forms a right-hand system of axes.

The iron yokes of both the primary and the secondary are assumed to be perfectly permeable, while due to high induction values in the tooth zones, the permeability of the iron in these zones is assumed to be finite with relative permeability μ_r.

The whole tooth area reveals a different magnetic reluctance in the x- and in the y-directions. For the purpose of the following analysis, the original alternating teeth and slots, of any toothed region, may be replaced by a homogeneous anisotropic magnetic mass with different relative permeabilities, μ_x in the x-direction and μ_y in the y-direction. The permeabilities of the equivalent anisotropic medium can be easily derived from the series and parallel laws of the reluctance of the magnetic circuit to get

$$\mu_x = \frac{\mu}{1 + (\mu_r - 1)\, b_o/\tau_s} \qquad (2.1a)$$

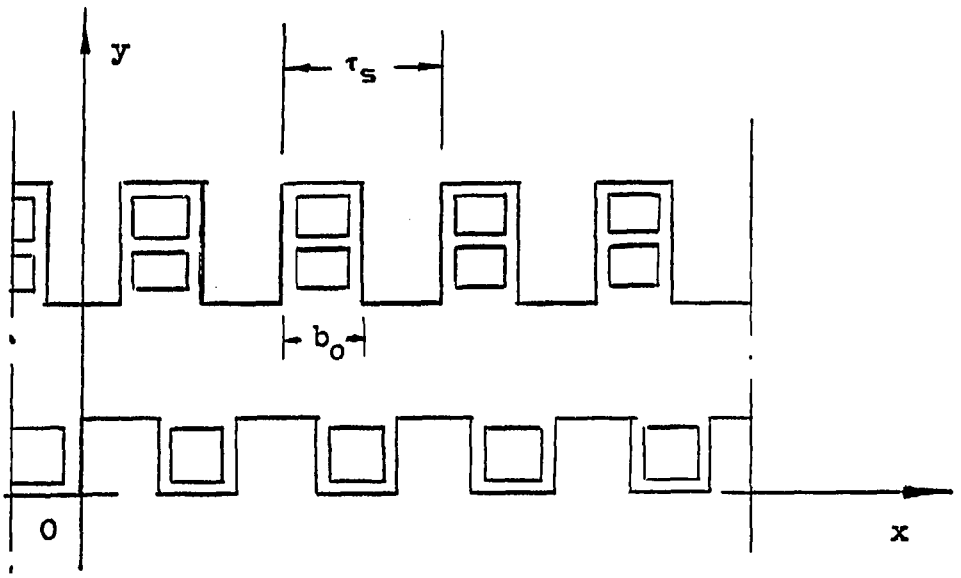

Figure 2.1a. Part of the developed motor

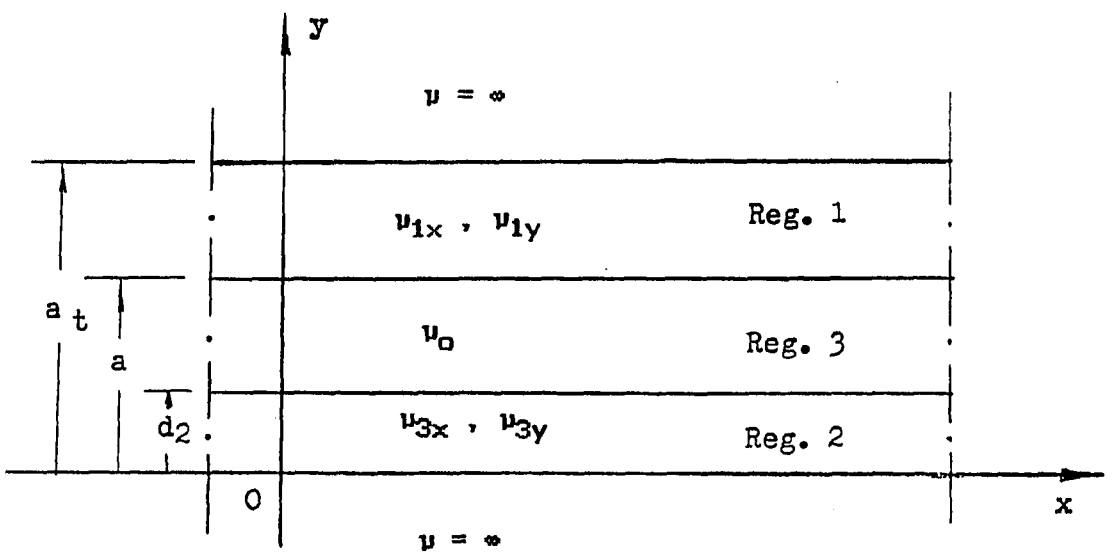

Figure 2.1b. The equivalent anisotropic magnetic regions 1, 2 and 3

$$\mu_y = \mu[1 + (1/\mu_r - 1)\, b_o/\tau_s] \tag{2.1b}$$

where

b_o = slot breadth,

τ_s = slot pitch,

μ_r = relative permeability of the tooth iron, and

μ = absolute permeability of the tooth iron.

From the electrical point of view, the above hypothetical magnetic mass must be conductive in the z-direction only, so that the model will represent faithfully (although in the form of a continuous distribution) the axially flowing electric currents.

It is clear that the attributed conductivity σ (S/m) should be

$$\sigma = \frac{b_s}{\tau_s} \gamma_s \bar{\sigma} \tag{2.2}$$

where γ_s is the slot space factor which is equal to the ratio between the area of the conductors to the area of the slot, and $\bar{\sigma}$ is the machine conductors' actual conductivity.

C. Basic Field Equations

Maxwell's field equations for stationary conducting medium are

$$\text{i. } \nabla \times \vec{E} = -\partial \vec{B}/\partial t, \qquad \text{ii. } \nabla \cdot \vec{D} = 0,$$
$$\text{iii. } \nabla \times H = \vec{J}, \qquad \text{iv. } \nabla \cdot \vec{B} = 0 \ . \tag{2.3}$$

To those, usually we add

$$\text{i. } \nabla \cdot \vec{J} + \partial \rho/\partial t = 0, \qquad \text{ii. } \vec{D} = \varepsilon \vec{E},$$
$$\text{iii. } \vec{B} = \mu \vec{H}, \qquad \text{iv. } \vec{J} = \sigma \vec{E} \ . \tag{2.4}$$

In moving media, where $\vec{E}$ is induced in a moving medium due to $\vec{B}$ in a stationary medium, only Eq. (2.3.i) should be modified to

$$\nabla \times \vec{E} = -\partial \vec{B}/\partial t + \nabla \times (\vec{B} \times \vec{V}) \tag{2.5}$$

where $\vec{V}$ is the velocity of the moving medium. Other equations of (2.3) and (2.4) remain unchanged.

In our analysis, we shall assume that the electric intensity $\vec{E}$ has only a z-component E, and the magnetic induction $\vec{B}$ has x- and y-components, B_x and B_y, respectively. Thus,

$$\vec{E} = E \hat{z} \tag{2.6}$$

$$\vec{B} = B_x \hat{x} + B_y \hat{y} \tag{2.7}$$

where $\hat{x}$, $\hat{y}$ and $\hat{z}$ are unit vectors along the coordinate axes x, y and z, respectively.

The relative permeability of the tooth regions has different values in the x- and y-directions, as given by Eqs. (2.1a) and (2.1b). Then, the magnetic induction (Eq. 2.7) can be rewritten in the form:

$$\vec{B} = \mu_x H_x \hat{x} + \mu_y H_y \hat{y} \tag{2.8}$$

where μ_x and μ_y are the permeabilities of the equivalent anisotropic mass to the tooth region.

Making use of the assumptions given by Eqs. (2.6) to (2.8), Maxwell's field equations (2.3) for stationary media will yield:

$$\partial E/\partial y = - \mu_x \partial H_x/\partial t \tag{2.9}$$

$$\partial E/\partial x = \mu_y \partial H_y/\partial t \tag{2.10}$$

$$\partial H_y/\partial x - \partial H_x/\partial y = J \ . \tag{2.11}$$

For media moving in the x-direction with a velocity V, Eqs. (2.9) through (2.11) should be modified by using Eq. (2.5) to take the form:

$$\partial E/\partial y = - \mu_x (\partial H_x/\partial t + V \partial H_x/\partial x) \tag{2.12}$$

$$\partial E/\partial x = \mu_y (\partial H_y/\partial t + V \partial H_y/\partial x) \tag{2.13}$$

$$\partial H_y/\partial x - \partial H_x/\partial y = J \quad . \tag{2.14}$$

Equations (2.9) through (2.14) constitute the basic field equations necessary to derive the basic partial differential equations which describe the field phenomena in the different regions of the motor.

In what follows, the indices 1, 2 and 3 will be used for the primary, the secondary and the air-gap quantities, respectively.

1. Primary tooth region

The primary tooth region is defined for values of $a < y < a_t$. It is a stationary region, so the set of equations (2.9) through (2.11) will be the one used in this case. To derive the partial differential equation for the electric intensity of this region, the following procedure can be carried out.

Differentiating Eq. (2.9) with respect to y, and introducing the subscript 1 for the field components in this region, we obtain

$$\frac{\partial^2 E_1}{\partial y^2} = - \mu_{1x} \frac{\partial^2 H_{1x}}{\partial y \partial t} \quad . \tag{2.15}$$

Similarly, on differentiating Eq. (2.10) with respect to x_1, we obtain

$$\frac{\partial^2 E_1}{\partial x^2} = \mu_{1y} \frac{\partial^2 H_{1y}}{\partial x \partial t} \quad . \tag{2.16}$$

Finally, differentiating Eq. (2.11) with respect to t, we obtain

$$\frac{\partial^2 H_{1y}}{\partial t \partial x} - \frac{\partial^2 H_{1x}}{\partial t \partial y} = \frac{\partial J_1}{\partial t} \quad . \tag{2.17}$$

If we assume that the field components are continuous to their second partial derivatives, then we can eliminate the partial derivatives of H_{1x} and H_{1y} using Eqs. (2.15) through (2.17), as well as Eq. (2.11) (with the subscript 1 for this region) to obtain

$$\frac{1}{\mu_{1y}} \frac{\partial^2 E_1}{\partial x^2} + \frac{1}{\mu_{1x}} \frac{\partial^2 E_1}{\partial y^2} = \frac{\partial J_1}{\partial t} \quad . \tag{2.18}$$

2. Secondary tooth region

The secondary tooth region is defined for values of $0 < y < d_2$. This region is a moving region, so the set of Eqs. (2.12) through (2.14) will be applicable to this case. By a procedure similar to that given in case 1 above, the partial differential equation of the electric intensity can be derived. Introducing the subscript 2 for the quantities of this region, the resulting equation will take the form:

$$\frac{1}{\mu_{2y}} \frac{\partial^2 E_2}{\partial x^2} + \frac{1}{\mu_{2x}} \frac{\partial^2 E_2}{\partial y^2} = \frac{\partial J_2}{\partial t} + V \frac{\partial J_2}{\partial x} \quad . \tag{2.19}$$

3. Air-gap region

This case can be derived directly, as a special case, either from Eq. (2.18) or (2.19). This is carried out by equating the permeabilities

in the x- and y-directions to that of the free space, and equating the current density to zero. The resulting equation will be Laplace's equation. Introducing the subscript 3 to the quantities in this region- we obtain

$$\frac{\partial^2 E_3}{\partial x^2} + \frac{\partial^2 E_3}{\partial y^2} = 0 \quad . \tag{2.20}$$

Equations (2.18) through (2.20) are the three basic equations, which describe the electric intensities in the secondary tooth, the air-gap and the primary tooth regions of the motor, respectively.

4. Secondary end-ring constraints

Figure 2.2a shows the developed rotor, as seen from the stator, together with its end rings. The squirrel-cage bars are not shown as they are replaced by the anisotropic inductive magnetic mass. Let σ_e be the conductivity of the end-ring material, σ_2 be the conductivity of the anisotropic equivalent mass of the secondary region, J_2 be the current density in the secondary region, I_e be the end-ring current, A_e the area of the secondary end ring, and $(2W_2)$ be the secondary width. The secondary is short-circuited; therefore, neglecting the field at the secondary end rings, the line integral of E_2 along the contour shown in Figure 2.2a yields

$$E_2 \cdot W_2 - (E_2 + \frac{\partial E_2}{\partial x}\delta x) \cdot W_2 = J_2 \cdot \frac{W_2}{\sigma_2} - (J_2 + \frac{\partial J_2}{\partial x}\delta x) \cdot \frac{W_2}{\sigma_2} + 2I_e \frac{\delta x}{\sigma_e A_e} \quad . \tag{2.21}$$

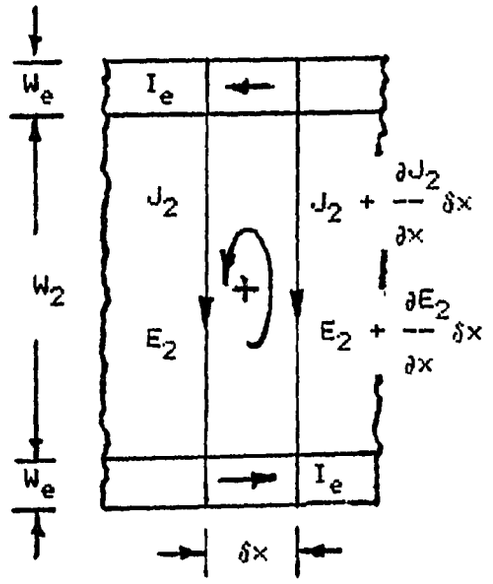

Figure 2.2a. The developed secondary, together with its end rings

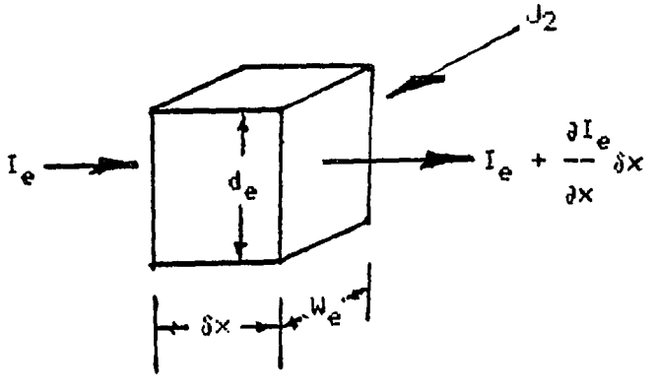

Figure 2.2b. The current distribution in an element end ring of length δx

Simplifying Eq. (2.21), and taking the limit as δx tends to zero, we obtain

$$\frac{\partial E_2}{\partial x} = \frac{1}{\sigma_2}\frac{\partial J_2}{\partial x} - \frac{2I_e}{\sigma_e A_e W_2} \quad . \tag{2.22}$$

The current continuity at the secondary end rings (see Figure 2.2b) implies that

$$J_2 = \frac{1}{d_2}\frac{\partial I_e}{\partial x} \quad . \tag{2.23}$$

To eliminate I_e between Eqs. (2.22) and (2.23), we differentiate Eq. (2.22) partially with respect to x, and then, eliminate $\partial I_e/\partial x$ between the resulting equation and Eq. (2.23) to obtain

$$\frac{\partial^2 E_2}{\partial x^2} = \frac{1}{\sigma_2}\frac{\partial^2 J_2}{\partial x^2} - \frac{2d_2 J_2}{\sigma_e A_e W_2} \quad . \tag{2.24}$$

Eq. (2.24) represents the constraint equation imposed by the secondary end rings on the electric intensity in the secondary region.

5. Primary overhang region

Figure 2.3 shows a sectional view of an induction motor. In order to represent the overhang on both sides of the primary, the secondary has been drawn in its full length, while the primary has been lengthened up to $(\ell_t/2)$, where ℓ_t is equal to one primary-turn's mean

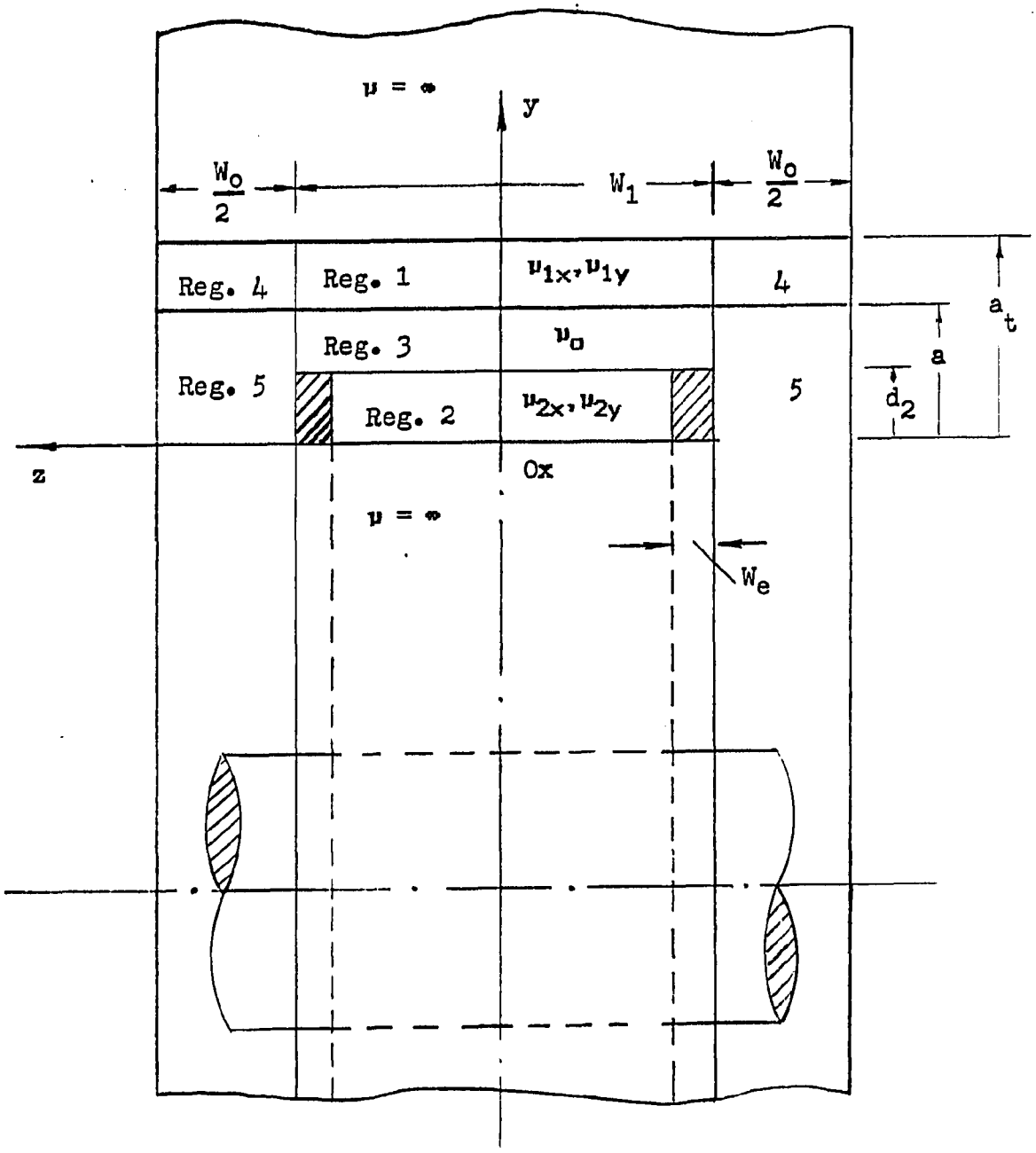

Figure 2.3. Sectional view of the induction motor showing regions 1, 2 and 3 (the primary, secondary and air-gap regions), as well as regions 4 and 5 (the primary overhang and air overhang regions)

length. The primary overhang conductors are normally bent so as to recline on the primary's yoke. This is taken into consideration by continuing the yoke, behind the primary conductors, up to the length $(\ell_t/2)$. Figure 2.3 shows also the relative permeability of the various regions. The system of coordinates is chosen similar to that used in the previous cases, so that this region is defined for values of $a < y < a_t$. The current density is assumed to be identical with that of case 1. The differential equation of the electric intensity E_4 in this region is similar to that given by Eq. (2.18) with the sole correction $\mu_{1x} = \mu_{1y} = \mu_o$; hence,

$$\frac{\partial^2 E_4}{\partial x^2} + \frac{\partial^2 E_4}{\partial y^2} = \mu_o \frac{\partial J_1}{\partial t} \quad . \tag{2.25}$$

6. Air overhang region

This is region 5, defined for values of $0 < y < a$. The differential equation in this air region, which now extends from the primary overhang to the motor's shaft, will be similar to that of case 3, which is Laplace's equation:

$$\frac{\partial^2 E_5}{\partial x^2} + \frac{\partial^2 E_5}{\partial y^2} = 0 \quad . \tag{2.26}$$

The previous results are summarized in Figure 2.4, which shows a sectional view of the motor, and the differential equations which hold in each of its regions.

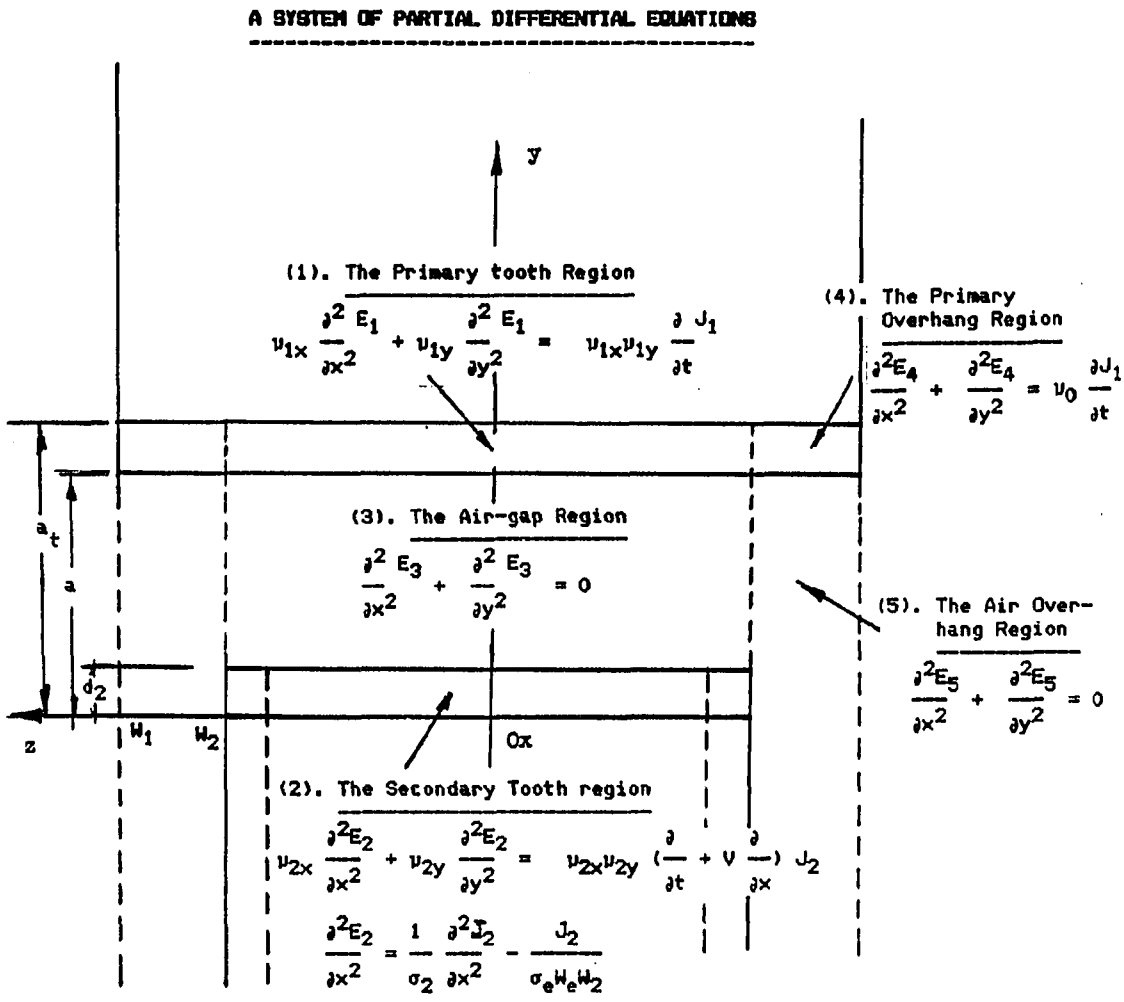

Figure 2.4. A sectional view of the induction motor showing the frame of reference, the main dimensions and the governing differential equations in each region

D. Boundary Conditions

The field conditions at the boundary between any two regions can be derived by using the integral form of the following two Maxwell equations:

$$\oint_L \vec{H}\cdot d\vec{L} = \iint_S \vec{J}\cdot d\vec{A} + \frac{\partial}{\partial t}\vec{D}\cdot d\vec{A} \tag{2.27}$$

$$\oint_A \vec{B}\cdot d\vec{A} = 0 \quad . \tag{2.28}$$

Applying Eq. (2.27) to any small closed path on the boundary between the two regions yields

$$H_x^- = H_x^+ \tag{2.29}$$

where H_x^- and H_x^+ are the magnetic field intensities just below and above the boundary. Equation (2.29) follows directly from Eq. (2.27) so long as current density and rate of change of electric flux density are finite, and then, the contribution from the right-hand side of Eq. (2.27) will be zero.

Similarly, applying Eq. (2.28) to any closed surface on the boundary between two regions yields

$$B_y^- = B_y^+ \tag{2.30}$$

where B_y^- and B_y^+ are the magnetic flux densities just below and above

the boundary.

Equations (2.29) and (2.30) represent the continuity of the tangential components of the magnetic field intensities and the normal components of the magnetic flux densities, respectively, at the boundary between any two regions.

To express Eqs. (2.29) and (2.30) in terms of the electric field intensity, we differentiate these equations partially with respect to t, and make use of Eqs. (2.9) and (2.10) to obtain

$$\left(\frac{1}{\mu_x}\frac{\partial E}{\partial y}\right)^{-} = \left(\frac{1}{\mu_x}\frac{\partial E}{\partial y}\right)^{+} \tag{2.31}$$

and

$$\left(\frac{\partial E}{\partial x}\right)^{-} = \left(\frac{\partial E}{\partial x}\right)^{+} . \tag{2.32}$$

Equations (2.29) through (2.32) are those necessary to obtain the field relations at the boundary between any two regions.

1. Main regions

Referring to Figure 2.3, the main regions are considered to be regions 1, 2 and 3. Now we can apply Eqs. (2.29) through (2.32) to the boundary between these regions. Due to the perfect permeability of the primary and secondary iron, i.e., $\mu=\infty$, the tangential magnetic field H_x must vanish along the planes $y=0$ and $y=a_t$; i.e.,

$$\text{at } y=0, \qquad \frac{\partial E_2}{\partial y} = 0 \tag{2.33}$$

$$\text{at } y=a_t, \qquad \frac{\partial E_1}{\partial y} = 0 \quad . \tag{2.34}$$

A direct application of Eqs. (2.31) and (2.32) to the boundary between the air-gap and the primary region yields:

$$\text{at } y=a, \qquad \frac{1}{\mu_{1x}} \frac{\partial E_1}{\partial y} = \frac{1}{\mu_o} \frac{\partial E_3}{\partial y} \tag{2.35}$$

$$\frac{\partial E_1}{\partial x} = \frac{\partial E_3}{\partial x} \quad . \tag{2.36}$$

The same continuity conditions of the tangential magnetic intensity and the normal induction at the boundary (Eqs. 2.29 and 2.30) still hold at $y=d_2$, but Eqs. (2.31) and (2.32) no longer hold. The reason is that Faraday's law of induction will take the form given by Eq. (2.5), as the secondary region is a moving medium in this case. The boundary conditions, therefore, between the secondary and the air-gap regions will be expressed in terms of Eqs. (2.29) and (2.30) to obtain

$$H_{2x} = H_{3x} \tag{2.37}$$

$$B_{2y} = B_{3y} \quad . \tag{2.38}$$

Expressing Eqs. (2.37) and (2.38) in terms of the electric field intensity will be carried out later, using Eq. (2.5), after getting the solution for $\vec{E}$ and $\vec{B}$.

2. Overhang regions

Referring to Figure 2.3, we see the overhang regions are the two regions 4 and 5. The condition given by Eqs. (2.31) and (2.32) still holds in this case with the sole modification $\mu_x = \mu_y = \mu_o$. Also, we have assumed the perfect permeability of the primary iron back. Therefore, we can write down the following boundary equations:

$$\text{at } y=a_t, \qquad \frac{\partial E_4}{\partial y} = 0 \tag{2.39}$$

$$\text{at } y=a, \qquad \frac{\partial E_4}{\partial y} = \frac{\partial E_5}{\partial y} \tag{2.40}$$

$$\frac{\partial E_4}{\partial x} = \frac{\partial E_5}{\partial x} \quad . \tag{2.41}$$

In addition to these conditions, we consider the distance between the primary overhang and the rotating shaft of the motor is very large. The field created by the overhang winding near the surface of the shaft can then be neglected. This yields the following condition:

$$\text{at } y=-\infty, \qquad \frac{\partial E_5}{\partial y} = 0 \quad . \tag{2.42}$$

According to the boundary conditions given above, we see that the boundaries of the problem are divided into two separate zones (see Figure 2.3). Zone I contains the three regions (1, 2 and 3); and zone II contains the two regions 4 and 5. The common boundaries of

these two zones are the two planes $z = \pm W_1/2$. Due to design considerations of the induction motor, there is negligible dependence on the z-coordinate. Therefore, the two zones are mathematically separate, and we can deal with the system of partial differential equations of each zone, together with its associated boundary conditions, individually.

E. Solution of the Field System of Equations

1. General considerations

Before going into the details of getting the solution of the system of partial differential equations, we shall discuss the outline that governs the functional form of the solution. This form is determined by the imposed nature of the primary current that generates all the electromagnetic phenomena inside the machine. The primary current, J_1, can be expressed in the form:

$$J_1 = \sum_{n=1}^{\infty} \sum_{\nu=-\infty}^{\infty} \bar{J}_1 \, e^{j(\frac{\nu\pi}{\tau}x + n\omega t)} \qquad (2.43)$$

where $\bar{J}_1$ is known as the Fourier coefficient of J_1, and is exclusively defined in terms of the wavenumber ν (also known as the space harmonic order), and the time harmonic order n.

In the case of a double layer, three-phase winding under unbalanced current operations, the expression of J_1 will be in the form:

$$\bar{J}_1 = \frac{1}{2t} a_n N_p K_w \left[I_1 + I_2 e^{-i \frac{2\pi}{3} \nu} + I_3 e^{-i \frac{4\pi}{3} \nu} \right] \qquad (2.44)$$

where

a_n = amplitude of the time harmonic component, equals unity for fundamental,

N_p = number of conductors/phase/pole pair,

I_1, I_2, I_3 = phase currents,

K_w = winding factor,

τ = pole pitch

The general expression of the winding factor, K_w, is given by

$$K_w = K_b K_c K_d K_o \qquad (2.45)$$

where

$$K_b = \frac{\sin(\nu\pi b_s/2\tau)}{(\nu\pi b_s/2\tau)} \quad . \qquad (2.46)$$

K_b is known as the slot breadth factor, b_s being the slot breadth.

$$K_c = \frac{1}{2} \left(1 - e^{-i\nu\pi\tau_c/\tau}\right) \quad . \qquad (2.47)$$

K_c is known as the chording factor, τ_c being the coil span in the same units as the pole pitch τ.

$$K_d = \frac{1 - e^{-jq\nu\alpha}}{q(1-e^{-j\nu\alpha})} \quad ; \quad \alpha = \pi\tau_s/\tau \quad . \tag{2.48}$$

K_d is known as the phase distribution factor, τ_s is the slot pitch and q is the number of slots/pole/phase.

$$K_o = \frac{1}{2}(1 - e^{-j\nu\pi}) \quad . \tag{2.49}$$

K_o is known as the odd harmonic factor; this factor is unity for odd values of ν, and is zero for even values of ν.

As mentioned before, the primary current, represented by Eq. (2.43), is the one that is responsible for generating all the electromagnetic phenomena inside the different machine regions. It seems very reasonable to assume that the functional dependence of the generated quantities (the effect) will have the same form as the primary current (the cause).

Therefore, any arbitrary electromagnetic quantity A(x,y,z,t), generated in any of the machine regions, can be represented in the form:

$$A(x,y,z,t) = \sum_{n=1}^{\infty} \sum_{\nu=-\infty}^{\infty} \bar{A}(\nu,n,y,z)\, e^{j(\frac{\nu\pi}{\tau}x + n\omega t)} \tag{2.50}$$

where $\bar{A}(\nu,n,y,z)$, or simply $\bar{A}$, is known as the Fourier coefficient (or

the harmonic component) of the function A(x,y,z,t). The expression of $\bar{A}$ will be determined from the solution of the system of partial differential equations, as well as the associated system of boundary conditions.

In the next sections, we shall consider the solution of the system of equations in the five different regions of the machine model under consideration.

2. Primary tooth region

The PDE of the electric field intensity, E_1, in the primary tooth region 1, is given by Eq. (2.18). According to the explanation given in the previous section, the solution of E_1 can be assumed in the form:

$$E_1 = \sum_{n=1}^{\infty} \sum_{\nu=-\infty}^{\infty} \bar{E}_1 \, e^{j(\frac{\nu\pi}{\tau} x + n\omega t)} \quad . \tag{2.51}$$

The reader will recall $\bar{E}_1 \equiv \bar{E}_1 (\nu,n,y,z)$. Equation (2.51), together with Eq. (2.43), should satisfy the PDE of E_1 as given by Eq. (2.18). Therefore, on substituting Eqs. (2.51) and (2.43) into Eq. (2.18), we can obtain:

$$\sum_{n=1}^{\infty} \sum_{\nu=-\infty}^{\infty} [\frac{1}{\mu_{1y}} (\frac{j\nu\pi}{\tau})^2 \bar{E}_1 + \frac{1}{\mu_{1x}} \frac{\partial^2 \bar{E}_1}{\partial y^2} + jn\omega \bar{J}_1] e^{j(\frac{\nu\pi}{\tau} x + n\omega t)} = 0. \tag{2.52}$$

Since Eq. (2.52) is true for any arbitrary values of x and t, it should follow that:

$$\frac{1}{\mu_{1y}} \left(\frac{j\nu\pi}{\tau}\right)^2 \bar{E}_1 + \frac{1}{\mu_{1x}} \frac{\partial^2 \bar{E}_1}{\partial y^2} + jn\omega\, \bar{J}_1 = 0$$

or in the form:

$$\left(\frac{\partial^2}{\partial y^2} - \eta_1^2\right) \bar{E}_1 = jn\omega . \mu_{1x}\, \bar{J}_1 \qquad (2.53)$$

where

$$\eta_1^2 = \frac{\mu_{1x}}{\mu_{1y}} \left(\frac{\nu\pi}{\tau}\right)^2 . \qquad (2.54)$$

The solution of Eq. (2.53) will be the sum of the complementary function and the particular integral. These two solutions can be obtained as shown in the following paragraph.

The complementary function is the solution of Eq. (2.53) with the right-hand side equal to zero. This solution will be in the form

$$\bar{E}_{11} = A_1 \cosh \eta_1 y + B_1 \sinh \eta_1 y \qquad (2.55)$$

where A_1 and A_2 are arbitrary constants to be determined from the boundary conditions. The particular integral is any solution that satisfies Eq. (2.53), and is given by

$$\bar{E}_{12} = \frac{1}{(D_y^2 - \eta_1^2)} (jn\omega\, \mu_{1x}\, \bar{J}_1) \qquad (2.56)$$

where D_y^2 stands for the differential operation $\partial^2/\partial y^2$. Since $\bar{J}_1$ is only a function of ν and n, and is independent of the y-coordinate, the solution of Eq. (2.56) can be obtained by simply substituting zero for D_y. The final result can be written in the form

$$\bar{E}_{12} = -i\alpha_{\nu n} \bar{J}_1 \tag{2.57a}$$

where

$$\alpha_{\nu n} = n\omega \mu_{1x}/\eta_1^2 \quad . \tag{2.57b}$$

The complete solution will be the sum of Eqs. (2.55) and (2.57).

$$\bar{E}_1 = A_1 \cosh \eta_1 y + B_1 \sinh \eta_1 y - i\alpha\nu_n \bar{J}_1 \quad . \tag{2.58}$$

The series expression of E_1 can be obtained by substituting Eq. (2.58) into Eq. (2.51). Other field components can be derived from Maxwell's equations (2.9 - 2.11), so long as E_1 is obtained and their functional form is defined by Eq. (2.50).

3. Secondary tooth region

The system of PDEs in the secondary tooth region is given by Eqs. (2.19) and (2.24). As explained before (see Section E.1), the functional form of both E_2 and J_2 can be assumed to be in the form

$$E_2 = \sum_{n=1}^{\infty} \sum_{\nu=-\infty}^{\infty} \bar{E}_2 \, e^{j(\frac{\nu\pi}{\tau} x + n\omega t)} \tag{2.59}$$

$$J_2 = \sum_{n=1}^{\infty} \sum_{\nu=-\infty}^{\infty} \bar{J}_2 \, e^{j(\frac{\nu\pi}{\tau} x + n\omega t)} \tag{2.60}$$

where both $\bar{E}_2$ and $\bar{J}_2$ are functions of ν, n and the y-coordinate. Equations (2.59) and (2.60) should satisfy Eqs. (2.19) and (2.24). To fulfill this requirement, after substituting Eqs. (2.59) and (2.60) into Eqs. (2.19) and (2.24), we should have

$$(\frac{\partial^2}{\partial y^2} - n_2^2) \bar{E}_2 = jn\omega \, \mu_{2x} S_{\nu n} \bar{J}_2 \tag{2.61}$$

and

$$(\frac{\nu\pi}{\tau})^2 \bar{E}_2 = [\frac{1}{\sigma_2} (\frac{\nu\pi}{\tau})^2 + \frac{2d_2}{\sigma_e A_e W_2}] \bar{J}_2 \tag{2.62}$$

where

$$n_2^2 = \frac{\mu_{2x}}{\mu_{2y}} (\frac{\nu\pi}{\tau})^2 \tag{2.63}$$

and $S_{\nu n}$ is the motor slip referred to any arbitrary moving wave with space order ν and time order n:

$$S_{\nu n} = 1 + \frac{\nu\pi}{n\omega\tau} V = 1 + \frac{V}{(nV_s/\nu)} \quad . \tag{2.64}$$

$S_{\nu n}$ will be less or greater than one depending on the direction of the motor speed, as well as the sequence of the voltage, i.e., the sign of ω, applied to the motor. It is evident that when both ν and n equal one, $S_{\nu n}$ will be the familiar slip of the induction motor.

After eliminating $\bar{J}_2$ between Eqs. (2.61) and (2.62), the resulting equation will take the form:

$$\left(\frac{\partial^2}{\partial y^2} - \gamma^2\right) \bar{E}_2 = 0 \tag{2.65}$$

where

$$\gamma^2 = n_2^2 \left[1 + j \frac{\mu_{2y}\sigma_2 n\omega S_{\nu n}}{\left(\frac{\nu\pi}{\tau}\right)^2 + \frac{2d_2\sigma_2}{\sigma_e A_e W_2}}\right] \quad . \tag{2.66}$$

The solution of Eq. (2.65) will be in the form

$$\bar{E}_2 = A_2 \cosh \gamma y + B_2 \sinh \gamma y \quad . \tag{2.67}$$

Once we get $\bar{E}_2$, the field components in the secondary tooth region can be derived from Eqs. (2.59) and (2.60), as well as Maxwell's Eqs. (2.12) through (2.14), noting that the functional form of all the other field components is known to be in the form of Eq. (2.50).

4. Air-gap region

The differential equation of the field intensity in the air-gap region is given by Eq. (2.20). As explained before, the functional form of the electric intensity will be assumed in the form

$$E_3 = \sum_{n=1}^{\infty} \sum_{\nu=-\infty}^{\infty} \bar{E}_3 \, e^{j(\frac{\nu\pi}{\tau} x + n\omega t)} \quad . \tag{2.68}$$

This equation should satisfy Eq. (2.20); therefore, this requires

$$(\frac{\partial^2}{\partial y^2} - \eta_3^2) \, \bar{E}_3 = 0 \tag{2.69}$$

where

$$\eta_3 = \nu\pi/\tau \quad . \tag{2.70}$$

The solution of Eq. (2.69) will take the form

$$\bar{E}_3 = A_3 \cosh \eta_3 y + B_3 \sinh \eta_3 y \quad . \tag{2.71}$$

The expression of $\bar{E}_3$ can be substituted into Eq. (2.68) to get the field component E_3. All other field components can be derived, on the assumption that their functional form is the same as in Eq. (2.50) and using Eqs. (2.9) and (2.10).

5. Primary overhang region

The differential equation of the field intensity in this region is that given by Eq. (2.25). Assume the solution in the form

$$E_4 = \sum_{n=1}^{\infty} \sum_{\nu=-\infty}^{\infty} \bar{E}_4 \, e^{j(\frac{\nu\pi}{\tau} x + n\omega t)} \quad . \tag{2.72}$$

Then, in order for Eqs. (2.72) and (2.43) to be a solution for Eq. (2.25), we should have

$$(\frac{\partial^2}{\partial y^2} - \eta_3^2) \, \bar{E}_4 = jn\omega\mu_o \, \bar{J}_1 \tag{2.73}$$

where $\eta_3 = \nu\pi/t$, given previously by Eq. (2.70).

The solution of Eq. (2.73) will be composed of the complementary function and the particular integral. Following the procedure given before in Section E.2, the solution can be derived and will take the form

$$\bar{E}_4 = A_4 \cosh \eta_3 y + B_4 \sinh \eta_3 y - \frac{jn\omega\mu_o}{\eta_3} \bar{J}_1 \quad . \tag{2.74}$$

Substitution of Eq. (2.74) into Eq. (2.72) will yield the electric field intensity in region 4. Other field components in region 4 can be derived from E_4 using Maxwell's equations (2.9) - (2.11), noting that their expression has been assumed to be in the form of Eq. (2.50).

6. Air overhang region

The differential equation of the field intensity in region 5 is given by Eq. (2.26). Assume the solution to be in the form

$$E_5 = \sum_{n=1}^{\infty} \sum_{\nu=-\infty}^{\infty} \bar{E}_5 \, e^{j(\frac{\nu\pi}{\tau} x + n\omega t)} \quad . \tag{2.75}$$

Then, Eq. (2.75) will satisfy Eq. (2.26) if

$$(\frac{\partial^2}{\partial y^2} - \eta_3^2) \, \bar{E}_5 = 0 \tag{2.76}$$

where $\eta_3 = \nu\pi/t$, previously given by Eq. (2.70). The solution of Eq. (2.76) may take the form

$$\bar{E}_5 = A_5 \, e^{\eta_3 y} + B_5 \, e^{-\eta_3 y} \quad . \tag{2.79}$$

Once we have $\bar{E}_5$, the electric intensity in region 5 is completely determined, and hence, all the other field components can be derived from it by using Maxwell's equations (2.9) and (2.10).

F. The Arbitrary Constants and the Field Expressions

1. Main regions

Referring to Figure 2.3, the main regions are those of zone I, which constitute regions 1, 2 and 3. The electric intensity in these regions is given by Eqs. (2.51), (2.59) and (2.68). Since we are

dealing with only single components, then the interesting part for us will be the expressions of $\bar{E}_1$, $\bar{E}_2$ and $\bar{E}_3$ which are given by Eqs. (2.58), (2.67) and (2.71), respectively. These equations contain six arbitrary constants: A_1, B_1, A_2, B_2, A_3 and B_3. Six equations are needed to obtain the values of these six arbitrary constants. The boundary conditions, given by Eqs. (2.33) - (2.38), satisfy this need. According to our assumption given in Section E.1, all the field components have the functional form given by Eq. (2.50). This implies that the partial derivative of the field component with respect to x will be replaced by $(jv\pi/t)$, and the partial derivative with respect to time t will be replaced by jn . Therefore, we can express the boundary conditions, Eqs. (2.33) - (2.38), in terms of $\bar{E}_1$, $\bar{E}_2$ and $\bar{E}_3$. Summarizing the results, Eqs. (2.33) - (2.36) will yield:

$$\left[\frac{\partial \bar{E}_1}{\partial y}\right]_{y=a_t} = 0 \tag{2.78}$$

$$\left[\frac{\partial \bar{E}_2}{\partial y}\right]_{y=0} = 0 \tag{2.79}$$

$$\left[\frac{1}{\mu_{1x}} \frac{\partial \bar{E}_1}{\partial y}\right]_{y=a} = \left[\frac{1}{\mu_o} \frac{\partial \bar{E}_3}{\partial y}\right]_{y=a} \tag{2.80}$$

$$\left[\bar{E}_1\right]_{y=a} = \left[\bar{E}_3\right]_{y=a} , \tag{2.81}$$

while Eqs. (2.37) and (2.38) will yield

$$\left[\frac{1}{\mu_{2x}} \frac{\partial \bar{E}_2}{\partial y}\right]_{y=d_2} = \left[\frac{S_{\nu n}}{\mu_o} \frac{\partial \bar{E}_3}{\partial y}\right]_{y=d_2} \tag{2.82}$$

$$[E_2]_{y=d_2} = [S_{\nu n} E_3]_{y=d_2} \tag{2.83}$$

where $S_{\nu n}$ is the motor slip referred to any arbitrary moving wave with space order ν and time order n, as previously given by Eq. (2.64).

Substituting Eq. (2.58) into Eq. (2.78), we obtain

$$A_1 \sinh \eta_1 a_t + B_1 \cosh \eta_1 a_t = 0$$

which yields

$$B_1 = -A_1 \frac{\sinh \eta_1 a_t}{\cosh \eta_1 a_t} \quad . \tag{2.84}$$

Eliminating B_1 between Eqs. (2.84) and (2.58) yields

$$\bar{E}_1 = \frac{A_1}{\cosh \eta_1 a_t} \cosh \eta_1 (a_t - y) - j \alpha_{\nu n} \bar{J}_1 \quad . \tag{2.85}$$

Substituting Eq. (2.67) into Eq. (2.79), we obtain

$$B_2 = 0 \quad . \tag{2.86}$$

Then, Eq. (2.67) will be reduced to

$$\bar{E}_2 = A_2 \cosh \gamma y \quad . \tag{2.87}$$

Substituting Eqs. (2.85) and (2.71) into Eq. (2.80), we obtain

$$\frac{1}{\mu_{1x}} \frac{-A_1 \eta_1}{\cosh \eta_1 a_t} \cdot \sinh \eta_1 d_1 = \frac{\eta_3}{\mu_o} [A_3 \sinh \eta_3 a + B_3 \cosh \eta_3 a] \tag{2.88}$$

where $d_1 = a_t - a$. Substituting Eqs. (2.85) and (2.71) into the boundary condition given by Eq. (2.81), we obtain

$$\frac{A_1}{\cosh \eta_1 a_t} \cosh \eta_1 d_1 - j \alpha_{\nu n} \bar{J}_1 = A_3 \cosh \eta_3 a + B_3 \sinh \eta_3 a \quad . \tag{2.89}$$

Substituting Eqs. (2.87) and (2.71) into the boundary condition given by Eq. (2.82), we obtain

$$\frac{\gamma}{\mu_{2x}} A_2 \sinh \gamma y = \frac{\eta_3 S_{\nu n}}{\mu_o} [A_3 \sinh \eta_3 d_2 + B_3 \cosh \eta_3 d_2] \quad . \tag{2.90}$$

Finally, substituting Eqs. (2.87) and (2.71) into Eq. (2.83), we obtain

$$A_2 \cosh \gamma d_2 = S_{\nu n} [A_3 \cosh \eta_3 d_2 + B_3 \sinh \eta_3 d_2] \quad . \tag{2.91}$$

Equations (2.88) through (2.91) are sufficient to determine the four arbitrary constants: A_1, A_2, A_3 and B_3. To solve these equations, we start by arranging them in the following matrix form:

$$\begin{bmatrix} -\frac{\mu_o \eta_1}{\mu_{1x} \eta_3} \frac{\sinh \eta_1 d_1}{\cosh \eta_1 a_t} & 0 & \sinh \eta_3 a & \cosh \eta_3 a \\ -\frac{\cosh \eta_1 d_1}{\cosh \eta_1 a_t} & 0 & \cosh \eta_3 a & \sinh \eta_3 a \\ 0 & -\frac{\mu_o \gamma}{\mu_{2x} \eta_3} \sinh \gamma d_2 & S_{\nu n} \sinh \eta_3 d_2 & S_{\nu n} \cosh \eta_3 d_2 \\ 0 & -\cosh \gamma d_2 & S_{\nu n} \cosh \eta_3 d_2 & S_{\nu n} \sinh \eta_3 d_2 \end{bmatrix} \begin{bmatrix} A_1 \\ A_2 \\ A_3 \\ B_3 \end{bmatrix} = \begin{bmatrix} 0 \\ -j\alpha_{\nu n} \bar{J}_1 \\ 0 \\ 0 \end{bmatrix}. \tag{2.92}$$

The determinant of the matrix coefficient D_o is given by

$$D_0 = \begin{bmatrix} \frac{\mu_o \eta_1}{\mu_{1x} \eta_3} \frac{\sinh \eta_1 d_1}{\cosh \eta_1 a_t} & 0 & \sinh \eta_3 a & \cosh \eta_3 a \\ -\frac{\cosh \eta_1 d_1}{\cosh \eta_1 a_t} & 0 & \cosh \eta_3 a & \sinh \eta_3 a \\ 0 & -\frac{\mu_o \gamma}{\mu_{2x} \eta_3} \sinh d_2 & S_{\nu n} \sinh \eta_3 d_2 & S_{\nu n} \cosh \eta_3 d_2 \\ 0 & -\cosh \gamma d_2 & S_{\nu n} \cosh \eta_3 d_2 & S_{\nu n} \sinh \eta_3 d_2 \end{bmatrix}.$$

Expanding this determinant along the first column, the final expression of D_0 will take the form:

$$D_0 = - S_{\nu n} H_c(\nu)/\cosh \eta_1 a_t \tag{2.93}$$

where

$$H_c(\nu) = \cosh\eta_1 d_1 * g_1(\nu) + \frac{\mu_o}{\sqrt{\mu_{1x}\mu_{1y}}} \sinh\eta_1 d_1 * g_2(\nu) \tag{2.94}$$

$$g_1(\nu) = \cosh\gamma d_2 * \sinh\eta_3(a-d_2) + \frac{\gamma\mu_o}{\eta_3\mu_{2x}} \sinh\gamma d_2 * \cosh\eta_3(a-d_2) \tag{2.95}$$

and

$$g_2(\nu) = \cosh\gamma d_2 * \cosh\eta_3(a-d_2) + \frac{\gamma\mu_o}{\eta_3\mu_{2x}} \sinh\gamma d_2 * \sinh\eta_3(a-d_2) \; . \tag{2.96}$$

It should be noted that $H_c(\nu)$ is also a function of the motor dimensions. It is also evident that for the case of an infinitely thin primary current layer, i.e., $d_1=0$, the second term of Eq. (2.94) will identically vanish, as $\sinh\eta_1 d_1=0$ and $H_c(\nu)$ are simply given by $g_1(\nu)$.

The determinant D_1 is formed from the coefficient matrix, with the first column replaced by the R.H.S. column of Eq. (2.92):

$$D_1 = \begin{bmatrix} 0 & 0 & \sinh\eta_3 a & \cosh\eta_3 a \\ -j\alpha_{\nu n}\bar{J}_1 & 0 & \cosh\eta_3 a & \sinh\eta_3 a \\ 0 & -\frac{\gamma\mu_o}{\eta_3\mu_{2x}}\sinh\gamma d_2 & S_{\nu n}\sinh\eta_3 d_2 & S_{\nu n}\cosh\eta_3 d_2 \\ 0 & -\cosh\gamma d_2 & S_{\nu n}\cosh\eta_3 d_2 & S_{\nu n}\sinh\eta_3 d_2 \end{bmatrix} .$$

Expanding this determinant along the first column, it takes the form:

$$D_1 = -j\alpha_{\nu n} S_{\nu n} \bar{J}_1 g_1(\nu) \qquad (2.97)$$

where $g_1(\nu)$ is given by Eq. (2.95). Similarly, the determinant D_2 is derived from D_o by replacing the second column by the R.H.S. of Eq. (2.92):

$$D_2 = \begin{bmatrix} \frac{\mu_o\eta_1}{\mu_{1x}\eta_3}\frac{\sinh\eta_1 d_1}{\cosh\eta_1 a_t} & 0 & \sinh\eta_3 a & \cosh\eta_3 a \\ -\frac{\cosh\eta_1 d_1}{\cosh\eta_1 a_t} & -j\alpha_{\nu n}\bar{J}_1 & \cosh\eta_3 a & \sinh\eta_3 a \\ 0 & 0 & S_{\nu n}\sinh\eta_3 d_2 & S_{\nu n}\cosh\eta_3 d_2 \\ 0 & 0 & S_{\nu n}\cosh\eta_3 d_2 & S_{\nu n}\sinh\eta_3 d_2 \end{bmatrix} .$$

This yields

$$D_2 = j \frac{\mu_o \eta_1}{\mu_{1x} \eta_3} \cdot S_{\nu n}^2 \alpha_{\nu n} \bar{J}_1 \frac{\sinh \eta_1 d_1}{\cosh \eta_1 a_t} \quad . \tag{2.98}$$

Similarly,

$$D_3 = \begin{bmatrix} \frac{\mu_o \eta_1}{\mu_{1x} \eta_3} \frac{\sinh \eta_1 d_1}{\cosh \eta_1 a_t} & 0 & 0 & \cosh \eta_3 a \\ - \frac{\cosh \eta_1 d_1}{\cosh \eta_1 a_t} & 0 & -j\alpha_{\nu n} \bar{J}_1 & \sinh \eta_3 a \\ 0 & - \frac{\gamma \mu_o}{\eta_3 \mu_{2x}} \sinh \gamma d_2 & 0 & S_{\nu n} \cosh \eta_3 d_2 \\ 0 & - \cosh \gamma d_2 & 0 & S_{\nu n} \sinh \eta_3 d_2 \end{bmatrix}$$

which yields:

$$D_3 = j \frac{\mu_o \eta_1}{\mu_{1x} \eta_3} \alpha_{\nu n} \bar{J}_1 S_{\nu n} \cdot \frac{\sinh \eta_1 d_1}{\cosh \eta_1 a_t} (\cosh \gamma d_2 \cosh \eta_3 d_2 - \frac{\gamma \mu_o}{\eta_3 \mu_{2x}} \sinh \gamma d_2 \cdot \sinh \eta_3 d_2) \quad . \tag{2.99}$$

Finally,

$$D_4 = \begin{bmatrix} \frac{\mu_o \eta_1}{\mu_{1x} \eta_3} \frac{\sinh \eta_1 d_1}{\cosh \eta_1 a_t} & 0 & \sinh \eta_3 a & 0 \\ -\frac{\cosh \eta_1 d_1}{\cosh \eta_1 a_t} & 0 & \cosh \eta_3 a & -j\alpha_{\nu n} \bar{J}_1 \\ 0 & -\frac{\gamma \mu_o}{\eta_3 \mu_{2x}} \sinh \gamma d_2 & S_{\nu n} \sinh \eta_3 d_2 & 0 \\ 0 & -\cosh \gamma d_2 & S_{\nu n} \cosh \eta_3 d_2 & 0 \end{bmatrix}$$

which yields:

$$D_4 = -j \frac{\mu_o \eta_1}{\mu_{1x} \eta_3} \alpha_{\nu n} \bar{J}_1 S_{\nu n} \cdot \frac{\sinh \eta_1 d_1}{\cosh \eta_1 a_t} (\cosh \gamma d_2 \sinh \eta_3 d_2 - \frac{\gamma \mu_o}{\eta_3 \mu_{2x}} \sinh \gamma d_2 \cdot \cosh \eta_3 d_2) \quad . \tag{2.100}$$

The arbitrary constants A_1, A_2, A_3 and B_3 can be determined using Eqs. (2.93) through (2.100).

The expression of A_1 will be given by

$$A_1 = D_1/D_0 \quad .$$

Using Eqs. (2.93) and (2.97), we obtain

$$A_1 = j \frac{\alpha_{\nu n} g_1(\nu)}{H_c(\nu)} \cosh \eta_1 a_t \bar{J}_1 \quad . \tag{2.101}$$

The expression of A_2 is given by

$$A_2 = D_2/D_0 \quad .$$

Using Eqs. (2.98) and (2.93), we obtain

$$A_2 = j \frac{\mu_o \eta_1}{\mu_{1x} \eta_3} \alpha_{\nu n} S_{\nu n} \frac{\sinh \eta_1 d_1}{H_c(\nu)} \bar{J}_1 \quad . \tag{2.102}$$

The expression of A_3 is given by

$$A_3 = D_3/D_0 \quad .$$

Using Eqs. (2.99) and (2.93), we obtain

$$A_3 = -j \frac{\mu_o \eta_1}{\mu_{1x} \eta_3} \alpha_{\nu n} \frac{\sinh \eta_1 d_1}{H_c(\nu)} (\cosh \gamma d_2 \cosh \eta_3 d_2$$

$$- \frac{\gamma \mu_o}{\eta_3 \mu_{2x}} \sinh \gamma d_2 \sinh \eta_3 d_2) \bar{J}_1 \quad . \tag{2.103}$$

Finally, the expression of B_3 is given by

$$B_3 = D_4/D_0 .$$

Using Eqs. (2.100) and (2.93), we obtain

$$B_3 = j \frac{\mu_o \eta_1}{\mu_{1x} \eta_3} \alpha_{\nu n} \frac{\sinh \eta_1 d_1}{H_c(\nu)} (\cosh \gamma d_2 \cdot \sinh \eta_3 d_2$$

$$- \frac{\mu_o \gamma}{\mu_{2x} \eta_3} \sinh \gamma d_2 \cosh \eta_3 d_2) \bar{J}_1 \quad . \tag{2.104}$$

Once the arbitrary constants are determined, the electric field intensity in the different regions can be determined. The electric field intensity component, $\bar{E}_1$, in region 1, is obtained by substituting Eq. (2.101) into Eq. (2.85) to obtain:

$$\bar{E}_1 = j \alpha_{\nu n} (\frac{g_1(\nu)}{H_c(\nu)} \cosh \eta_1 (a_t - y) - 1) \bar{J}_1 \tag{2.105}$$

where $a \leqq y \leqq a_t$. The electric intensity component, $\bar{E}_2$, in the secondary conductive region, can be obtained by substituting Eq. (2.102) into Eq. (2.87):

$$\bar{E}_2 = j \frac{\mu_o \eta_1}{\mu_{1x} \eta_3} \frac{\sinh \eta_1 d_1}{H_c(\nu)} \alpha_{\nu n} S_{\nu n} \cosh \gamma y \bar{J}_1 \tag{2.106}$$

where $0 \leqq y \leqq d_2$. Finally, the electric field intensity component, $\bar{E}_3$, in the air-gap region, can be obtained by substituting Eqs. (2.103) and (2.104) into Eq. (2.71):

$$\bar{E}_3 = j \frac{\mu_o \eta_1}{\mu_{1x} \eta_3} \frac{\sinh \eta_1 d_1}{H_c(\nu)} \alpha_{\nu n} [\cosh \gamma d_2 \cosh \eta_3 (y-d_2)$$

$$+ \frac{\gamma \mu_o}{\eta_3 \mu_{2x}} \sinh \gamma d_2 \sinh \eta_3 (y-d_2)] \bar{J}_1 \quad . \tag{2.107}$$

Equations (2.105) through (2.107) give the expressions of the electric intensity components $\bar{E}_1$, $\bar{E}_2$ and $\bar{E}_3$ in the primary, the secondary and the air-gap regions, respectively. As a check, we can easily see that $\bar{E}_1$, $\bar{E}_2$ and $\bar{E}_3$ satisfy the boundary conditions given by Eqs. (2.78) through (2.83).

Other field expressions can be derived using Eqs. (2.9) - (2.11) for stationary media, and Eqs. (2.12) - (2.14) for moving media. Since the expressions of all the field components should be in the form given by Eq. (2.50), then Eqs. (2.9) and (2.11) can be expressed in terms of the Fourier coefficients (the bar quantities) by

$$\bar{H}_x = \frac{-1}{jn\omega\mu_x} \frac{\partial \bar{E}}{\partial y} \tag{2.108}$$

and

$$\bar{H}_y = \frac{\nu\pi/t}{n\omega\mu_y} \bar{E} \quad . \tag{2.109}$$

Similarly, Eqs. (2.12) and (2.13) will yield

$$\bar{H}_x = \frac{-1}{jn\omega S_{\nu n}\mu_x} \frac{\partial \bar{E}}{\partial y} \tag{2.110}$$

and

$$\bar{H}_y = \frac{\nu\pi/\tau}{n\omega S_{\nu n}\mu_y}\bar{E} \quad . \tag{2.111}$$

Equations (2.108) through (2.111) are sufficient to determine the magnetic field components $\bar{H}_x$, $\bar{H}_y$ in the different regions of the motor.

2. Overhang regions

Referring to Figure 2.3, the overhang regions are those of zone II that constitute regions 4 and 5. The electric intensity in these regions is given by Eqs. (2.74) and (2.75). The boundary conditions of these regions are given by Eqs. (2.39) through (2.42). These equations can be expressed in terms of the Fourier coefficients of Eqs. (2.74) and (2.75), which will take the form:

$$[\frac{\partial\bar{E}_4}{\partial y}]_{y=a_t} = 0 \tag{2.112}$$

$$[\frac{\partial\bar{E}_4}{\partial y}]_{y=a} = [\frac{\partial\bar{E}_5}{\partial y}]_{y=a} \tag{2.113}$$

$$[\bar{E}_4]_{y=a} = [\bar{E}_5]_{y=a} \tag{2.114}$$

$$[\frac{\partial\bar{E}_5}{\partial y}]_{y=-\infty} = 0 \quad . \tag{2.115}$$

Equations (2.74) and (2.77) should satisfy Eqs. (2.112) - (2.115), which provide the necessary equations to determine the arbitrary constants A_4,

B_4, A_5 and B_5. Equation (2.115) requires

$$B_5 = 0 \quad . \tag{2.116}$$

Then, the expression of $\bar{E}_5$ will be given by

$$\bar{E}_5 = A_5 \, e^{\eta_3 y} \quad . \tag{2.117}$$

Substituting Eqs. (2.74) and (2.117) into Eqs. (2.112) - (2.114), we can get the following equations:

$$A_4 \sinh\eta_3 a_t + B_4 \cosh\eta_3 a_t = 0 \tag{2.118}$$

$$A_3 \sinh\eta_3 a + B_4 \cosh\eta_3 a - A_5 \, e^{\eta_3 a} = 0 \tag{2.119}$$

$$A_4 \cosh\eta_3 a + B_4 \sinh\eta_3 a - A_5 \, e^{\eta_3 a} = \frac{jn\omega\mu_o}{\eta_3} \bar{J}_1 \quad . \tag{2.120}$$

We can follow the same procedure, as given in the previous section, to obtain the arbitrary constants A_4, B_4 and A_5. The final expressions will take the following forms:

$$A_4 = j \frac{\mu_o \, n\omega \cosh\eta_3 a_t}{\eta_3(\cosh\eta_3 d_1 + \sinh\eta_3 d_1)} \bar{J}_1 \tag{2.121}$$

$$B_4 = - \tanh \eta_3 a_t \, A_4 \tag{2.122}$$

$$A_5 = -j \frac{\mu_o n\omega \sinh\eta_3 d_1 \, e^{-a\eta_3}}{\cosh\eta_3 d_1 + \sinh\eta_3 d_1} \bar{J}_1 \quad . \tag{2.123}$$

Substituting Eqs. (2.121) - (2.123) into Eq. (2.74) and (2.117), the Fourier coefficient of the field components will take the form:

$$\bar{E}_4 = j \frac{\mu_o n\omega}{\eta_3} \left(\frac{\cosh(a_t - y)\eta_3}{\cosh\eta_3 d_1 + \sinh\eta_3 d_1} - 1 \right) \bar{J}_1 \tag{2.124}$$

$$\bar{E}_5 = - j \frac{\mu_o n\omega \sinh\eta_3 d_1 \, e^{(y-a)\eta_3}}{\cosh \eta_3 d_1 + \sinh \eta_3 d_1} \bar{J}_1 \quad . \tag{2.125}$$

Once we have the expressions of the electric intensity in regions 4 and 5, other magnetic components in these two regions can be derived using Eqs. (2.108) and (2.109).

G. Voltage Equations

So far, the field equations have been solved in terms of the primary current of the machine. In the constant voltage drive system, the applied voltages are known quantities, and it is required to get the machine currents in order to determine the machine performance. So, our task now is to write down the voltage equations for the different machine phases, and then solve these equations to get the machine currents.

The voltage induced in the primary winding is due to the electric intensity in both the primary region 1 and the overhang region 4. If we consider only a single harmonic of space order ν, and time order n,

acting on the primary winding, then the voltage, $V_{n\nu}$, induced per phase due to this harmonic component will be given by

$$V_{n\nu} = -\int_{\substack{\text{primary}\\\text{width}}} NK_w^* \bar{E}_1 e^{j\frac{\nu\pi}{\tau}X_o} dZ - \int_{\substack{\text{overhang}\\\text{width}}} N K_w^* \bar{E}_4 e^{j\frac{\nu\pi}{\tau}X_o} d_z \quad (2.126)$$

where

N = the total number of conductors per phase of the machine ($P*N_p$),

K_w^* = the complex conjugate of the winding factor K_w, as defined by Eq. (2.45), and

X_o = the arbitrary distance measured from the origin to the first coil side of the phase under consideration.

It is evident from Eqs. (2.105) and (2.124) that $\bar{E}_1$ and $\bar{E}_4$ are independent of the z-coordinate. Then, Eq. (2.126) will take the form

$$V_{n\nu} = -N K_w^* [W_1\bar{E}_1 + W_o\bar{E}_4] e^{j\frac{\nu\pi}{\tau}X_o} \quad (2.127)$$

where W_1 is the primary iron width and W_o is the total overhang width (see Figure 2.3). Summing the voltage induced in the primary winding, due to all the space harmonic components of the electric intensity, the resulting voltage, V_n, will be given by

$$V_n = -N \sum_{\nu=-\infty}^{\infty} K_w^* (W_1\bar{E}_1 + W_o\bar{E}_4) e^{j\frac{\nu\pi}{\tau}X_o} . \quad (2.128)$$

Substituting the expressions of $\bar{E}_1$ and $\bar{E}_4$, as given by Eqs. (2.105) and (2.124), into Eq. (2.128), the resulting equation can take the form

$$V_n = -N \sum_{\nu=-\infty}^{\infty} G(\nu,y) K_w^* \bar{J}_1 \, e^{j \frac{\nu\pi}{\tau} X_o} \tag{2.129}$$

where

$$G(\nu,y) = j \, W_1 \alpha_{\nu n} \left[\frac{g_1(\nu)}{H_c(\nu)} \cosh\eta_1 \, (a_t - y) - 1\right]$$

$$+ j \, W_o \frac{\mu_o \eta \omega}{\eta_3} \left[\frac{\cosh\eta_3 \, (a_t - y)}{\cosh\eta_3 d_1 + \sinh\eta_3 d_1} - 1\right] \, . \tag{2.130}$$

Substituting the expression of $\bar{J}_1$, as given by Eq. (2.44), into Eq. (2.129), we obtain

$$V_n = -a_n \frac{NN_p}{2t} \sum_{\nu=-\infty}^{\infty} G(\nu,y) \, K_w K_w^* \left[I_1 + I_2 \, e^{-j \frac{2\pi}{3} \nu}\right.$$

$$\left. + I_3 \, e^{-j \frac{4\pi}{3} \nu}\right] e^{j \frac{\nu\pi}{t} X_o} \, . \tag{2.131}$$

Equation (2.131) gives the voltage induced per phase of the machine, at any plane y, due to all space harmonics ν, and a single time harmonic of order n (a_n=1, corresponding to the fundamental harmonic component). It is evident that the voltage given by Eq. (2.131) is a function of y, as the electric intensity is varying with the coordinate

y. The terminal phase voltage will be the average value of Eq. (2.131). This average value is defined by

$$V_{ph} = \frac{1}{d_1} \int_{a}^{a_t} v_n \, dy \quad . \tag{2.132}$$

Substituting Eq. (2.131) into Eq. (2.132) and noting that the expression of $G(\nu,y)$ is given by Eq. (2.130), the final expression of the average voltage induced per phase will be in the form

$$V_{ph} = \sum_{\nu=-\infty}^{\infty} f(\nu) \left[I_1 + I_2 e^{-j\frac{2\pi}{3}\nu} + I_3 e^{-j\frac{4\pi}{3}\nu}\right] e^{j\frac{\nu\pi}{\tau}X_o} \tag{2.133}$$

where

$$f(\nu) = j\, a_n \frac{NN_p}{2\tau} K_w K_w^* \left[W_1 \alpha_{\nu n}\left(1 + \frac{g_1(\nu)}{H_c(\nu)} \frac{\sinh\eta_1 d_1}{\eta_1 d_1}\right)\right.$$

$$\left. + W_o \frac{\mu_o n \omega}{\eta_3}\left(1 + \frac{\sinh\eta_1 d_1/\eta_1 d_1}{\cosh\eta_3 d_1 + \sinh\eta_1 d_1}\right)\right] \quad . \tag{2.134}$$

Once we obtain the voltage induced in an arbitrary phase of the machine, the voltage equations for the different phases can be developed as follows.

For Phase I, $X_o = 0$. Let the phase resistance equal R_1 and the applied voltage equal V_1. The applied voltage, V_1, will be balanced with the voltage induced per phase, plus the IR drop in the phase. Using Eq. (2.133) with $X_o = 0$, as given above, the voltage equation will

take the form

$$I_1R_1 + \sum_{\nu=-\infty}^{\infty} f(\nu)\left[I_1 + I_2 e^{-j\frac{2\pi}{3}\nu} + I_3 e^{-j\frac{4\pi}{3}\nu}\right] = V_1 \quad . \quad (2.135)$$

For Phase II:

$$X_o = 2\tau/3 \ .$$

Let the phase resistance equal R_2 and the applied voltage equal V_1. Then, as above, the voltage equation will take the form

$$I_2R_2 + \sum_{\nu=-\infty}^{\infty} f(\nu)\left[I_1 + I_2 e^{-j\frac{2\pi}{3}\nu} + I_3 e^{-j\frac{4\pi}{3}\nu}\right] e^{j\frac{2\pi}{3}\nu} = V_2 \ . \quad (2.136)$$

For Phase III:

$$X_o = 4\tau/3 \ .$$

Let the phase resistance equal R_3 and the applied voltage equal V_3. Then, in a similar procedure as given above, the voltage equation will take the form

$$I_3R_3 + \sum_{\nu=-\infty}^{\infty} f(\nu)\left[I_1 + I_2 e^{-j\frac{2\pi}{3}\nu} + I_3 e^{-j\frac{4\pi}{3}\nu}\right] e^{j\frac{4\pi}{3}\nu} = V_3 \ . \quad (2.137)$$

Equations (2.135) through (2.137) are the voltage equations of the different phases of the machine, required to get the phase currents. Equations (2.135) through (2.137) can be rearranged and written in the following matrix form:

$$\begin{bmatrix} R_1 + \sum_{\nu=-\infty}^{\infty} f(\nu) & \sum_{\nu=-\infty}^{\infty} f(\nu)e^{-j\frac{2\pi}{3}\nu} & \sum_{\nu=-\infty}^{\infty} f(\nu)e^{-i\frac{4\pi}{3}\nu} \\ \sum_{\nu=-\infty}^{\infty} f(\nu)e^{j\frac{2\pi}{3}\nu} & R_2 + \sum_{\nu=-\infty}^{\infty} f(\nu) & \sum_{\nu=-\infty}^{\infty} f(\nu)e^{-i\frac{2\pi}{3}\nu} \\ \sum_{\nu=-\infty}^{\infty} f(\nu)e^{j\frac{4\pi}{3}\nu} & \sum_{\nu=-\infty}^{\infty} f(\nu)e^{j\frac{2\pi}{3}\nu} & R_3 + \sum_{\nu=-\infty}^{\infty} f(\nu) \end{bmatrix} \begin{bmatrix} I_1 \\ I_2 \\ I_3 \end{bmatrix} = \begin{bmatrix} V_1 \\ V_2 \\ V_3 \end{bmatrix}$$

(2.138)

Equation (2.138) permits the representation of unbalanced voltage operations, as well as fault conditions, as the voltages V_1, V_2 and V_3 are quite arbitrary values. The entries of the coefficient matrix are the self and the mutual impedances of the different phases of the machine. Once we solve Eq. (2.138) for the phase currents, the field components in the different regions can be obtained, and hence, the machine performance can be fully predicted.

H. Force and Power Expressions

1. Force expressions

The force, $\vec{dF}$, acting on a current carrying conductor, $Id\vec{S}$, placed in a magnetic field of magnetic induction, $\vec{B}$, is given in magnitude and direction by the following cross product:

$$\vec{dF} = I\, d\vec{S} \times \vec{B} \quad . \tag{2.139}$$

In our case I is given by $(J_1 d_x d_y)$ and is in the z-direction, so that dS will be equal to dz. To get the force component in the x-direction, B will be substituted by B_{1y} in the primary region 1, and B_{4y} in the primary overhang region 4. Denoting this force component by dF_x, its expression will take the form

$$dF_x = -J_1(B_{1y} + B_{4y})\,dxdydz \quad . \tag{2.140}$$

The negative sign is introduced to make the force positive in the positive x-direction. It is evident that dxdydz is the elementary volume, $\delta_{vol.}$, occupied by the current. If we denote the total force developed by the motor in the x-direction by F_x, then its value can be derived from the integration of Eq. (2.140) over the whole volume occupied by the primary current, i.e.,

$$F_x = -\iiint_{\text{reg. 1}} J_1 B_{1y}\,dxdydz - \iiint_{\text{reg. 4}} J_1 B_{4y}\,dxdydz \quad . \tag{2.141}$$

Since J_1, B_{1y} and B_{4y} are independent of the z-coordinate, the integration with respect to the z-coordinate can be simply replaced by the multiplication by the primary width, W_1, for the first term, and the multiplication by the overhang width, W_o, for the second term of Eq. (2.141).

Recall that J_1, as well as the field components, has the form given by Eq. (2.50), where their harmonic components are now fully defined. Therefore, on replacing J_1, B_{1y} and B_{4y} by their series forms and taking the average, first, with respect to time, and then integrating with respect to x and y, the resulting force expression will take the form

$$F_x = -\frac{1}{2}(2\tau P)\,\mathrm{Re}\sum_{n=1}^{\infty}\sum_{\nu=-\infty}^{\infty}(W_1\bar{B}_{1y} + W_o\bar{B}_{4y})\bar{J}_L^* \qquad (2.142)$$

where

$\bar{J}_L$ = the linear current density defined by $(\bar{J}_1 d_1)$,

$*$ = the conjugate of the complex quantity, and

$\bar{B}_{1y}$, $\bar{B}_{4y}$ = the average values of the y-components of the magnetic inductions as given by Eq. (2.109) with $\bar{E}_1$ replacing $\bar{E}$ for $\bar{B}_{1y}$ and $\bar{E}_4$ replacing $\bar{E}$ for $\bar{B}_{4y}$, i.e.,

$$\bar{B}_{1y} = -j\,\frac{(\nu\pi/\tau)}{n\omega}\,\alpha_{\nu n}\left(\frac{g_1(\nu)}{H_c(\nu)}\,\frac{\sinh\eta_1 d_1}{\eta_1 d_1} + 1\right)\bar{J}_1 \qquad (2.143)$$

$$\bar{B}_{4y} = -j\,\mu_o\left(\frac{\sinh\eta_3 d_1/\eta_3 d_1}{\cosh\eta_3 d_1 + \sinh\eta_3 d_1}\right) + 1) \quad . \qquad (2.144)$$

The normal force expressions can be derived in a similar way as above, with $\bar{B}_{1x}$ and $\bar{B}_{4x}$ substituted for $\bar{B}_{1y}$ and $\bar{B}_{4y}$ in Eq. (2.142). However, this force is of less importance in the theory of rotating machines.

2. Power expressions

The flow of electromagnetic power through a closed surface is obtained from the surface integral of the time instantaneous quantity

$$\vec{P} = \vec{E} \times \vec{H} \tag{2.145}$$

where $\vec{P}$ is the Poynting vector. The ingoing power-flux over the surface S, assuming that the element of surface area $d\vec{s}$ is outward directed, is given by

$$- \iint_S \vec{P} \cdot d\vec{s} \quad . \tag{2.146}$$

Using the above definition as well as the divergence theorem and Maxwell's field equations, we can expand Eq. (2.146) as follows:

$$\begin{aligned} - \iint_S \vec{P} \cdot d\vec{s} &= - \iiint_V \nabla \cdot (\vec{E} \times \vec{H}) dv \\ &= \iiint_V (\vec{E} \cdot \nabla \times \vec{H} - \vec{H} \cdot \nabla \times \vec{E}) dv \\ &= \iiint_V [\vec{E} \cdot (\vec{J} + \partial \vec{D}/\partial t) - \vec{H} \cdot (-\partial \vec{B}/\partial t)] dv \\ &= \iiint_V (\vec{E} \cdot \partial \vec{D}/\partial t + \vec{H} \cdot \partial \vec{B}/\partial t) dv + \iiint_V \vec{E} \cdot \vec{J} \, dv \end{aligned}$$

i.e.,

$$- \iint_S \vec{P} \cdot d\vec{s} = \frac{\partial}{\partial t} \iiint \left(\frac{1}{2} \vec{E} \cdot \vec{D} + \frac{1}{2} \vec{H} \cdot \vec{B}\right) dv + \iiint_V \vec{E} \cdot \vec{J} \, dv \quad . \tag{2.147}$$

The first term on the right-hand side is the time rate of increase of the electromagnetic energy, and the second term is the total dissipated power ($\vec{E}$ and $\vec{J}$ are in the same directions) or generated power ($\vec{E}$ and $\vec{J}$ are in opposite directions) in the system. Equation (2.147) is the Poynting Theorem.

Now, Eq. (2.147) can be applied to our case, but in the opposite sense, viz., the increase in the electromagnetic energy plus the energy dissipated in the system is equal to

$$- \iint_S \vec{P} \cdot d\vec{s} \quad . \tag{2.148}$$

Note that the closed surface S is composed of the cylindrical surface of length $2\tau P$, as well as the circular area closing this cylinder on the sides. According to our assumption regarding the field components,

$$\vec{P} = \vec{E} \times \vec{H}$$

$$= - E_z H_y \vec{i} + E_z H_x \vec{j} \quad . \tag{2.149}$$

The expression of $d\vec{s}$ will be:

over the cylindrical surface,

$$ds = dxdy\ \vec{j} \quad , \tag{2.150}$$

over the circular sides,

$$ds = \pm\ dxdy\ \vec{K} \quad . \tag{2.151}$$

Using Eqs. (2.149) through (2.151) to form the surface integral given by Eq. (2.148), yields:

$$- \iint_S \vec{P} \cdot \vec{ds} = - \iint E_z H_x\ dxdy \quad . \tag{2.152}$$

Since both E_z and H_x are independent of the z-coordinate, then the integration with respect to the z-coordinate will be replaced by the multiplication by the field width. The left-hand side of Eq. (2.152) will be the secondary input power, P_{sec}, if E_z and H_x are the values of the fields at the boundary between the air gap and the primary region. Thus, we can write

$$P_{sec} = - W_1 \int_0^{2\tau P} [E_z H_x]_{\substack{y=a \\ \text{zone I}}} dx - W_o \int_0^{2\tau P} [E_z H_x]_{\substack{y=a \\ \text{zone II}}} dx \quad . \tag{2.153}$$

Equation (2.153) is similar to Eq. (2.141) (note that the integration of Eq. (2.141) with respect to z and y means the multiplication by the field width, and replacing the field components B by their average values). Then, we can follow the same procedures given in the previous section to show that the secondary input will be given by

$$P_{sec} = -\frac{1}{2}(2\tau P)\ \mathrm{Re} \sum_{n=1}^{\infty} \sum_{\nu=-\infty}^{\infty} (W_1 E_{1z} + W_0 E_{4z})\bar{J}_L^* \qquad (2.154)$$

where E_{1z} and E_{4z} are the harmonic components of the electric intensity at the boundary surface between regions 3 and 1, and between regions 4 and 5.

This secondary power includes all the secondary losses, mechanical losses, stray losses, as well as the mechanical output of the machine. The input power to the motor is simply given by

$$P_{in} = \mathrm{Re} \sum_{r=1} V_r I_r^* \qquad (2.155)$$

where V_r (r=1,2,3) are the applied voltages to the motor and I_r^* (r=1,2, 3) are the complex conjugate of the motor currents.

Equations (2.142), (2.154) and (2.155) are those required to predict the machine performance, in terms of its design parameters.

I. Conclusion

In this chapter, the electromagnetic theory of induction motors has been developed. The theory is based on a five-region model consisting of primary, secondary, air gap, overhang and air overhang regions. The basic field equations in each region have been derived from Maxwell's field equations. The additional constraint field equations arising from the secondary end rings are also derived. The resulting field equations form a system of elliptic partial differential equations. This system has been solved simultaneously to obtain the field expressions in each individual region. The solution is developed from its most general approach. It includes both the whole space and time harmonics which can act on the motor. The motor force and power expressions have been derived also. This permits the prediction of the motor performance, as well as the determination of the effects of the motor parameters on its performance.

III. WAVE IMPEDANCE CONCEPT FOR SOLVING THE FIELD PROBLEM IN INDUCTION MOTORS

A. Introduction

In the previous chapter, the solution of Maxwell's equation for a five-region mathematical model of an induction motor has been developed. The model replaces the practical toothed structure of the stator and rotor by continuous, though inhomogeneous, regions having appropriately averaged resistivities, and different permeabilities in directions parallel to, and perpendicular to, the air gap. The effect of the end winding is taken into account in the analysis. In general, the analysis given in the previous chapter is lengthy and needs simplification without substantial sacrifice of details.

The purpose of this chapter is to present a simplified electromagnetic theory of the induction motor, using the concept of wave impedance. A different mathematical model has been developed to widen the scope of the work, and to study the effect of more parameters on the motor performance.

For simplicity, the end effects of the motor are neglected in the mathematical model considered, while the tooth top of the motor secondary has been added (see Figures 3.1a and 3.1b). Thus, the new model permits studying the effect of the secondary tooth top, as well as the zigzag leakage flux, on the performance of the induction motor.

Figure 3.1b shows that the stationary frame of reference is chosen to coincide with the lower surface of the secondary slot region. Regions 1 and 2 are the slot and tooth-top regions of the motor

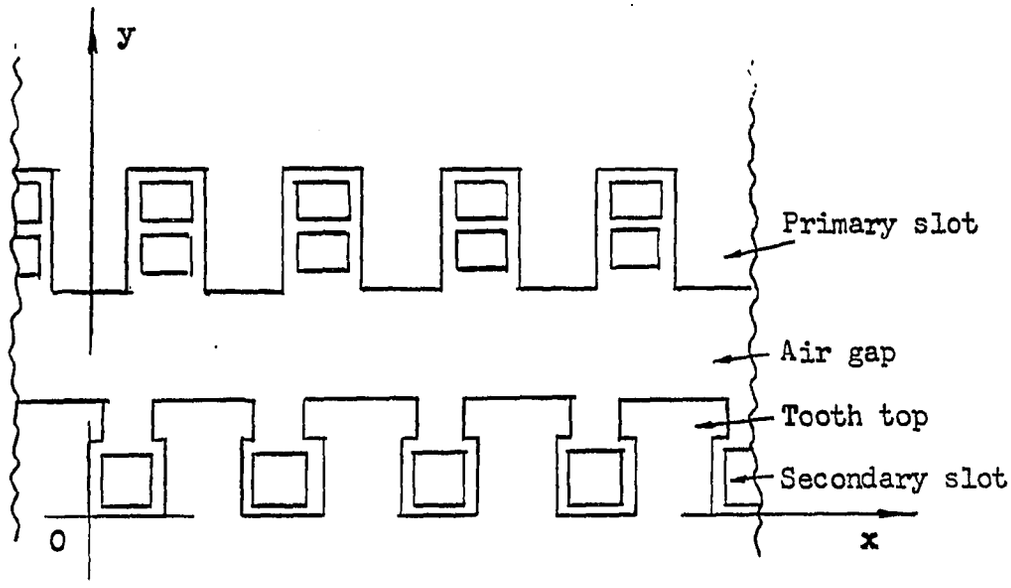

Figure 3.1a. Part of the developed slotted structure of the induction motor

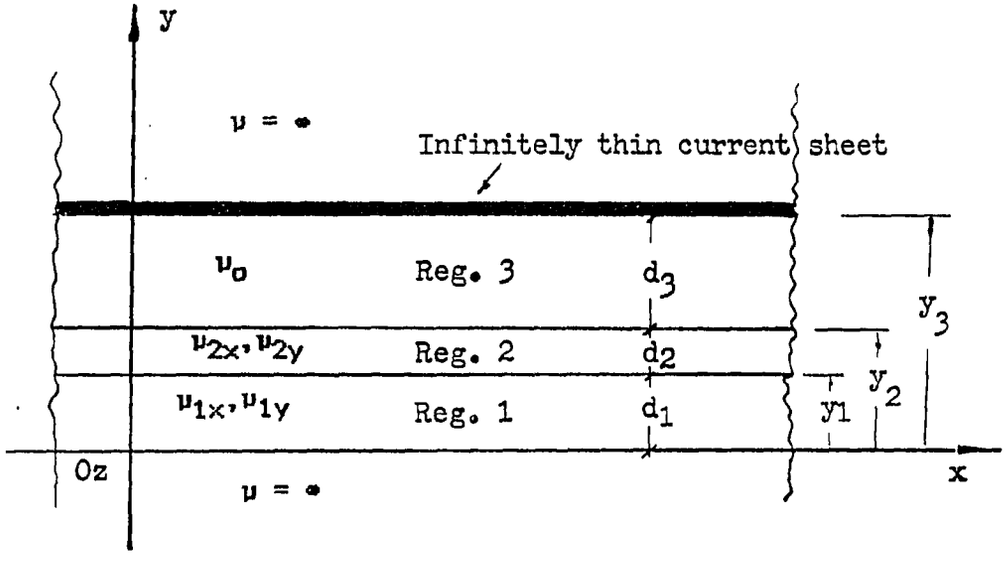

Figure 3.1b. The equivalent anisotropic magnetic regions 1, 2 and 3

secondary (the rotor). Tooth regions 1 and 2 are moving with the same speed, V, with respect to the stationary frame of reference. The air gap region 3 is a stationary region. The primary current is approximated by an infinitely thin current sheet of linear density, J_L. The toothed structure of the secondary part is replaced, as before, by inhomogeneous regions having different permeabilities in the x and y directions as shown. The average conductivity of the secondary region 1 is z-direction, while the conductivity of other regions is zero. The permeabilities of both the secondary and primary iron yokes are considered to be infinitely large.

B. Field Analysis

Following the same steps as given in Chapter II, Section C, Maxwell's equations in region 1 are given by

$$\partial E_1/\partial y = - \mu_{1x} (\partial H_{1x}/\partial t + v \partial H_{1x}/\partial x) \tag{3.1}$$

$$\partial E_1/\partial x = \mu_{1y} (\partial H_{1y}/\partial t + v \partial H_{1y}/\partial x) \tag{3.2}$$

$$\partial H_{1y}/\partial x - \partial H_{1x}/\partial y = \sigma_1 E_1 \quad . \tag{3.3}$$

Assume all the field components have the functional form previously given by Eq. (2.50), i.e., they vary with x and t as $e^{j(\nu\pi/\tau\, x + n\omega t)}$. Therefore, in Eqs. (3.1) - (3.3), we can substitute

$jn\omega$ for $\partial/\partial t$, and $j\nu\omega/t$ for $\partial/\partial x$, to get

$$\partial \bar{E}_1/\partial y = -jS_{\nu n} n\omega\mu_{1x} \bar{H}_{1x} \tag{3.4}$$

$$(j\nu\pi/t)\ \bar{E}_1 = jS_{\nu n} n\omega\mu_{1y} \bar{H}_{1y} \tag{3.5}$$

$$(j\nu\pi/t)\ \bar{H}_{1y} - \partial \bar{H}_{1x}/\partial y = \sigma_1 \bar{E}_1 \quad . \tag{3.6}$$

In these equations, $\bar{E}_1$, $\bar{H}_{1x}$ and $\bar{H}_{1y}$ are the Fourier coefficients of E_1, H_{1x} and H_{1y}, respectively, as explained in Chapter II, Section E.1. Eliminating $\bar{H}_{1y}$ between Eqs. (3.5) and (3.6), we get

$$\partial \bar{H}_{1x}/\partial y = -\left(\sigma_1 + \frac{(\nu\pi/t)^2}{jS_{\nu n} n\omega\mu_{1y}}\right) \bar{E}_1 \quad . \tag{3.7}$$

If a solution of Eqs. (3.4) and (3.7) for $\bar{E}_1$ can be found, the problem is solved, for $\bar{H}_{1y}$ can easily be found from $\bar{E}_1$ using Eq. (3.5). Thus, Eqs. (3.4) and (3.7) are the basic equations. Their solution is easily found by making use of the wave impedance concept and employing a transmission-line analog. Corresponding quantities in the analog are most easily seen by setting out the relevant equations side by side, as Booker [12] has done in dealing with other electromagnetic problems.

Induction motor	Transmission line
$\frac{\partial \bar{E}_1}{\partial y} = - (jS_{\nu n} n\omega\mu_{1x})\ \bar{H}_{1x}$	$\frac{\partial V}{\partial y} = - Z_1 I$
$\frac{\partial \bar{H}_{1x}}{\partial y} = - (\sigma_1 + \frac{(\nu\pi/\tau)^2}{jS_{\nu n} n\omega\mu_{1y}})\ \bar{E}_1$	$\frac{\partial I}{\partial y} = -Y_1 V$

There is clearly a one-to-one correspondence between the following quantities:

$$\begin{aligned} \bar{E}_1 &\rightarrow V \\ \bar{H}_{1x} &\rightarrow I \\ jS_{\nu n} n\omega\mu_{1x} &\rightarrow Z_1 \\ \sigma_1 + \frac{(\nu\pi/\tau)^2}{jS_{\nu n} n\omega\mu_{1y}} &\rightarrow Y_1 \end{aligned} \qquad (3.8)$$

Since Z and Y represent respectively the series impedance and shunt admittance per unit length of the transmission line, we can construct for the induction motor a transmission line equivalent circuit which represents exactly the relationship between $\bar{E}_1$ and $\bar{H}_{1x}$ in region 1. An elementary section of this line is shown in Figure 3.2. The expressions for the characteristic wave impedance Z_{01} and the propagation factor γ_1 for the y-direction can be written by analogy:

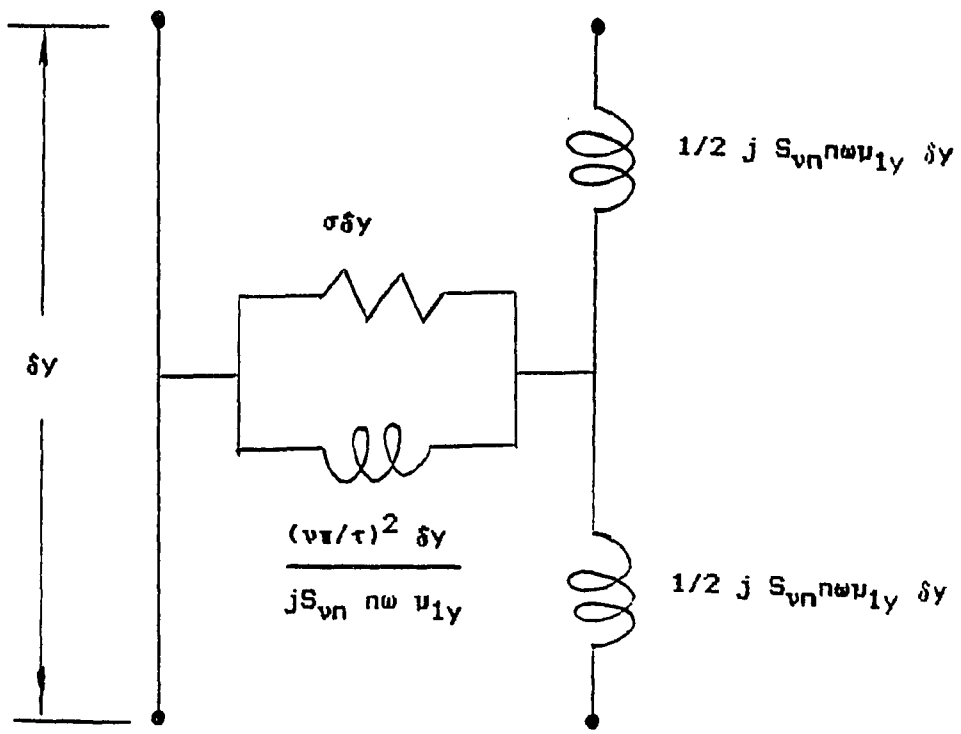

Figure 3.2. Element of equivalent circuit of induction motor or transmission line

$$Z_{01} = \sqrt{\frac{Z}{Y}} = \sqrt{\left[\frac{jS_{\nu n}^{n\omega\mu_{1x}}}{\sigma_1 + \frac{(\nu\pi/\tau)^2}{jS_{\nu n}^{n\omega\mu_{1y}}}}\right]} \tag{3.9}$$

$$\gamma_1 = \sqrt{ZY} = \sqrt{\left[jS_{\nu n}^{n\omega\mu_{1x}}(\sigma_1 + \frac{(\nu\pi/\tau)^2}{jS_{\nu n}^{n\omega\mu_{1y}}})\right]} \quad . \tag{3.10}$$

The subscript '1', as stated previously, refers to region 1.

By exactly the same argument, we can set up a transmission-line model for region 2. The characteristic wave impedance Z_{02} and the propagation factor γ_2 can be obtained from Eqs. (3.9) and (3.10) by replacing μ_{1x} with μ_{2x}, μ_{1y} with μ_{2y}, and putting $\sigma_1 = 0$. This gives

$$Z_{02} = j \frac{S_{\nu n}^{n\omega}}{(\nu\pi/\tau)} \sqrt{\mu_{2x}\mu_{2y}} \tag{3.11}$$

$$\gamma_2 = (\nu\pi/\tau)\sqrt{\frac{\mu_{2x}}{\mu_{2y}}} \quad . \tag{3.12}$$

In order to complete the analogy, we must consider the boundary conditions. Referring to Figure 3.1b at the interface A between regions 1 and 2, both the electric and magnetic intensities must be continuous. This implies that the Fourier coefficients must be equal also, i.e.,

$$\bar{E}_A^+ = \bar{E}_A^-$$

$$\bar{H}_{Ax}^+ = \bar{H}_{Ax}^- \qquad (3.13)$$

where the superscripts '+' and '-' denote just above and below the interface A. Thus, in the analog, V and I must be continuous at the junction of the two dissimilar transmission lines representing regions 1 and 2. This continuity follows from Kirchhoff's laws.

In region 0, H_x must be zero everywhere since the permeability is infinite. In particular,

$$H_{0x} = 0 \qquad (3.14)$$

at the boundary between region 1 and 0. In the analog, we must have I = 0 at the corresponding point. The transmission line for region 1 is, therefore, open-circuited at the corresponding end. The open circuit condition can alternatively be obtained by noting that since $\mu = \infty$ in region 0, the associated characteristic wave impedance is infinite, and this is the 'termination' of region 1.

Similarly, we can set up a transmission-line model for region 3, the air gap region. The characteristic wave impedance Z_{03} and the propagation factor γ_3 can be obtained from Eqs. (3.9) and (3.10) by putting $\mu_{2x} = \mu_{2y} = \mu_0$, $\sigma_1 = 0$ and $S_{\nu n} = 1$. This gives

$$Z_{03} = j \frac{n\omega\mu_0}{(\nu\pi/\tau)} \tag{3.15}$$

$$\gamma_3 = \nu\pi/\tau \quad . \tag{3.16}$$

Referring to Figure 3.1b, at the interface B, the magnetic induction, as well as the magnetic intensity, must be continuous. This implies that the Fourier coefficients must be equal also:

$$\begin{aligned} \bar{B}_{By}^{+} &= \bar{B}_{By}^{-} \\ \bar{H}_{Bx}^{+} &= \bar{H}_{Bx}^{-} \end{aligned} \quad . \tag{3.17}$$

The first equation of Eq. (3.16) can be expressed in terms of the electric intensity, noting that $\bar{B}_{By}^{+}$ lies in the air gap, i.e., a stationary region, and $\bar{B}_{By}^{-}$ lies in the tooth-top region, i.e., a moving region. Faraday's laws of induction for moving regions are given by Eqs. (3.1) and (3.2), and for stationary regions, the same equations hold with $\nu = 0$. Thus, we can use Eq. (3.2) to express the magnetic induction in terms of the electric intensity, and Eq. (3.17) will take the form

$$\begin{aligned} \bar{E}_B^{+} &= S_{\nu n}\bar{E}_B \\ \bar{H}_{Bx}^{+} &= \bar{H}_{Bx}^{-} \end{aligned} \quad . \tag{3.18}$$

Ampere's circuital law,

$$\oint \vec{H} \cdot \vec{dS} = \iint_S \vec{J} \cdot \vec{dA} \tag{3.19}$$

can be applied at the interface C, between regions 3 and 4. This gives the following relations between the Fourier coefficients:

$$\bar{H}_{cx}^{-} = \bar{J}_L \tag{3.20}$$

where $\bar{J}_L$ represents the Fourier coefficient of the linear current density of the primary winding.

Figure 3.3 shows the transmission-line analog of the interaction regions of the induction motor. The figure also shows the boundary conditions at each junction or interface between the different regions.

C. Solution of the Field Equations

As described in the previous section, the field equations have the transmission line form in each region of the induction motor, with their relevant expressions of the characteristic impedance Z_0 and the propagation factor γ.

In region 1, the field equations, in terms of the Fourier coefficient, are given by

TRANSMISSION LINE ANALOGY

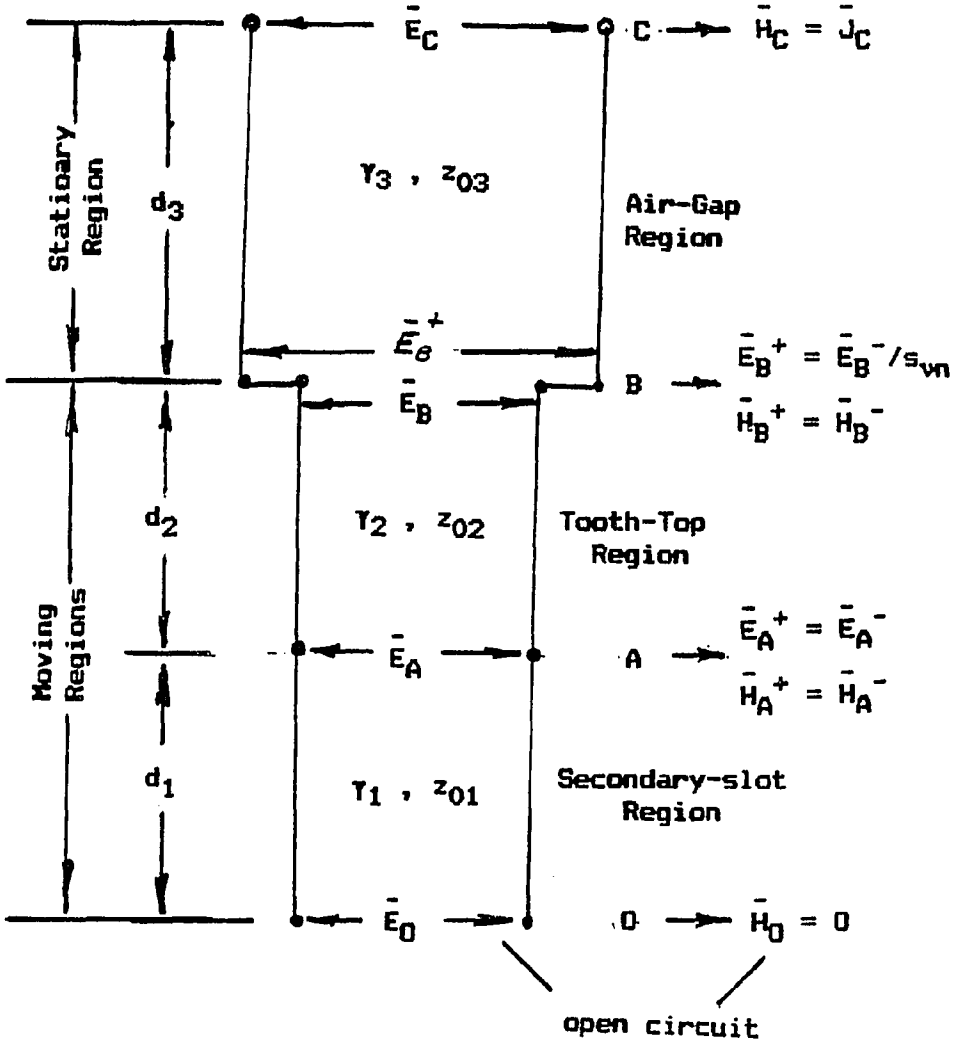

Figure 3.3. Transmission line analogy of the different regions of the induction motor and the boundary conditions at the different sections

$$\partial \bar{E}_1/\partial y = - Z_1 \bar{H}_{1x}$$

$$\partial \bar{H}_{1x}/\partial y = - Y_1 \bar{E}_1 \qquad (3.21)$$

where Z_1 and Y_1 are given by Eq. (3.8). According to the chosen system of coordinates, as shown in Figure 3.1b, the solution of the system given by Eq. (3.21) will take the following matrix form:

$$\begin{bmatrix} \bar{E}_A^- \\ \bar{H}_{Ax}^- \end{bmatrix} = \begin{bmatrix} \cosh \gamma_1 d_1 & -Z_{01} \sinh \gamma_1 d_1 \\ -\frac{1}{Z_{01}} \sinh \gamma_1 d_1 & \cosh \gamma_1 d_1 \end{bmatrix} \begin{bmatrix} \bar{E}_0^+ \\ \bar{H}_{0x}^+ \end{bmatrix} \qquad (3.22)$$

where Z_{01} and γ_1 are given by Eqs. (3.9) and (3.10). The subscript A means the field quantity is at the interface A, and 0 has the same meaning at the interface 0.

Equation (3.22) can be rewritten in the following abbreviated form:

$$\begin{bmatrix} \bar{E}_A^- \\ \bar{H}_{Ax}^- \end{bmatrix} = D_1 \begin{bmatrix} \bar{E}_0^+ \\ \bar{H}_{0x}^+ \end{bmatrix} \qquad (3.23)$$

where D_1 is the transfer matrix of region 1, and is given by

$$D_1 = \begin{bmatrix} \cosh \gamma_1 d_1 & -Z_{01} \sinh \gamma_1 d_1 \\ -\frac{1}{Z_{01}} \sinh \gamma_1 d_1 & \cosh \gamma_1 d_1 \end{bmatrix} . \tag{3.24}$$

By exactly the same argument, we can set up the solution of the field quantities in region 2, the tooth-top region, which can be written in the form:

$$\begin{bmatrix} \bar{E}_B^- \\ \bar{H}_{Bx}^- \end{bmatrix} = D_2 \begin{bmatrix} \bar{E}_A^+ \\ \bar{H}_{Ax}^+ \end{bmatrix} \tag{3.25}$$

where the superscripts '-' and '+' denote the values of the field quantities just below and above the interface between the two regions, and D_2 is the region matrix

$$D_2 = \begin{bmatrix} \cosh \gamma_2 d_2 & -Z_{02} \sinh \gamma_2 d_2 \\ -\frac{1}{Z_{02}} \sinh \gamma_2 d_2 & \cosh \gamma_2 d_2 \end{bmatrix} \tag{3.26}$$

where γ_2 and Z_{02} are given by Eqs. (3.11) and (3.12). The boundary conditions at the interface A between regions 1 and 2 are given by Eq. (3.13). Then, on eliminating the column matrix on the right-hand

side of Eq. (3.25) using Eq. (3.13), Eq. (3.25) will take the form:

$$\begin{bmatrix} \bar{E}_B^- \\ \bar{H}_{Bx}^- \end{bmatrix} = D_2 \begin{bmatrix} \bar{E}_A^- \\ \bar{H}_{Ax}^- \end{bmatrix} . \tag{3.27}$$

On eliminating the column matrix on the right-hand side of Eq. (3.27), by using Eq. (3.23), we can write

$$\begin{bmatrix} \bar{E}_B^- \\ \bar{H}_{Bx}^- \end{bmatrix} = D_2 D_1 \begin{bmatrix} \bar{E}_0^+ \\ \bar{H}_{0x}^+ \end{bmatrix} . \tag{3.28}$$

By exactly the same argument, we can set up the solution for the field quantities in the air gap region 3 as:

$$\begin{bmatrix} \bar{E}_C^- \\ \bar{H}_{Cx}^- \end{bmatrix} = D_3 \begin{bmatrix} \bar{E}_B^+ \\ \bar{H}_{Bx}^+ \end{bmatrix} \tag{3.29}$$

where the superscripts '-' and '+' denote the values of the field quantities just below and above the two interfaces C and B, respectively; and D_3 is the region matrix given by

$$D_3 = \begin{bmatrix} \cosh \gamma_3 d_3 & Z_{03} \sinh \gamma_3 d_3 \\ -\frac{1}{Z_{03}} \sinh \gamma_3 d_3 & \cosh \gamma_3 d_3 \end{bmatrix} \tag{3.30}$$

where γ_3 and Z_{03} are given by Eqs. (3.15) and (3.16).

The boundary conditions at the interface B are given by Eq. (3.18). This equation can be rewritten in the following matrix form:

$$\begin{bmatrix} \bar{E}_B^+ \\ \bar{H}_{Bx}^+ \end{bmatrix} = T \begin{bmatrix} \bar{E}_B^- \\ \bar{H}_{Bx}^- \end{bmatrix} \tag{3.31}$$

where the matrix T is given by

$$T = \begin{bmatrix} S_{\nu n} & 0 \\ 0 & 1 \end{bmatrix} . \tag{3.32}$$

The matrix can be called 'The Transition Matrix', as it represents the transition relations between the field quantities at an interface separating moving and stationary regions. It is evident that if the moving region becomes stationary, $S_{\nu n} = 1$, then the transition matrix T becomes the identity matrix I.

Substituting Eq. (3.31) into (3.29) and then, using Eq. (3.28), we get:

$$\begin{bmatrix} \bar{E}_C^- \\ \bar{H}_{Cx}^- \end{bmatrix} = D_3 T D_2 D_1 \begin{bmatrix} \bar{E}_0^+ \\ \bar{H}_{0x}^+ \end{bmatrix} . \tag{3.33}$$

In Eq. (3.33), the entries of the region matrices D_1, D_2, D_3 and T are known quantities. Then, Eq. (3.33) defines the two field components at the boundary C in terms of those at the boundary 0. The two boundary conditions necessary to get any two of the four unknowns, are given by Eqs. (3.14) and (3.20). On substituting Eqs. (3.14) and (3.20) into Eq. (3.33), we can get:

$$\begin{bmatrix} \bar{E}_C^- \\ \bar{J}_L \end{bmatrix} = D_3 T D_2 D_1 \begin{bmatrix} \bar{E}_0^+ \\ 0 \end{bmatrix} . \tag{3.34}$$

Let e_1, e_2, e_3 and e_4 be the entries of the equivalent matrix formed from the product of the four matrices D_1, D_2, D_3 and T; then we can write

$$\begin{bmatrix} \bar{E}_C \\ \bar{J}_L \end{bmatrix} = \begin{bmatrix} e_1 & e_2 \\ e_3 & e_4 \end{bmatrix} \begin{bmatrix} \bar{E}_0^+ \\ 0 \end{bmatrix} . \tag{3.35}$$

The solution of Eq. (3.35) for $\bar{E}_C^-$ and $\bar{E}_0^+$ will yield:

$$\bar{E}_0^{+} = \frac{1}{e_3}\,\bar{J}_L \tag{3.36}$$

$$\bar{E}_C^{-} = \frac{e_1}{e_3}\,\bar{J}_L \quad . \tag{3.37}$$

The Fourier coefficient of the y-component of the magnetic induction at the interface can be derived from Eq. (3.5), by putting $S_{\nu n} = 1$ and replacing the suffix 1 by C to get

$$\bar{B}_{Cy} = \frac{(\nu\pi/\tau)}{n\omega}\,\bar{E}_C \quad . \tag{3.38}$$

Eqs. (3.36) - (3.38), as well as Eq. (3.20), constitute the basic equations needed to obtain the field components in any region of the motor.

Once we obtain the Fourier coefficients of the field components, the expressions of these field components can be set up. Their form will be that of Eq. (2.50). Therefore, the field components at the interface C will be

$$E_C = \sum_{n=1}^{\infty}\sum_{\nu=-\infty}^{\infty} \frac{e_1}{e_3}\,\bar{J}_L\, e^{j(\frac{\nu\pi}{\tau}x + n\omega t)} \tag{3.39}$$

$$B_{Cy} = \sum_{n=1}^{\infty}\sum_{\nu=-\infty}^{\infty} \frac{(\nu\pi/\tau)}{n\omega}\,\frac{e_1}{e_3}\,\bar{J}_L\, e^{j(\frac{\nu\pi}{\tau}x + n\omega t)} \tag{3.40}$$

$$H_{Cx} = \sum_{n=1}^{\infty}\sum_{\nu=-\infty}^{\infty} \bar{J}_L\, e^{j(\frac{\nu\pi}{\tau}x + n\omega t)} \quad . \tag{3.41}$$

Equations (3.39) and (3.40) are those required to predict the machine performance.

D. Motor Currents and Performance

1. Current equations

By exactly the same argument, as previously given in Chapter II, Section G, the voltage induced per phase of the primary winding due to a certain electric field component having time harmonic order, n, will be given by

$$V_{ph} = - NW_1 \sum_{\nu=-\infty}^{\infty} K_w^* \bar{E}_C e^{j \frac{\nu\pi}{\tau} x_o} \tag{3.42}$$

where x_o, N, W_1 and K_w^* have the definitions as previously given in Chapter II, Section G. Substituting the expression of $\bar{E}_C$, as given by Eq. (3.37), and then eliminating $\bar{J}_L$ by using Eq. (2.44) gives the voltage equation for any arbitrary phase, distance x_o from the origin:

$$V_{ph} = \sum_{\nu=-\infty}^{\infty} f(\nu) \left[I_1 + I_2 e^{j \frac{2\pi}{3} \nu} + I_3 e^{j \frac{4\pi}{3} \nu}\right] e^{j \frac{\nu\pi}{\tau} x_o} \tag{2.43}$$

where

$$f(\nu) = - \left(\frac{a_n}{2\tau} NN_p W_1\right) \frac{e_1}{e_3} K_w K_w^* \quad . \tag{3.44}$$

The comparison between Eq. (3.43) and (2.133) shows that both equations are identical with the sole difference in the expressions of $f(\nu)$. Thus, the analysis from Eq. (2.133) to Eq. (2.139) will also hold here, and the voltage equations will be given by:

$$\begin{bmatrix} R_1 + \sum_{\nu=-\infty}^{\infty} f(\nu) & \sum_{\nu=-\infty}^{\infty} f(\nu)\, e^{-j\frac{2\pi}{3}\nu} & \sum_{\nu=-\infty}^{\infty} f(\nu)\, e^{-i\frac{4\pi}{3}\nu} \\ \sum_{\nu=-\infty}^{\infty} f(\nu)\, e^{j\frac{2\pi}{3}\nu} & R_2 + \sum_{\nu=-\infty}^{\infty} f(\nu) & \sum_{\nu=-\infty}^{\infty} f(\nu)\, e^{-j\frac{2\pi}{3}\nu} \\ \sum_{\nu=-\infty}^{\infty} f(\nu)\, e^{j\frac{4\pi}{3}\nu} & \sum_{\nu=-\infty}^{\infty} f(\nu)\, e^{j\frac{2\pi}{3}\nu} & R_3 + \sum_{\nu=-\infty}^{\infty} f(\nu) \end{bmatrix} \begin{bmatrix} I_1 \\ I_2 \\ I_3 \end{bmatrix} = \begin{bmatrix} V_1 \\ V_2 \\ V_3 \end{bmatrix} \tag{3.45}$$

Equation (3.45) permits the representation of unbalanced voltage operations, as well as fault conditions, as the voltages V_1, V_2 and V_3 are arbitrary quantities. The entries of the coefficient matrix are self and the mutual impedances of the different phases of the machine. Once we solve Eq. (3.45) for the phase currents, the field components in the different regions can be determined, and hence, the machine performance can be fully predicted.

2. Performance equations

The analysis of Chapter II, Section H.1 also holds in this case with the sole modification that the overhang length of the primary

winding is neglected, i.e., $W_0 = 0$. Therefore, the tangential force component, F_x, as follows from Eq. (2.142), will be given by

$$F_x = -\frac{1}{2}(2\tau p\, W_1)\, \mathrm{Re} \sum_{n=1}^{\infty} \sum_{\nu=-\infty}^{\infty} \bar{B}_{Cy}\, \bar{J}_L^{\,*} \tag{3.46}$$

where $\bar{J}_L^{\,*}$ is the complex conjugate of the linear current density, and $\bar{B}_{Cy}$ is the Fourier coefficient of the y-component of the magnetic induction at the interface C, as given by Eq. (3.38).

Similarly, the analysis of Section H.2 in Chapter II also holds in this case, with $W_0 = 0$. Thus, the secondary input power, P_{sec}, can be derived from the Poynting theorem, and the final result will take the form:

$$P_{sec} = -\frac{1}{2}(2\tau P W_1)\, \mathrm{Re} \sum_{n=1}^{\infty} \sum_{\nu=-\infty}^{\infty} \bar{E}_C\, \bar{J}_L^{\,*} \tag{3.47}$$

where $\bar{J}_L^{\,*}$ is the complex conjugate of the linear current density of the primary winding, and $\bar{E}_C$ is the Fourier coefficient of the electric intensity at the interface C, as given by Eq. (3.37).

Finally, the input power to the motor will be given by:

$$P_{in} = \mathrm{Re} \sum_{r=1}^{3} V_r I_r^{\,*} \quad . \tag{3.48}$$

Equations (3.46) - (3.48) are those required to predict the motor performance in terms of its design parameters.

E. Conclusion

In this chapter, a simplified electromagnetic theory of induction motors has been developed. The theory is based on the wave impedance concept, or in other words, on the analogy found between the differential equations of the Fourier coefficients of the field quantities and those of the transmission lines. The analysis presented in this chapter represents a generalization and extension to the work of Cullen and Barton [26], Freeman [37, 38], Freeman and Smith [40] and Greig and Freeman [45]. The analysis establishes a general approach capable of describing any arbitrary electric or magnetic loading, as well as a general method for calculating the machine currents. The analysis can be equally applied to fault conditions, as well as single-phase machines. The expression of force, input power and secondary input power is also derived, which enables the prediction of motor performance.

IV. EXTENSION OF THE FIELD ANALYSIS

A. Introduction

The analysis presented in Chapter II is based on the solution of the field equations in a five-region model. These regions are: the primary slot, the air gap, the secondary slot, the primary overhang and the air overhang. The analysis of Chapter II ignores the important part played by tooth-top and zigzag leakage flux in practical machines. This omission leads to performance equations in which the rotor slot is a principal component of the leakage reactance. The rotor-slot leakage reactance is exceedingly dependent upon the slip. Moreover, the tooth tops in both the primary and secondary members entirely control the flow of the electromagnetic energy from the primary to the secondary side. This effect of the tooth tops can considerably affect the machine performance.

The purpose of this chapter is to extend the field analysis to a more accurate and elaborate model. This model consists of the five regions developed in Chapter II, plus the two regions corresponding to the tooth tops of the primary and secondary members. Another purpose of this chapter is to derive a systematic field analysis, in a way similar to that developed in Chapter III, when the effect of the secondary end ring is taken into account.

B. Mathematical Model

Figure 4.1 shows a sectional view of the mathematical model of a seven-region induction motor. The figure is the same as the model given

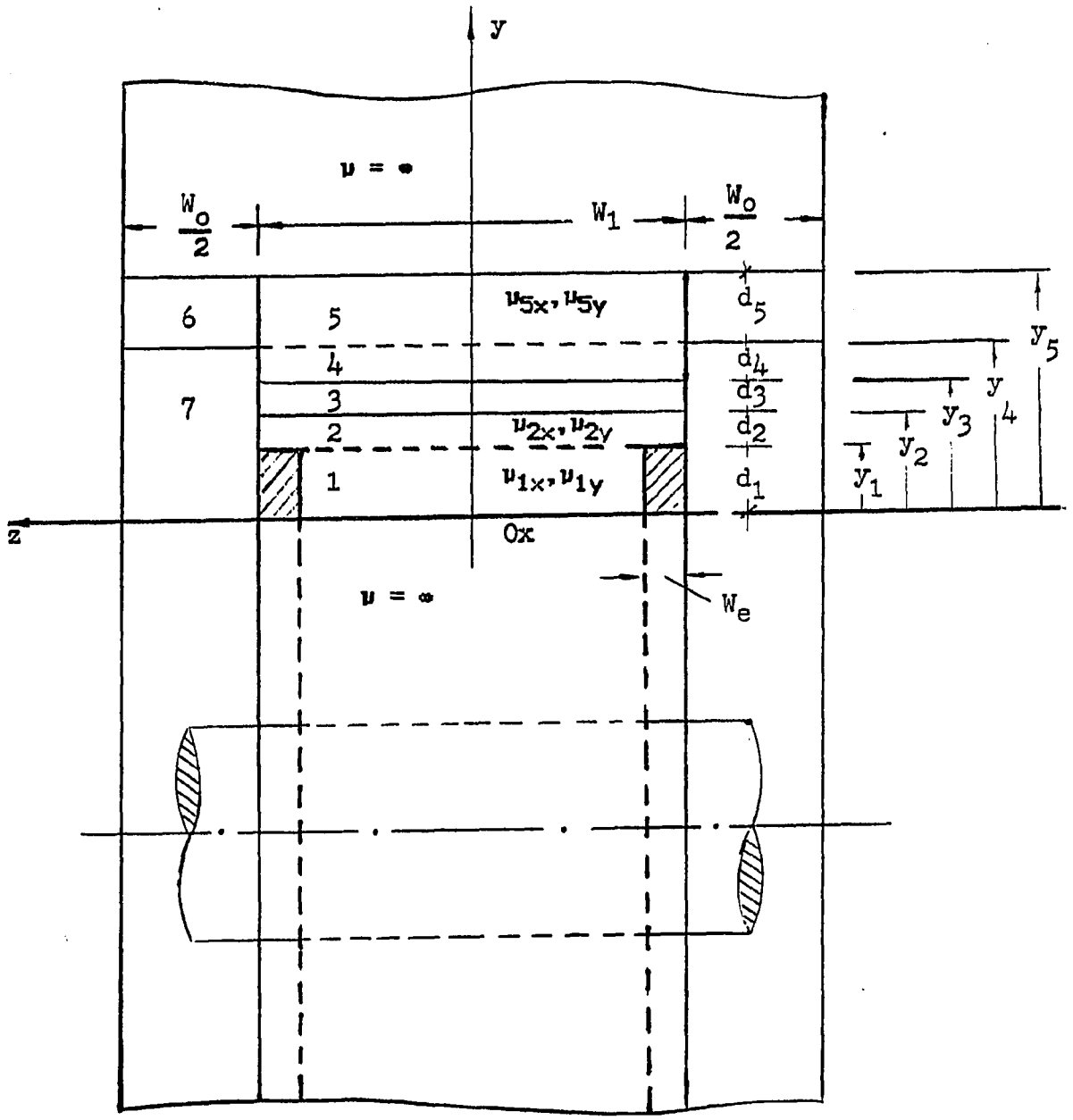

Figure 4.1. Sectional view of the induction motor showing the seven regions (1, 2, ..., 7) considered in the analysis

in Figure 2.3, with two additional regions: the primary and secondary tooth tops. To achieve generality in representation, the thickness of regions 1, 2, ..., 5 are denoted by d_1, d_2, ..., d_5, while their interfaces measured from the OX^2 plane are denoted by y_1, y_2, ..., y_5. Other dimensions are as shown in the figure. The directional permeabilities are denoted by μ_{ix} and μ_{iy}, where i = 1, 2, ..., 5. The overhang regions 6 and 7 are kept without change, as previously given in Chapter II (see Figure 2.3).

C. Field Analysis

The procedure of deriving the basic differential equations and their solutions in the different regions of the motor are exactly the same as previously developed in Chapter II. To avoid repetition, the results of Chapter II will be used directly with their appropriate formulation on the basis of the notation adopted in this chapter. Then, the basic equations in the different regions of the mathematical model can be summarized as follows.

Region 1:

The differential equations in this region are previously given by Eqs. (2.19) and (2.24). Therefore, according to the notation adopted in Figure 4.1, these equations can be written in the form

$$\mu_{1x} \frac{\partial^2 E_1}{\partial x^2} + \mu_{1y} \frac{\partial^2 E_1}{\partial y^2} = \mu_{1x}\mu_{1y} \left(\frac{\partial}{\partial t} + V \frac{\partial}{\partial x}\right) J_1 \qquad (4.1)$$

$$\frac{\partial^2 E_1}{\partial x^2} = \frac{1}{\sigma_1} \frac{\partial^2 J_1}{\partial x^2} - \frac{2d_1}{\sigma_e A_e W_1} J_1 \tag{4.2}$$

where the subscript 1 denotes the quantities of region 1 and the subscript e denotes those of the end ring.

It is clear that the elimination of J_1 between Eqs. (4.1) and (4.2) will yield a fourth order PDE in E_1. This PDE represents the field equation in region 1 subjected to the constraint imposed by the end ring of the secondary member.

As explained in Chapter II, the functional form of all the field quantities, as well as the current distribution, should be that given by Eq. (2.50). Therefore, we can express Eqs. (4.1) and (4.2) in terms of their Fourier coefficients (this is simply done by replacing the operations $\partial/\partial x$ and $\partial^2/\partial x^2$ by $(j\nu\pi/\tau)$ and $(j\nu\pi/\tau)^2$, respectively), and on eliminating $\bar{J}_1$ between the resulting equations, we can get

$$\frac{\partial^2 \bar{E}_1}{\partial y^2} - \eta_1^2 \bar{E}_1 = 0 \tag{4.3}$$

where

$$\eta_1^2 = \frac{\mu_{1x}}{\mu_{1y}} \left(\frac{\nu\pi}{\tau}\right)^2 + j\, \mu_{1x}\, S_{\nu n} \frac{n\omega\sigma_1}{K_e} \tag{4.4}$$

$$K_e = 1 + \frac{2d_1\sigma_1/\sigma_e}{A_e W (\nu\pi/\tau)^2} \quad . \tag{4.5}$$

We retain the bar to denote the Fourier coefficient of the field quantity. The solution of Eq. (4.3) will be given by

$$\bar{E}_1 = A_1 \cosh \eta_1 y + B_1 \sinh \eta_1 y \quad . \tag{4.6}$$

Regions 2, 3 and 4:

In a similar way, the differential equation of the Fourier coefficient of the field components of regions 2, 3 and 4 can be written in the form

$$\frac{\partial^2 \bar{E}_i}{\partial x^2} - \eta_i^2 \bar{E}_i = 0, \quad i = 2, 3, 4 \tag{4.7}$$

where

$$\eta_i^2 = \frac{\mu_{ix}}{\mu_{iy}} \left(\frac{\nu\pi}{\tau}\right)^2 \quad . \tag{4.8}$$

Note that in region 3, $\mu_{3x} = \mu_{3y} = \mu_0$. The solution of Eq. (4.8) can be written in the form

$$\bar{E}_i = A_i \cosh \eta_i (y-y_{i-1}) + B_i \sinh \eta_i (y-y_{i-1}) \tag{4.9}$$

where i = 2, 3, 4 as defined above.

Region 5:

The differential equation of the Fourier coefficient of the field intensity in this region is given by

$$\frac{\partial^2 \bar{E}_5}{\partial x^2} - \eta_5^2 \bar{E}_5 = j \mu_{5x} n\omega \bar{J}_5 \qquad (4.10)$$

where

$$\eta_5^2 = \frac{\mu_{5x}}{\mu_{5y}} \left(\frac{\nu\pi}{\tau}\right)^2 \quad . \qquad (4.11)$$

Note that $\bar{J}_5$ is the Fourier coefficient of the primary current, which is a completely defined quantity (see Eq. (2.44)).

The solution of Eq. (4.10) is composed of the complimentary function and the particular integral, and can be written in the form

$$\bar{E}_5 = A_5 \cosh \eta_5(y-y_4) + B_5 \sinh \eta_5(y-y_5)$$

$$- i \frac{n\omega\mu_{5x}}{\eta_5^2} \bar{J}_5 \quad . \qquad (4.12)$$

Equations (4.6), (4.9) and (4.12) constitute the necessary equations to get the solution of the field components in the different regions of the induction motor. These equations contain ten arbitrary constants which can be determined from the boundary conditions.

D. Boundary Conditions

As follows from Eqs. (2.31) and (2.32), the boundary conditions at any interface between any two adjacent regions can be expressed in terms of the Fourier coefficients and are given by

$$\left(\frac{1}{S_{\nu n}}\bar{E}\right)^{-} = \left(\frac{1}{S_{\nu n}}\bar{E}\right)^{+} \qquad \text{(i)}$$

$$\left(\frac{1}{S_{\nu n}\mu_x}\frac{\partial\bar{E}}{\partial y}\right)^{-} = \left(\frac{1}{S_{\nu n}\mu_x}\frac{\partial\bar{E}}{\partial y}\right)^{+} \qquad \text{(ii)} \tag{4.13}$$

where the '-' and '+' denote the value of the field components, or its derivative, just above and below the interface under consideration.

E. The Arbitrary Constants and the Field Expressions

Consider the ith and the (i+1)th regions to be any two adjacent regions. Equations (4.13i) and (4.13ii) can be applied to the interface between these two adjacent regions. The relation between the arbitrary constants of the field expressions can be written in the form

$$\begin{pmatrix} A_{i+1} \\ B_{i+1} \end{pmatrix} = D_i \begin{pmatrix} A_i \\ B_i \end{pmatrix}, \quad i = 1, 2, 3 \tag{4.14}$$

where

$$D_i = \frac{S_{\nu n i+1}}{S_{\nu n i}} \begin{pmatrix} 1 & 0 \\ 0 & \dfrac{\eta_i/\mu_{ix}}{\eta_{i+1}/\mu_{i+1x}} \end{pmatrix} \begin{pmatrix} \cosh \eta_i d_i & \sinh \eta_i d_i \\ \sinh \eta_i d_i & \cosh \eta_i d_i \end{pmatrix} . \tag{4.15}$$

The advantage of using Eq. (4.14) for the first four regions is that it permits expressing the arbitrary constants of region 4 in terms of those of region 1. This is carried out by letting i take the values of 1, 2 and 3, and substituting the resulting matrix equation iteratively to get

$$\begin{pmatrix} A_4 \\ B_4 \end{pmatrix} = D_3 D_2 D_1 \begin{pmatrix} A_1 \\ B_1 \end{pmatrix} . \tag{4.16}$$

In region 5, at $y = y_4$, the boundary conditions will lead to the following matrix equation:

$$\begin{pmatrix} A_5 \\ B_5 \end{pmatrix} = D_4 \begin{pmatrix} A_4 \\ B_4 \end{pmatrix} + \begin{pmatrix} jS_{\nu n5} n\omega\mu_{5x}\bar{J}_5/n_5^2 \\ 0 \end{pmatrix} \tag{4.17}$$

where D_4 has the same definition as given by Eq. (4.15), with $i = 4$. Clearly, the slip $S_{\nu n5} = 1$, as region 5 is a stationary region, i.e., $v = 0$ (see Eq. 2.64).

Eliminating $(A_4 B_4)$ between Eqs. (4.16) and (4.17), we can write

$$\begin{pmatrix} A_5 \\ B_5 \end{pmatrix} = \begin{pmatrix} e_1 & e_2 \\ e_3 & e_4 \end{pmatrix} \begin{pmatrix} A_1 \\ B_1 \end{pmatrix} + \begin{pmatrix} jn\omega\mu_{5x}\bar{J}_5/n_5^2 \\ 0 \end{pmatrix} \tag{4.18}$$

where

$$\begin{pmatrix} e_1 & e_2 \\ e_3 & e_4 \end{pmatrix} = D_4 D_3 D_2 D_1 . \tag{4.19}$$

Evidently, e_1, e_2, e_3 and e_4 are the entries of the equivalent matrix formed from the product of the matrices of the first four regions. Equation (4.18) shows that the field expressions in regions 1 and 5, Eqs. (4.6) and (4.12), can be expressed by the same arbitrary constants A_1 and B_1. The two additional boundary conditions required to get the values of A_1 and B_1 are:

$$\text{at } y = 0, \qquad \partial E/\partial y = 0$$

$$\text{at } y = y_5, \qquad \partial E/\partial y = 0 \quad . \tag{4.20}$$

Equation (4.20) together with Eqs. (4.18), (4.6) and (4.12) can be solved to get the values of the arbitrary constants A_5 and B_5. Their expressions will be given by

$$A_5 = j \frac{n\omega\mu_{5x}}{n_5^2} \cdot \frac{e_3}{e_3 + e_1 \tanh n_5 d_5} \bar{J}_5 \tag{4.21}$$

$$B_5 = - j \frac{n\omega\mu_{5x}}{n_5^2} \cdot \frac{e_3 \tanh n_5 d_5}{e_3 + e_1 \tanh n_5 d_5} \bar{J}_5 \quad . \tag{4.22}$$

Once we get the expressions of the arbitrary constants A_5 and B_5, the field expression in region 5, Eq. (4.12), is fully determined. The magnetic intensity, as well as the magnetic induction, can be derived from the expression of the electric intensity by using the relations given by Eqs. (2.9) and (2.10).

F. Other Considerations

The above analysis gives the solution of the field problem in the five main regions (1, 2, ..., 5) of the induction motor. The solution of the field problem in the other overhang regions 6 and 7 is exactly similar to that previously developed in Chapter II (see Sections C.5, C.6, D.2, E.5 and F.2), with the sole modification of the number of regions. The voltage equations, as well as the force and power expressions, are exactly similar to those developed in Chapter II (see Sections G and H). Therefore, the analysis will not be repeated here and the results of those sections will be used directly.

G. Conclusion

In this chapter, the field analysis is developed for a more elaborate mathematical model. The model consists of seven regions that can represent faithfully the induction motor with its actual regions. The purpose of this chapter, in addition to extending the regions of the mathematical model, is to develop a systematic analysis capable of handling larger region models with relative mathematical ease. The approach developed in this chapter permits the determination of the fields in the required region only, without the need to determine the fields in the other regions. This differs from the analysis developed in Chapter II. This is a short cut procedure and avoids the solution of ten simultaneous algebraic equations to get the the arbitrary constants for the solution of the differential equations. The method developed here is a combination of the methods developed in

Chapters II and III. It is similar to that developed in Chapter II as it deals with the differential equations of a single field component in all the regions of the mathematical model. It is also similar to that developed in Chapter III as it deals with the matrices of the different regions, permitting the elimination of the arbitrary constants of the regions not involved directly in getting the machine performance.

V. NUMERICAL CALCULATIONS AND DISCUSSIONS

A. Introduction

In order to achieve a reasonable demonstration of the newly developed analysis of the previous chapters, the performance characteristics of an induction motor, designed for this purpose, will be studied.

The performance characteristics of the given model have been calculated under the normal, constant voltage drive system. Some considerations have also been given to varying some of the motor parameters to obtain their effects on the motor performance. Both the space and time harmonics have been taken into account in the calculations. Harmonic time effects have been studied individually, as well as globally.

A computer program has been developed for this purpose, and is shown in the Appendix.

B. Induction Motor Model

The induction motor designed for the purpose of this investigation is assumed to have the following specifications.

Primary side:

Slot depth	10 mm
Slot width	12 mm
Tooth top thickness	2 mm (4 mm)
Tooth top opening	12 mm (8, 4, 1 mm)

Slot pitch	24 mm
Pole pitch	216 mm
Core length	200.6 mm
Relative permeability of core iron	500
No. of slots/pole/phase	3
Coil pitch	1-8
No. of poles	4
No. of conductors/slot	40
Resistance/phase	0.5 ohm
Slot factor	0.7
Overhang length (both sides)	50 mm (0, 100 mm)
No. of phases	3
Frequency	60 Hz

Type of winding:

3 phase, double layer, star connected.

Voltage:

3 phase, balanced system, 220V (rms).

Time harmonics:

Fundamental	100%
Third harmonic	9%
Fifth and higher harmonics	(9.0/harmonic order) %

Space harmonics:

-11, -5, 1, 7, 13 (or fundamental only).

Secondary side:

Slot depth	20 mm (15, 10 mm)
Slot width	12 mm
Tooth top thickness	2 mm (4 mm)
Tooth top opening	10 mm (semi-closed)
Slot pitch	24 mm
Conductivity of squirrel cage conductors (AL.)	3.45×10^7 s/m
Secondary core length	200.2 mm
End ring width (if considered)	5 mm
Conductivity of end ring (Cu)	1.148×10^6 s/m

(Other conductivities have been also considered.)

Relative permeability of secondary iron	500 mm

Air gap length:

2 mm

The numbers in parentheses have been investigated too.

C. Results and Discussion

The following paragraphs describe the basic results as concluded from the study of the given model using the analyses developed in the previous chapter.

Figures 5.1 and 5.2 show the thrust-speed characteristics of the motor when the end ring effects are neglected and when they are taken into account. Curves A and C show the characteristics when both the space and time harmonics, in the sense indicated in Section B above, are taken into account. Curves B and D are the characteristics when harmonics are neglected. The figures clearly show that the effects of harmonics are pronounced at the low speed range.

Figure 5.3 shows the exact shape of the irregularity in the thrust-speed curve in the low speed range. The figure shows almost two coincident curves, the lower curve is drawn when the space harmonics are acting only in the air gap, while the time harmonics are neglected. The upper curve is drawn when both the space and time harmonics are acting together on the motor. It is evident that the effect of the time harmonics is almost negligible. Both curves of Figure 5.3 are drawn for a motor with end rings.

Figures 5.4 and 5.5 show the effect of the conductivity of the end rings of the squirrel cage structure on the thrust-speed characteristics. Figure 5.4 is drawn when both space and time harmonics are neglected, while Figure 5.5 shows the characteristics when the effects of these harmonics are taken into account. Clearly, the performance of the motor is considerably improved when the end-ring conductivity is increased. This suggests a motor design with end-ring conductivity higher than that of the squirrel cage structure.

Figure 5.6 shows the thrust-speed characteristics for the given model with different values of primary tooth top openings. Both space

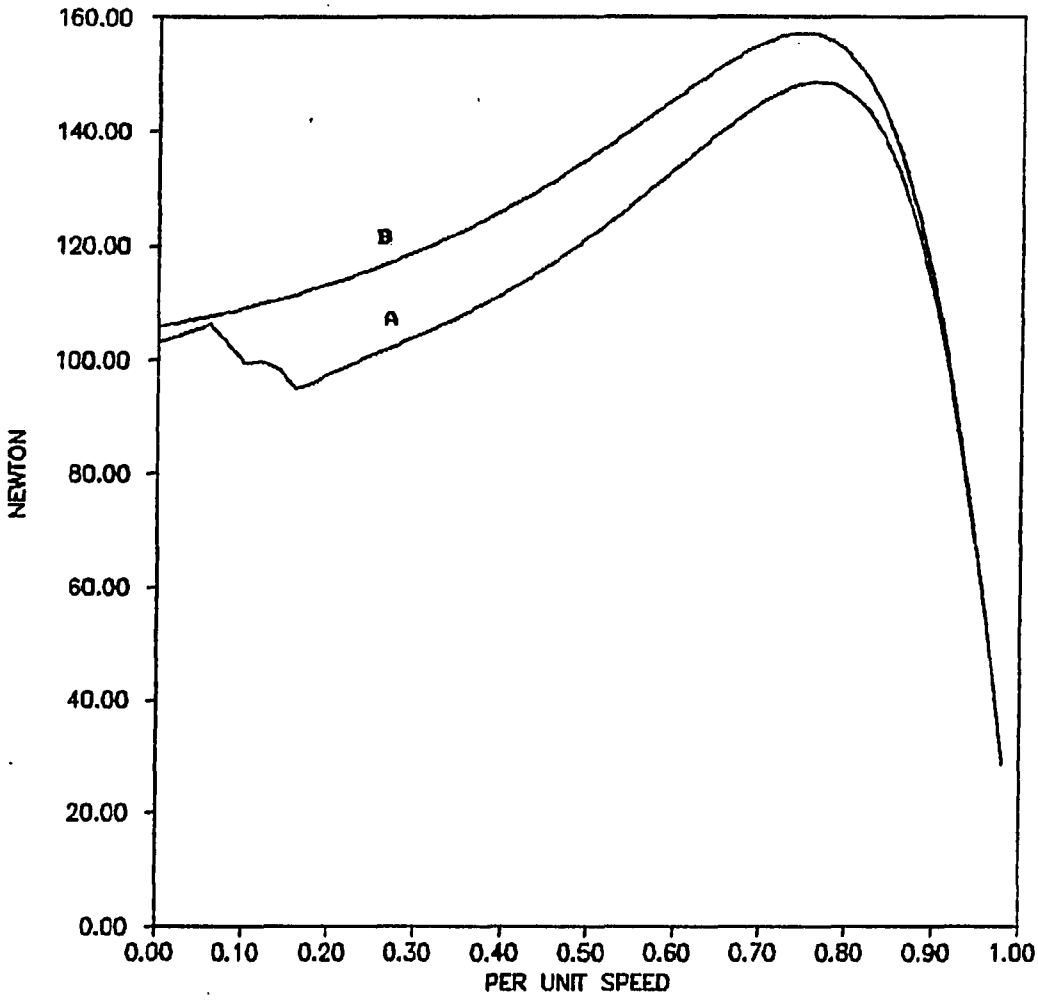

Figure 5.1. Thrust-speed characteristics for the motor without end rings. Curve A: space and time harmonics are taken into account. Curve B: space and time harmonics are neglected. (Without end rings means that the secondary core length is assumed to be infinite)

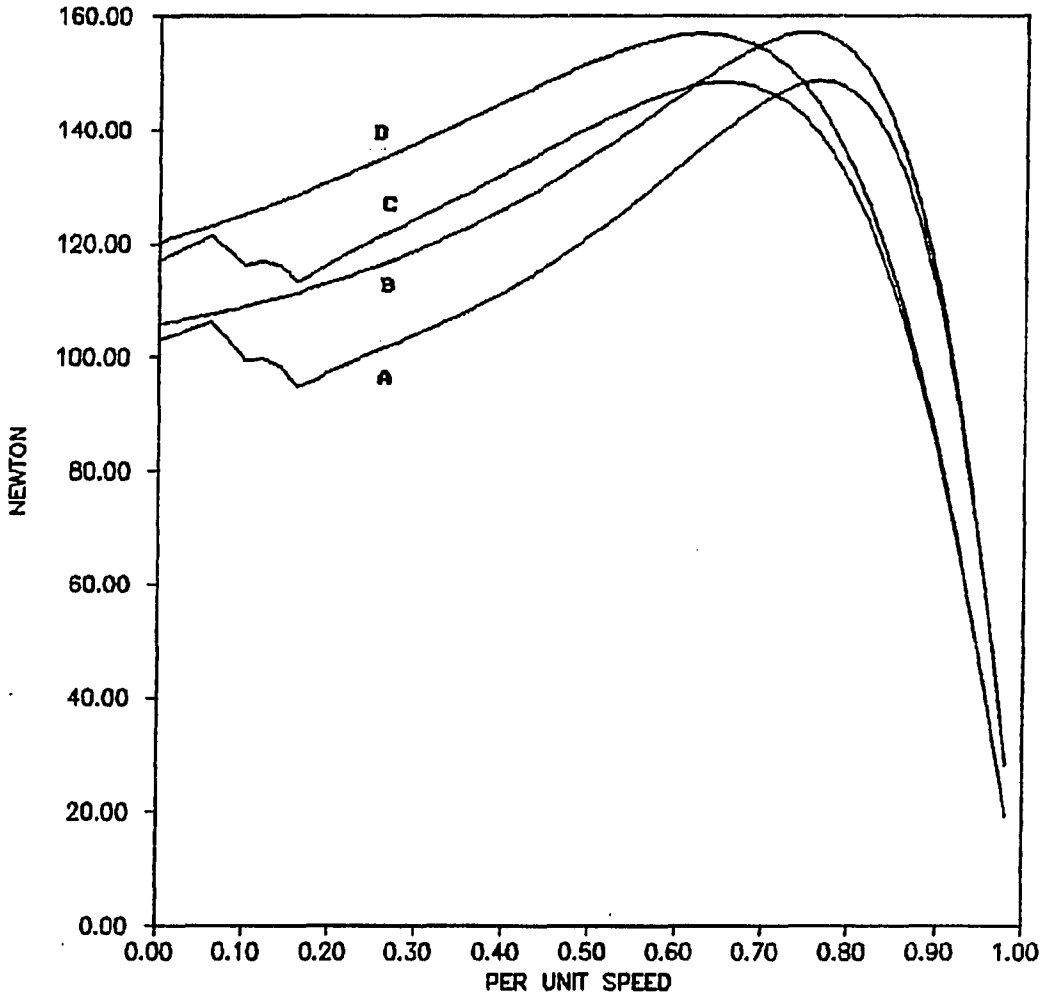

Figure 5.2. Thrust-speed characteristics for the motor with and without end rings. Curves C and D are for the motor with end rings when harmonics are taken into account and are neglected, respectively. Curves A and B are those of Figure 5.1 for the purpose of comparison. (Without end rings means that the secondary core length is assumed to be infinite)

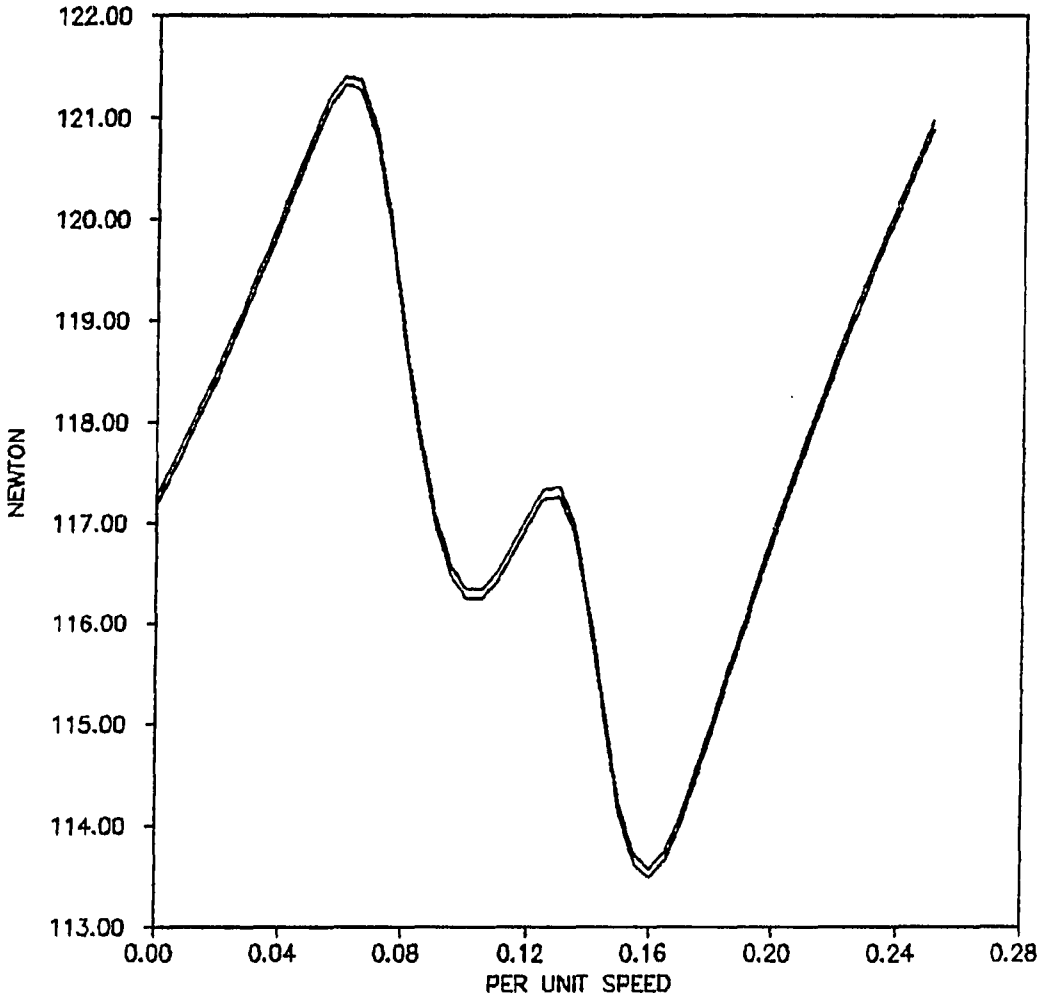

Figure 5.3. Thrust-speed curve at the low speed range for the motor with end rings. Lower curve: space harmonics only are considered. Upper curve: both space and time harmonics are considered

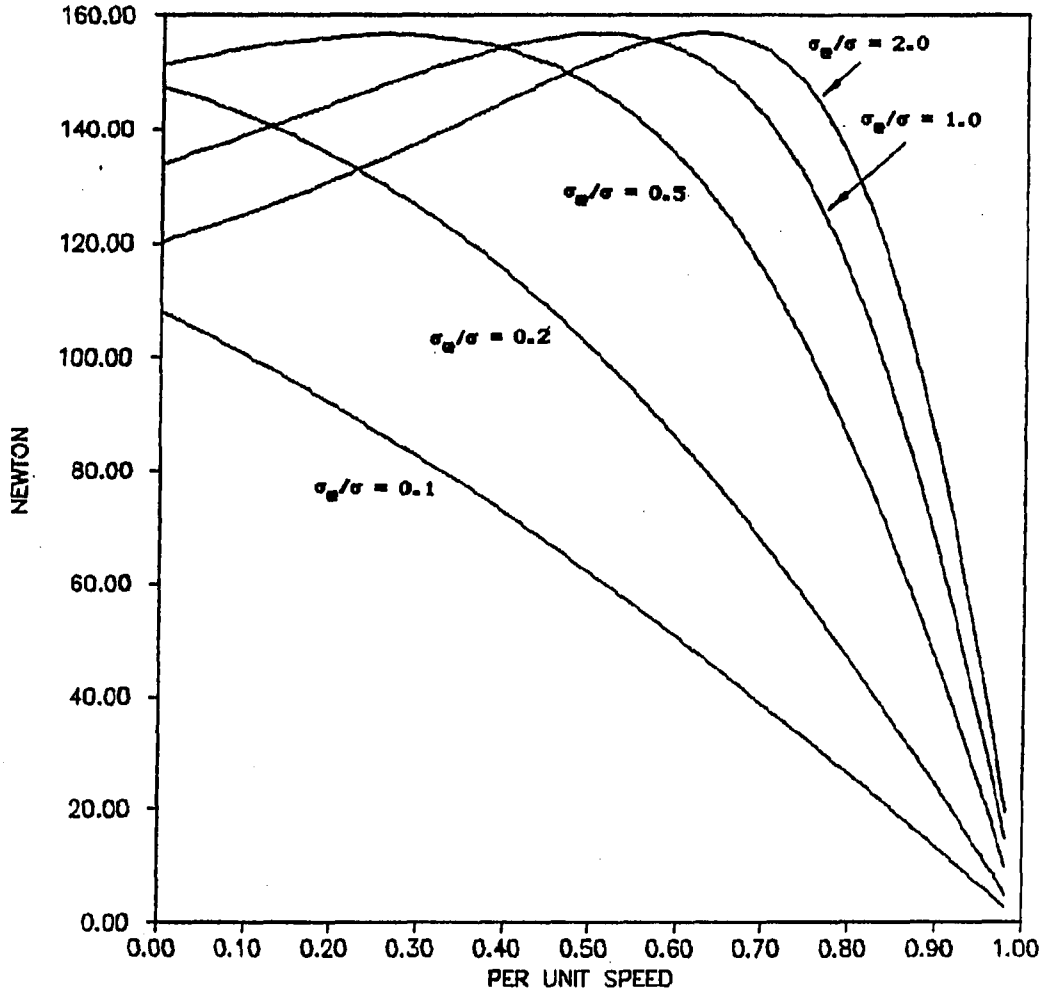

Figure 5.4. Thrust-speed characteristics for the motor with different end-ring conductivities. Space and time harmonics are not taken into account. (σ_e/σ) is the ratio between the end-ring conductivity and the squirrel cage conductivity

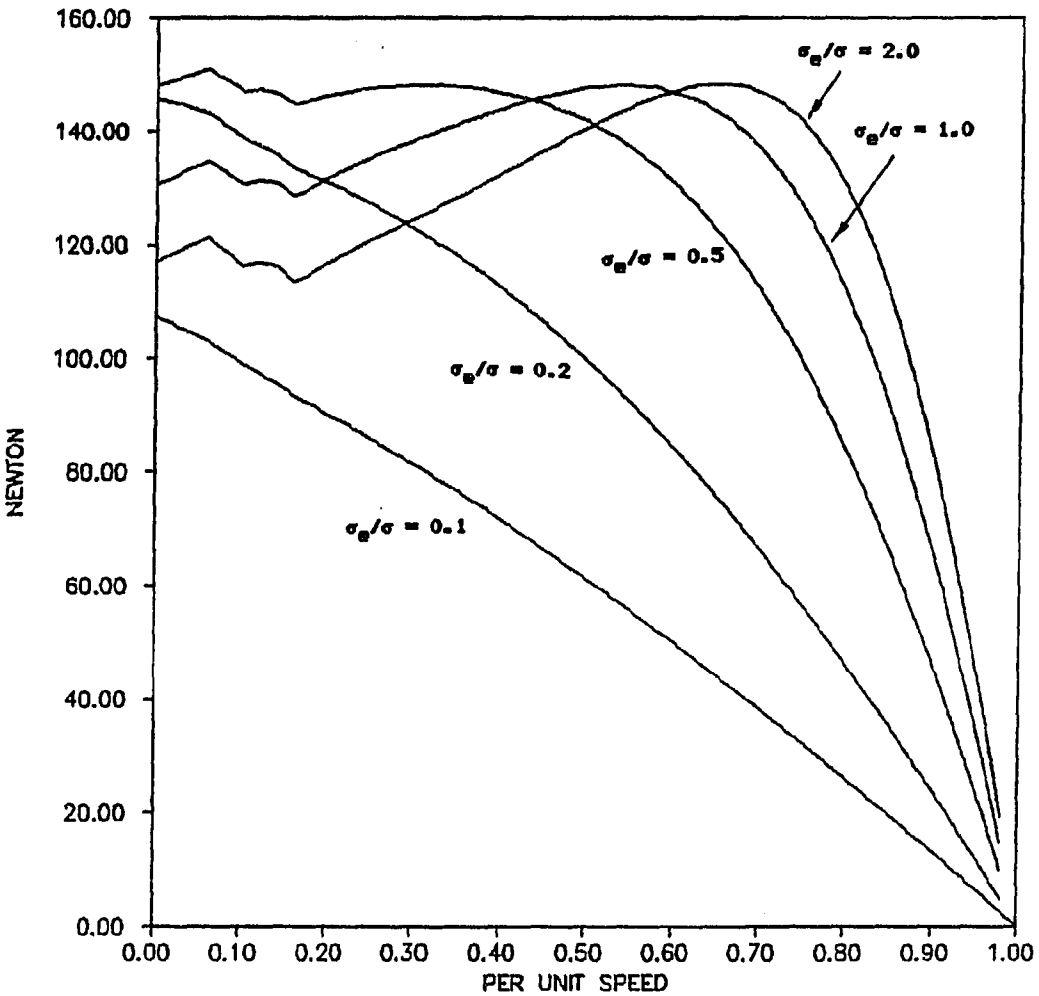

Figure 5.5. Thrust-speed characteristics for the motor with different end-ring conductivities. Space and time harmonics are taken into account. (σ_e/σ) is the ratio between the end-ring conductivity and the squirrel cage conductivity

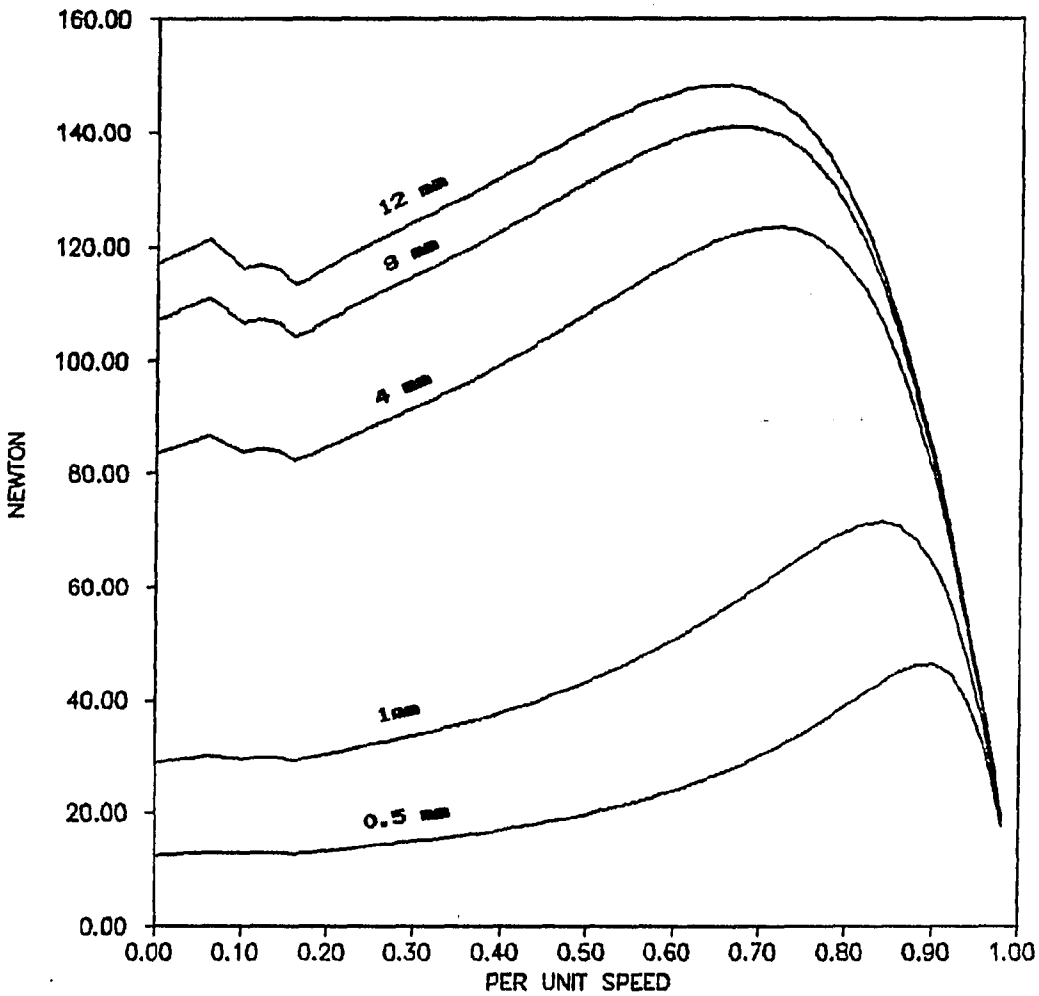

Figure 5.6. Thrust-speed characteristics for the motor with different primary tooth-top openings. Space and time harmonics are taken into account

and time harmonics are taken into account. The figure shows that the pattern of the thrust-speed curves does not change as the tooth-top opening gets narrower, but the thrust magnitude is distinctly reduced with the reduction of the tooth-top opening. The figure clearly shows that the tooth-top opening can behave as a gate that controls the flow of the electromagnetic energy from the primary side to the air gap of the motor. It is evident from Figure 5.6 that the usual replacement of the motor winding by a single current sheet irrespective of the dimension of the tooth top of the electrical machine is questionable.

Figure 5.7 shows the effect of the conductivity of the end rings on the efficiency-speed characteristics of the given motor. Space and time harmonics are taken into account in the calculation of Figure 5.6, as well as for all of the efficiency and power factor curves. The figure shows clearly that the lower the conductivity of the end ring, the poorer is the performance of the motor in the working speed range.

Figure 5.8 shows the effect of the primary tooth-top opening on the primary efficiency of the motor. Clearly, as the primary tooth opening gets narrower, the motor performance is degraded.

Figure 5.9 shows the effect of the conductivity of the end rings on the power factor of the secondary input power. The figure shows that as the conductivity of the end rings is increased, the power factor is improved in the low speed range, but decreases in the high speed range.

Figure 5.10 shows the effect of the primary tooth-top opening on the power factor of the secondary input power. Clearly, the power

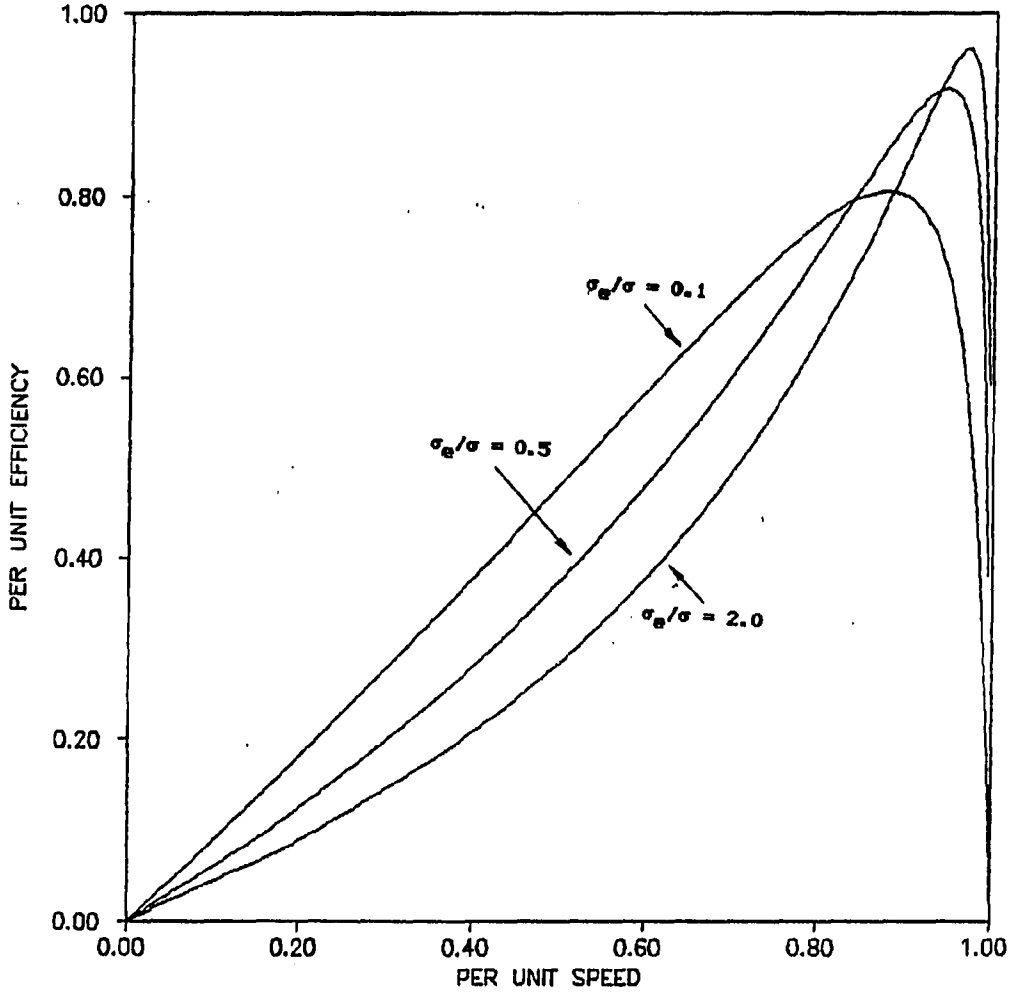

Figure 5.7. Primary efficiency-speed characteristics for the motor with different end-ring conductivities. Space and time harmonics are taken into account. (σ_e/σ) is the ratio between the end-ring conductivity and the squirrel cage conductivity

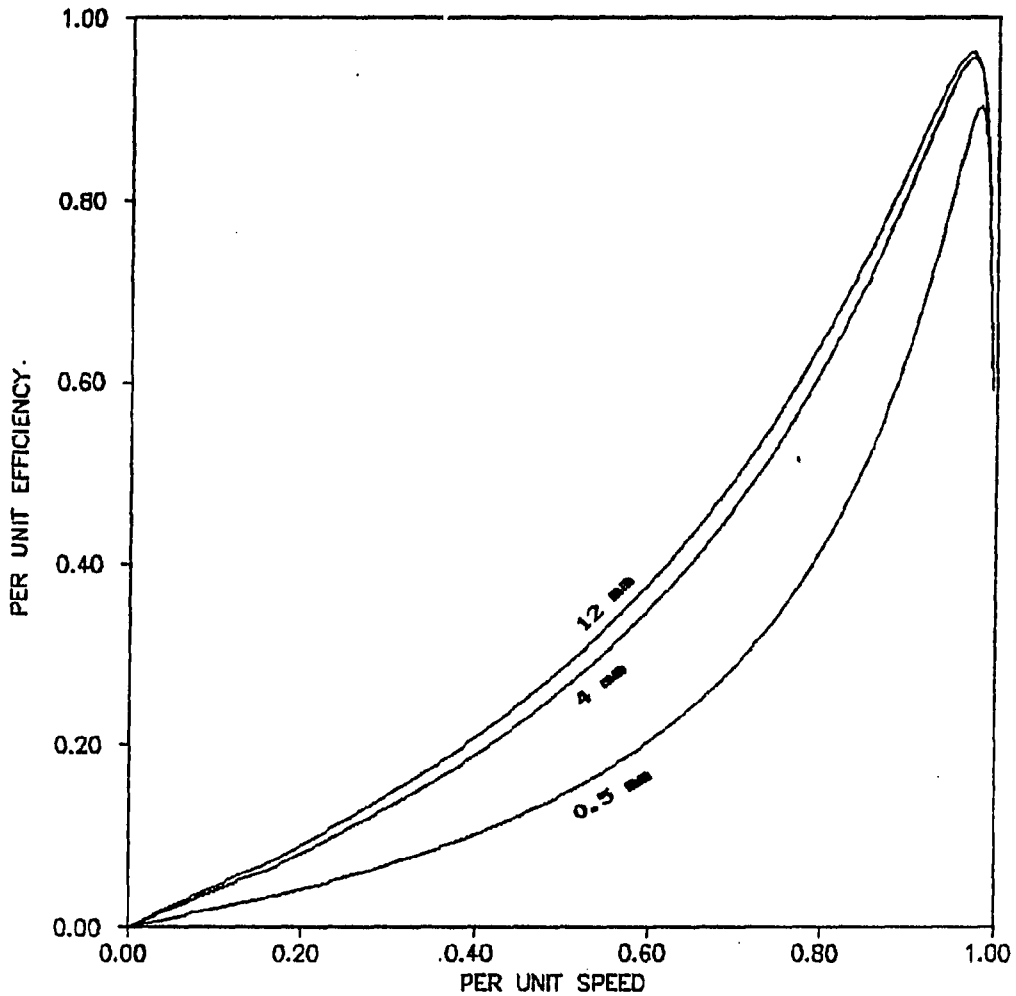

Figure 5.8. Primary efficiency-speed characteristics for the motor with different primary tooth-top openings. Space and time harmonics are taken into account

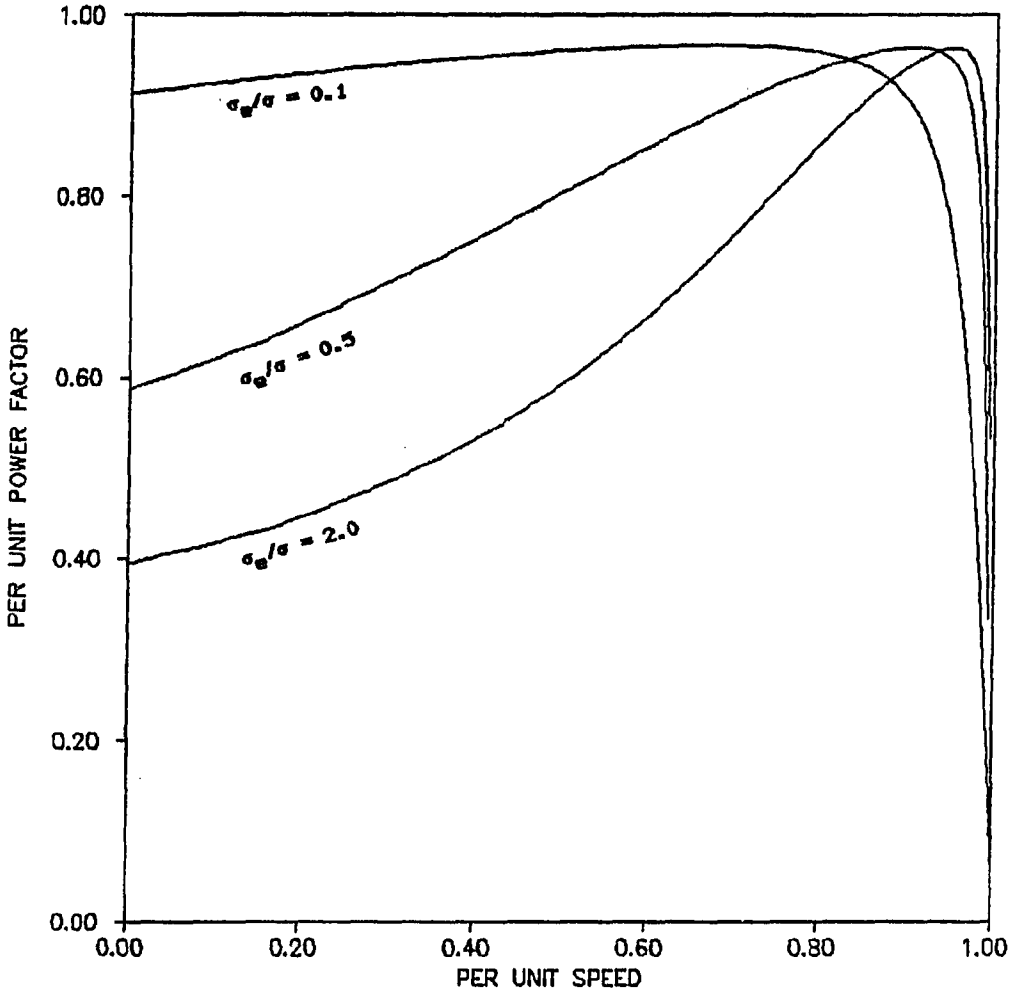

Figure 5.9. Secondary power factor-speed characteristics for the motor with different end-ring conductivities. Space and time harmonics are taken into account. (σ_e/σ) is the ratio between the end-ring conductivity and the squirrel cage conductivity

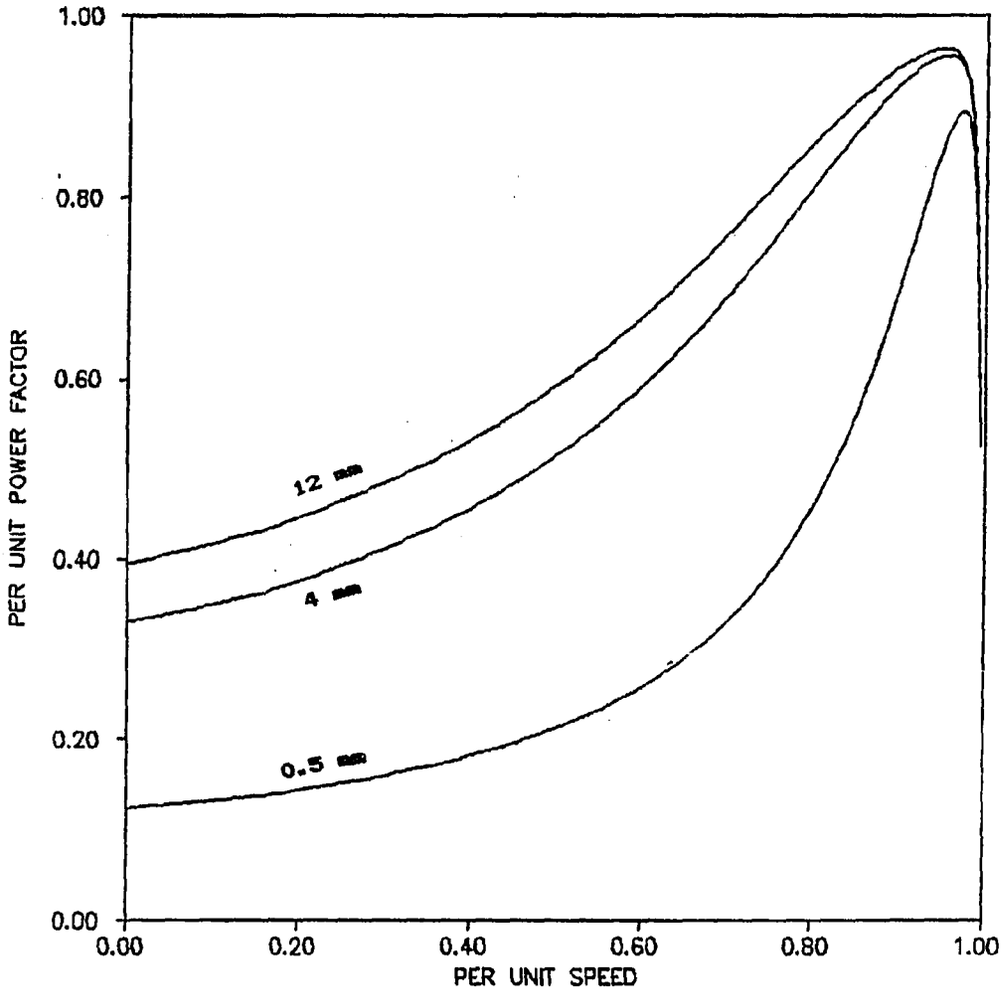

Figure 5.10. Secondary power factor-speed characteristics for the motor with different primary tooth-top openings. Space and time harmonics are taken into account

factor is degraded as the tooth-top opening is decreased.

Table 5.1 shows that the values of the currents drawn by the motor due to time harmonics in the voltage system are almost constant over the whole speed range (about 4.8% decrease from standstill to the synchronous speed). For the relatively high distortion in the given voltage, the values of the harmonic currents are slightly larger than 3.5% in most of the speed range. The value can reach 12% in the working speed range. The effect of these harmonic currents on the thrust force is very small, as shown in Table 5.2. The harmonic currents decrease the primary efficiency of the motor by about 1% in the working speed range, as shown in Table 5.3.

Table 5.1. Harmonic currents and their percentage values with respect to the fundamental[a]

Per unit speed	Fundamental current A	3rd harmonic current A	%	5th harmonic current A	%
0.00	20.9380	0.7455	3.5603	0.0971	0.4638
0.05	20.7586	0.7436	3.5819	0.0970	0.4671
0.10	20.5818	0.7416	3.6032	0.0968	0.4704
0.15	20.3897	0.7396	3.6274	0.0967	0.4741
0.20	20.2214	0.7373	3.6463	0.0965	0.4772
0.25	19.9701	0.7355	3.6831	0.0963	0.4824
0.30	19.6774	0.7349	3.7347	0.0962	0.4888
0.35	19.3375	0.7332	3.7918	0.0960	0.4963
0.40	18.9394	0.7309	3.8592	0.0958	0.5058
0.45	18.4690	0.7297	3.9511	0.0958	0.5190
0.50	17.9084	0.7292	4.0720	0.0958	0.5347
0.55	17.2347	0.7276	4.2215	0.0856	0.5549
0.60	16.4188	0.7258	4.4204	0.0955	0.5817
0.65	15.4242	0.7240	4.6936	0.0954	0.6182
0.70	14.2063	0.7221	5.0826	0.0950	0.6689
0.75	12.7141	0.7201	5.6638	0.0952	0.7484
0.80	10.8945	0.7181	6.5915	0.0951	0.8730
0.85	8.7036	0.7161	8.2274	0.0950	1.0912
0.90	6.1259	0.7140	11.6554	0.0948	1.5480
0.95	3.2026	0.7119	22.2280	0.0947	2.9563
1.00	0.3761	0.7097	188.7042	0.0945	25.1333

[a]Fundamental voltage = 220.0 V (rms), 3rd harmonic voltage = 19.8 V (rms), and 5th harmonic voltage = 3.96 V (rms).

Table 5.2. Harmonic forces and their percentage values with respect to the fundamental[a]

Per unit speed	Fundamental force N	3rd harmonic force N	%	5th harmonic N	%
0.00	310.8450	0.3442	0.1107	0.0054	0.0017
0.05	310.1975	0.3438	0.1108	0.0054	0.0017
0.10	305.9543	0.3435	0.1123	0.0054	0.0018
0.15	299.7314	0.3433	0.1146	0.0054	0.0018
0.20	290.3235	0.3443	0.1186	0.0054	0.0019
0.25	284.6108	0.3434	0.1207	0.0054	0.0019
0.30	278.7537	0.3361	0.1206	0.0054	0.0019
0.35	272.4097	0.3333	0.1224	0.0054	0.0020
0.40	265.4331	0.3323	0.1252	0.0054	0.0021
0.45	257.6414	0.3295	0.1279	0.0053	0.0021
0.50	248.8066	0.3243	0.1304	0.0053	0.0021
0.55	238.6402	0.3219	0.1349	0.0052	0.0022
0.60	226.7850	0.3198	0.1410	0.0052	0.0023
0.65	212.7924	0.3178	0.1494	0.0052	0.0024
0.70	196.1072	0.3160	0.1611	0.0052	0.0027
0.75	176.0505	0.3142	0.1785	0.0051	0.0029
0.80	151.8320	0.3125	0.2058	0.0051	0.0033
0.85	122.6192	0.3109	0.2535	0.0050	0.0041
0.90	87.7399	0.3093	0.3525	0.0050	0.0057
0.95	47.1066	0.3077	0.6532	0.0050	0.0106
1.00	5.5126	0.3062	5.5547	0.0050	0.0901

[a]Fundamental voltage = 220.0 V (rms), 3rd harmonic voltage = 19.8 V (rms), and 5th harmonic voltage = 3.96 V (rms).

Table 5.3. Effect of harmonics on the primary efficiency (space harmonics are taken into account)[a]

Per unit speed	Prim. eff. (no time harmonics)	Prim. eff. (with time harmonics)
0.00	0.000000	0.000000
0.05	0.023261	0.023212
0.10	0.044861	0.044767
0.15	0.066207	0.066070
0.20	0.090217	0.090030
0.25	0.116902	0.116649
0.30	0.145158	0.144837
0.35	0.175602	0.175209
0.40	0.208743	0.208269
0.45	0.245065	0.244484
0.50	0.285111	0.284419
0.55	0.329515	0.328688
0.60	0.379033	0.378041
0.65	0.434579	0.433375
0.70	0.497259	0.495768
0.75	0.568390	0.566485
0.80	0.649505	0.646950
0.85	0.742171	0.738470
0.90	0.846966	0.840842
0.95	0.955545	0.942120
1.00	-0.337778	-0.245724

[a]Fundamental voltage = 220.0 V (rms), 3rd harmonic voltage = 19.8 V (rms), and 5th harmonic voltage = 3.96 V (rms).

VI. CONCLUSIONS

Comprehensive and rigorous electromagnetic field analyses for induction motors have been presented in this dissertation. These analyses may be used to predict motor performance and to enhance the methods of motor design. The analyses presented are based on the solution of a system of partial differential equations that faithfully express the field phenomena in the different regions of the induction motor. The following paragraphs describe the principal contributions of this dissertation.

1. The field analyses are presented from a very general point of view that can be used to get the field structure in the different zones of the machine under any electric and magnetic loading designs. The approach used in these analyses can be equally applied to single- and two-phase machines, as well as to the theories of linear machines. It also can be applied to the magnetohydrodynamics area as in the case of liquid metal induction pumps.

2. A short cut method for the field analysis has been developed to determine the fields in only the required regions of the motor. This method greatly simplifies the analytical expression used to describe the field quantities, as well as the computer work required to get these values.

3. A generalization of the transmission-line concept for solving the field problem has been introduced, for the first time, in a way that permits the inclusion of the field constraints imposed by the

complicated structure of the induction machine.

4. The analyses presented suggest new design features and parameters to improve the motor performance. The following paragraphs describe some of these examples.

i. The tooth-top opening of the slotted structure plays a dominant role in controlling the transfer of electromagnetic energy from the primary side to the secondary side. This energy is greatly reduced by the decrease of the slot opening and will be zero for a closed slot structure with highly permeable iron.

ii. The end ring of the squirrel cage structure can greatly influence the performance of the induction motor. This dissertation presents, for the first time, the detailed equations necessary to get the optimal machine performance by properly designing the end ring of the rotor structure.

iii. The effect of the space harmonics is limited to the low speed range, so its effect on the machine performance can be neglected in the operating range of the machine (in the low slip range).

iv. Time harmonic voltage (9% third harmonic and 1.8% fifth) has a very small effect on the torque-speed characteristic. This amount of time harmonic voltage reduces the overall efficiency of the motor by about 1% in the working speed range.

5. This dissertation suggests a reformulation of some of the basic ideas used in the electromagnetic theory of electrical machine analysis. An example is the use of an equivalent current sheet for the primary windings. This practice may not allow a proper understanding of the phenomena taking place in the machines.

VII. BIBLIOGRAPHY

1. Alden, R. T. H. "Transfer-matrix Analysis of Linear Induction Machines with Finite Width and Depth." Proc. IEE 121 [11] (November 1974): 1393-1398.

2. Alger, P. L. and West, H. R. "The Air Gap Reactance of Polyphase Machines." AIEE Transactions 66 (1947): 1331-1343.

3. Alger, P. L. The Nature of Polyphase Induction Machines. New York: John Wiley and Sons, 1951.

4. Alger, P. L. "Induced High-Frequency Currents in Squirrel Cage Windings." AIEE Transactions PAS-76, Part III (1957): 724-729.

5. Alger, P. L., Angst, G. and David, E. J. "Stray-Load Losses in Polyphase Induction Machines." AIEE Transactions PAS-78, Part III-A (June 1959): 349-357.

6. Anderson, G. R. "The 'Copperspun' Squirrel Cage Rotor." AIEE Transactions 66 (1947): 1312-1314.

7. Barton, T. H. and Ahmad, V. "The Measurement and Prediction of Induction Motor Stray Loss at Large Slips." Proc. IEE 104, Part C (September 1957): 299-304.

8. Behrend, B. A. The Induction Motor. 2nd ed. New York: McGraw-Hill, 1921.

9. Binns, K. J. and Lawrenson, P. J. Analysis and Computation of Electric and Magnetic Field Problems. New York: Pergamon Press, 1963.

10. Binns, K. J. and Dye, M. "Effects of Slot Skew and Iron Saturation on Cogging Torques in Induction Machines." Proc. IEE 117 [7] (July 1970): 1249-1252.

11. Bird, B. M. "Measurement of Stray Load Losses in Squirrel-Cage Induction Motors." Proc. IEE 111 [10] (October 1964): 1697-1705.

12. Booker, H. G. "The Elements of Wave Propagation Using the Wave-Impedance Concept." Journal IEE 94, Part III (May 1947): 171-202.

13. Burbridge, R. E. "A Rapid Method of Analyzing the M.M.F. Wave of a Single or Polyphase Winding." Proc. IEE 105, Part C (January 1958): 307-311.

14. Burbridge, R. F. and Fryett, M. L. "Synchronous and Asynchronous Torques in Squirrel Cage Induction Motors." Proc. IEE 114 [11] (November 1967): 1665-1673.

15. Carter, F. W. "Note on Air-Gap and Interpolar Induction." Journal Proc. IEE 29, Part 146 (1900): 925-933.

16. Carter, F. W. "Air-Gap Induction." Electrical World and Engineering 38 [22] (November 1901): 884-888.

17. Charlmers, B. J. and Williamson, A. C. "Stray Losses in Squirrel-Cage Induction Motors. Validity of the Reverse-Rotation Test Method." Proc. IEE 110 [10] (October 1963): 1773-1778.

18. Charlmers, B. J. and Richardson, J. "Investigation of High-Frequency No-Load Losses in Induction Motors with Open Stator Slots." Proc. IEE 113 [10] (October 1966): 1597-1605.

19. Charlmers, B. J. and Sarker, B. R. "High-Frequency Effects in Induction Motors." Proc. IEE 114 [10] (October 1967): 1518-1519.

20. Charlmers, B. J. and Sarker, B. R. "Induction Motor Losses due to Nonsinusoidal Supply Wave Forms." Proc. IEE 115 [12] (December 1968): 1777-1782.

21. Christofides, N. and Adkins, B. "Determination of Load Losses and Torques in Squirrel-Cage Induction Motors." Proc. IEE 113 [12] (December 1966): 1995-2005.

22. Christofides, N. "Origin of Load Losses in Induction Motors with Cast Aluminum Rotors." Proc. IEE 112 [12] (December 1965): 2317-2332.

23. Ciganek, L. "Air Gap Under the Saturated Tooth of an Induction Motor." IEEE Transactions PAS-87 [11] (November 1968): 1918-1924.

24. Correspondence. "Tooth-Ripple Losses in Solid Poles." Proc. IEE 113 [11] (November 1966): 1864-1867.

25. Creedy, F. "Electric Wave Phenomena in the Dynamo-Electric Machine." Journal IEE 55 (1917): 450-472.

26. Cullen, A. L. and Barton, T. H. "A Simplified Electromagnetic Theory of the Induction Motor, Using the Concept of Wave Impedance." Proc. IEE 105, Part C (September 1958): 331-336.

27. Davey, K. R. and Barnes, W. J. "Three-Dimensional Eddy Current Problems Using the Tee-Omega Method and Fredholm Integral Equations." IEEE Transactions on Magnetics MAG-19 (March 1983): 120-125.

28. Discussion on "Electromagnetic Theory of Electrical Machines." Proc. IEE 112 [10] (October 1965): 1927-1932.

29. Discussion on "Application of Linear Induction Motors to High Speed Transport System." Proc. IEE 117 [7] (July 1970): 1253-1256.

30. Dorairaj, K. R. and Krishnamurthy, M. R. "Polyphase Induction Machine with a Slitted Ferromagnetic Rotor: I. Experimental Investigations and a Novel Slipmeter." IEEE Transactions PAS-86 [7] (July 1967): 835-843.

31. Dorairaj, K. R. and Krishnamurthy, M. R. "Polyphase Induction Machine with a Slitted Ferromagnetic Rotor: II. Analysis." IEEE Transactions PAS-85 [7] (July 1967): 844-855.

32. Douglas, J. F. H. "The Reluctance of Some Irregular Magnetic Fields." AIEE Transactions 34, Part 1 (1915): 1067-1134.

33. Ellison, A. J. and Moore, C. J. "Acoustic Noise and Vibration of Rotating Electric Machines." Proc. IEE 115 (1968): 1633-1640.

34. Fitzgerald, A. E., Kingsley, C. J. and Umans, S. D. Electric Machinery. 4th ed. New York: McGraw-Hill, 1983.

35. Fortiscue, C. L. "Method of Symmetrical Coordinates Applied to the Solution of Polyphase Networks." AIEE Transactions 37, Part II (1918): 1027-1140.

36. Freeman, E. M. "The Calculations of Harmonics, Due to Slotting, in the Flux-Density Waveforms of a Dynamo-Electric Machine." Proc. IEE 109 [16], Part C (June 1962): 581-588.

37. Freeman, E. M. "Travelling Waves in Induction Machines: Input Impedance and Equivalent Circuits." Proc. IEE 115 [12] (December 1968): 1772-1776.

38. Freeman, E. M. "Equivalent Circuits from Electromagnetic Theory Low-Frequency Induction Devices." Proc. IEE 124 [10] (October 1974): 1117-1121.

39. Freeman, E. M. "Computer-Aided Steady-State and Transient Solutions of Field Problems in Induction Devices." Proc. IEE 124 [11] (November 1977): 1057-1061.

40. Freeman, E. M. and Smith, B. E. "Surface-Impedance Method Applied to Multilayer Cylindrical Induction Devices with Circumferential Exciting Currents." Proc. IEE 117 [10] (October 1970): 2012-2013.

41. Fuchs, E. F., Roesler, D. J. and Alashhab, F. S. "Sensitivity of Electrical Appliances to Harmonics and Fractional Harmonics of the Power System Voltage. Part I: Transformers and Induction Machines." Paper 86 WM 170-5, IEE/PES Winter Meeting, New York (February 1986).

42. Fuchs, E. F., Roesler, D. J. and Kovas, K. P. "Aging of Electrical Appliances to Harmonics of the Power System's Voltage." Paper 86 WM 169-7, IEE/PES Winter Meeting, New York (February 1986).

43. Gieras, J. F., Dawson, G. E. and Eastham, A. R. "Performance Calculation for Single-Sided Linear Induction Motors with a Double-Layer Reaction Rail Under Constant Current Excitation." IEEE Transactions on Magnetics MAG-22 (January 1986): 54-62.

44. Graham, Q. "Dead Points in Squirrel-Cage Motors." AIEE Transactions 59 (1940): 637-642.

45. Greig, J. and Freeman, E. M. "Travelling-Wave Problem in Electrical Machines." Proc. IEE 114 [11] (November 1967): 1681-1683.

46. Hague, B. The Principles of Electromagnetism Applied to Electrical Machines. New York: Dover Publications, Inc., 1962.

47. Harris, M. R. and Fam, W. Z. "Analysis and Measurement of Radial Power Flow in Machine Air Gaps." Proc. IEE 113 [10] (October 1966): 1607-1615.

48. Heartz, R. A. and Saunders, R. M. "Harmonics Due to Slots in Electric Machines." AIEE Transactions 73, Part III-B (1954): 946-949.

49. Hellmond, R. E. "Graphical Treatment of Zigzag and Slot Leakages in Induction Motors." Journal IEE 45 [202] (1910): 239-273.

50. Hesmondhalgh, D. E. and Tipping, D. "Miniature Sheet-Rotor Induction Motors for Extremely High Speeds." Proc. IEE 130, Part B [4] (July 1983): 265-277.

51. Hesmondhalgh, D. E. and Tipping, D. "Effect of Stator Slotting on the Performance of Sheet-Rotor Induction Motors." Proc. IEE 130, Part B [6] (November 1983): 381-391.

52. Jain, G. C. "The Effect of Voltage Wave Shape on the Performance of a 3-Phase Induction Motor." IEEE Transactions PAS-83 (June 1964): 561-566.

53. Klingshirn, E. A. and Jordan, H. E. "Polyphase Induction Motor Performance and Losses on Non-sinusoidal Voltage Sources." IEEE Transactions PAS-87 (March 1968): 624-631.

54. Krause, P. C. Analysis of Electric Machinery. New York: McGraw-Hill, 1986.

55. Kron, G. "Equivalent Circuit for the Hunting Electrical Machinery." AIEE Transactions 61 (1942): 290-296.

56. Kron, G. "Tensorial Analysis and Equivalent Circuit of a Variable-Ratio Frequency Changer." AIEE Transactions 66 (1947): 1503-1506.

57. Langsdorf, A. S. Theory of Alternating-Current Machinery. New York: McGraw-Hill, 1955.

58. Lawrenson, P. J., Reece, P. and Ralph, M. C. "Tooth-Ripple Losses in Solid Poles." Proc. IEE 113 [4] (April 1966): 657-662.

59. Liwschitz, M. M. "Field Harmonic in Induction Motors." AIEE Transactions 61 (1942): 797-803.

60. Liwschitz, M. M. "Differential Leakage with Respect to the Fundamental Wave and to the Harmonics." AIEE Transactions 63 (1944): 1139-1149.

61. Liwschitz, M. M. "Leakage Reactance of the Squirrel Cage Rotor with Respect to the Stator Harmonics and the Equivalent Circuit of the Induction Motor." AIEE Transactions 66 (1947): 1407-1408.

62. Liwschitz, M. M. and Formhals, W. H. "Some Phases of Calculation of Leakage Reactance of Induction Motors." AIEE Transactions 66 (1947): 1409-1413.

63. Moore, A. D. Fundamentals of Electrical Design. New York: McGraw-Hill, 1927.

64. Morill, W. J. "Harmonic Theory of Noise in Induction Motors." AIEE Transactions 59 (1940): 474-480.

65. Nasar, N. A. "Electromagnetic Theory of Electrical Machines." Proc. IEE 111 [6] (June 1964): 1123-1131.

66. Neville, S. "Use of Carter's Coefficient with Narrow Teeth." Proc. IEE 114 [9] (September 1967): 1245-1250.

67. Odok, A. M. "Stray-Load Losses and Stray Torques in Induction Machines." AIEE Transactions PAS-77, Part III (April 1958): 43-53.

68. Piggot, L. S. "A Theory of the Operation of Cylindrical Induction Motors with Squirrel-Cage Rotors." Proc. IEE 108 (December 1961): 270-282.

69. Poloujadoff, M. and El-Khashab, H. "A Finite Difference Model of Linear Induction Motors, Taking Into Account the Finite Length of Iron." IEEE Transactions PAS-101 [8] (August 1982): 2966-2974.

70. Puchstein, A. F. "Calculation of Slot Constants." AIEE Transactions 66 (1947): 1315-1323.

71. Rawcliff, G. H. and Menon, A. M. "Test for Harmonic-Frequency Losses in A.C. Machines." Proc. IEE 104, Part II (April 1952): 145-150.

72. Reece, A. B. J. and Pramanic, A. "Calculation of the End-Region Field of a.c. Machines." Proc. IEE 112 [7] (July 1965): 1355-1368.

73. Silvester, P. "Eddy-Current Modes in Linear Solid-Iron Bars." Proc. IEE 112 [8] (August 1965): 1589-1594.

74. Silvester, P. "Dynamic Resistance and Inductances of Slot-Embedded Conductors." IEEE Transactions PAS-87 (January 1968): 250-256.

75. Singh, G. and Singh, B. "Asymmetric Three-Phase Induction Motors, Crossed-Field Analysis: Extension to Single- and Two-Phase Motors." IEEE Transactions PAS-98 [4] (July/August 1979): 1251-1258.

76. Spooner, T. and Kinnard, I. F. "Surface Iron Losses with Reference to Laminated Materials." AIEE Transactions 43 (1924): 262-281.

77. Stratford, R. P. "Harmonic Pollution on Power Systems - A Change in Philosophy." IEEE Transactions on Industry Applications 1A-16 [5] (September/October 1980): 43-49.

78. Subrahmanyam, V. "Axial Forces in Induction Motors with Skewed Slots." Proc. IEE 118 [12] (December 1971): 1759-1760.

79. Vickers, H. The Induction Motor. 2nd ed. London: Sir Isaac Bitman and Sons, 1953.

80. Walker, J. H. "Theory of Induction Motor Surface Losses." Journal IEE 95, Part II (October 1948): 597-606.

81. Ware, D. H. "Measurement of Stray-Load Loss in Induction Motors." AIEE Transactions 64 (1945): 194-196.

82. Weber, C. A. and Lee, F. W. "Harmonics Due to Slot Openings." AIEE Transactions 43 (1924): 939-941.

83. West, J. C. and Hesmondhalgh, D. E. "The Analysis of Thick-Cylinder Induction Machines." Proc. IEE 108 (November 1961): 172-181.

84. Williams, F. C. and Mamark, R. S. "Electromagnetic Forces in Slotted Structures." Proc. IEE 108 (July 1961): 11-17.

85. Williams, F. C., Laithwaite, E. R. and Piggott, L. S. "Brushless Variable-Speed Induction Motors." Proc. IEE 104, Part A (April 1957): 102-122.

86. Williamson, S. "Calculation of the Resistance of Induction Motor End Rings." Proc. IEE 133, Part B [2] (March 1986): 54-60.

VIII. ACKNOWLEDGMENTS

The author wishes to express his gratitude to his co-major professors, Dr. Robert E. Post and Dr. A. L. Day, for their helpful discussions and assistance during the research work.

Special thanks are given to Professor A. A. Read, and thanks to the committee members, Dr. K. C. Kruempel and Dr. R. J. Lambert.

The author wishes to express his gratitude to his wife, Samia Zaki, for her understanding and patience throughout this research work. God bless them all.

IX. APPENDIX: FORTRAN PROGRAM FOR CALCULATING THE MOTOR PERFORMANCE

```
C
C
C
C
C
C
C
C
C
C
C     THIS PROGRAM COMPUTES THE PERFOERMANCE OF AN INDUCTION MOTOR.
C                        EIGHT-REGION MODEL
C   SECONDARY SLOT, SECONDARY TOOTH TOP, AIR GAP, PRIMARY TOOTH TOP
C                 AND PRIMARY CURRENT REGION
C         SECONDARY END RING IS TAKEN INTO ACCOUNT
C   SEE SUBROUTINE RGMTRX. BOTH THE PRIMARY AS WELL AS THE PRIMARY
C   OVERHANG REGIONS ARE MODELLED BY FINITE THICKNESS REGIONS. THE
C   UPPER AND THE LOWER REGIONS ADJACENT TO THESE REGIONS ARE EITHER
C   OF FINITE OR INFINIT PERMEABILITIES. Z0E IS CALCULATED FROM
C   THE E-H APPROACH, THEN CHANGED TO B-H APPROACH, SEE SUB. RGMTRX.
C
      COMPLEX CIH(3),FTH,FNH,PSH,PINH
      COMPLEX VLTG(3),ENT(3),Z(3,3),CI(3),FT,FN,PS,PINC
      REAL D(4),R(3)
C
C     THE FOLLOWING ARE THE DRAWING PARAMETERS :
      COMPLEX CIDR(3,25)
      REAL FDR(25),FNDR(25),PSDR(25),PPDR(25),EFSDR(25),EFPDR(25),
     *     PFSDR(25),PFPDR(25),SPRDR(25)
C
      COMMON NRG,DP,BO,BS,BOS,BSS,TAUS,TAUSS,SLTF,W2,WI,WH,WE
     $,PRM0,PRMR,EM,P,Q,TAU,U,CNDPP,HZ,PI,SEG,SEGE,OMG,VS
      COMMON /MPIMFP/ SSPH,NSPH,DSPH
C
C     MOTOR DESIGN PARAMETERS :
C
C     D(I), I=1,4 : region thickness,   DP : prim. thick.,  BS : prim
C     slot open.,  BO : prim. tooth top open,  BSS : sec. slot open.,
C     BOS : sec tooth top open.,    TAUS : prim. slot pitch,  TAUSS :
C     sec. slot pitch, SLTF : sec. slot factor (cu. area/ slot area),
C     W2 : sec. width,   WI : prim. iron width,   WH : prim. overhang
C     width, WE : sec. end ring width, PRMR : sec. and prim. relative
C     permeability,    EM : no. of phases,     P : no. of pole pairs,
C     Q : no. of slots/ pole/ phase,       U : no. of chording slots,
C     TAU : prim pole pitch,       CNDPP : no. of cond./ pole pairs,
C     R(I), I=1,3 : prim. phase resist.,   HZ : frequency, SEG : sec.
C     conductivity,   NSPH : no. of space harmonics,  SSPH : starting
```

```
C     space harmonic,     DSPH : difference bet. two successive space
C     harmonics,   NTH : no. of time harmonics,   STH : starting time
C     harmonic,  DTH : difference bet. two successive time harmonics.
C
C    READING THE MOTOR PARTICULARS :
C
      READ (12,*) NRG
      READ (12,*) (D(I),I=1,4),DP
      READ (12,*) BO,BS,BOS,BSS,TAUS,TAUSS,SLTF
      READ (12,*) W2,WI,WH,WE,PRMR,EM,P,Q,U
      READ (12,*) CNDPP,(R(I),I=1,3),HZ
      TAU  =  EM*Q*TAUS
      SEG  = 0.574E+08 * 0.6
      SEGE = 2.0 * SEG
      PI   = 4.0*ATAN(1.0)
      PRM0 = 4.0*PI*1.0E-07
      OMG  = 2.0 * PI * HZ
      VS   = 2.0 * TAU * HZ
C
C    Specifications of space and time harmonics, time Harmonics are
C   only in Main Program. For balanced operations, DSPH = 2.0*EM.
C
      SSPH =  -11.0
      NSPH =  13
      DSPH =  2.0
      STH  =  1.0
      NTH  =  3
      DTH  =  2.0
C
C   No. of data points, NDTP :
C
      NDTP = 20
C
C          THE WRITING STAEMENTS OF THE MTOR DESIGN PARAMETERS
C
      WRITE (6,19)
   19 FORMAT (/10X,'****************************************',/)
      WRITE (6,11)
   11 FORMAT (/17X,'MOTOR DESIGN PARAMETERS (ROTDRW3, Y-CONN) :'/)
      WRITE (6,12)
   12 FORMAT (/5X,'NRG, D(1), D(2), D(3), D(4), DP, BO, BS, BOS :'/)
      WRITE (6,13) NRG,(D(I),I=1,4),DP,BO,BS,BOS
   13 FORMAT (I8,8F12.5)
      WRITE (6,14)
   14 FORMAT (/5X,'BSS, TAUS, TAUSS, SLTF, W2, WI, WH, PRMR, EM :'/)
      WRITE (6,18) BSS,TAUS,TAUSS,SLTF,W2,WI,WH,PRMR,EM
      WRITE (6,15)
   15 FORMAT (/5X,'U, TAU, CNDPP, R(I): I=1,3 , HZ, SEG, SEGE :'/)
      WRITE (6,185) U,TAU,CNDPP,(R(I),I=1,3),HZ,SEG,SEGE
   18 FORMAT (9F12.5)
```

```
 185  FORMAT (7F11.4,2E14.4)
      WRITE (6,186)
 186  FORMAT (/5X,'SSPH, NSPH, DSPH, STH, NTH, DTH and (NDTP) : '/)
      WRITE (6,187) SSPH,NSPH,DSPH,STH,NTH,DTH,NDTP
 187  FORMAT (F12.4,I8,2F12.4,I8,F12.4,5X,'NDTP =',I6)
      WRITE (6,19)
C
      SPR = 0.0
      DSPR = - 0.1
      DO 90 II = 1,NDTP
C
      IF (ABS(SPR).GT.0.7) DSPR = -0.05
      IF (ABS(SPR).GT.0.8) DSPR = -0.025
      IF (ABS(SPR).EQ.1.0) SPR = 1.005 * SPR
      V = SPR * VS
C
C     THE LINE VOLTAGES (Y-CONN.), GIVEN HERE IS -ive PHASE SEQUENCE,
C
      VLTG(1) = (0.0,220.0)
      VLTG(2) = (0.0,220.0) * (-0.500000, 0.866025)
      VLTG(3) = (0.0,220.0) * (-0.500000,-0.866025)
C
C     Initialization the parameters :
C
      DO 17 I = 1,3
      CIH(I) = (0.0,0.0)
  17  CONTINUE
      FTH = (0.0,0.0)
      FNH = (0.0,0.0)
      PSH = (0.0,0.0)
      PINH = (0.0,0.0)
C
      EN = STH
      DO 35 KK = 1,NTH
C
      IF (KK.EQ.1) GO TO 25
      IF (KK.EQ.2) HRAT = 0.09
      IF (KK.EQ.3) HRAT = 1.0 / EN
      IF (KK.GE.4) HRAT = (EN-DTH) / EN
C
      DO 23 I = 1,3
      VLTG(I) = HRAT * VLTG(I)
  23  CONTINUE
  25  CONTINUE
C
      CALL IMPEDN(EN,R,D,V,Z)
C
C    Formation of the R.H. entries of the VLTG-CURR  Matrix
```

```
C
      DO 51 I = 1,3
      ENT(I) = VLTG(I)
      IF (I.EQ.3) ENT(I) = (0.0,0.0)
   51 CONTINUE
C
      CALL CURRNT(Z,ENT,CI,JJ)
C        JJ is a control integer which stpos the program, if the value
C     of the determinant is zero as comming from the subroutine CURRNT
C
      IF (JJ.EQ.0) GO TO 200
C
      CALL FRCENP(EN,V,D,CI,FT,FN,PS)
C
      PINC = (0.0,0.0)
      DO 29 I = 1,3
      PINC = PINC + VLTG(I) * CONJG(CI(I)) / SQRT(3.0)
   29 CONTINUE
      PINH = PINH + PINC
C
      DO 27 I = 1,3
      CIH(I) = CIH(I) + CI(I)
      CIDR(I,II) = CIH(I)
   27 CONTINUE
C
      FTH = FTH + FT
      FNH = FNH + FN
      PSH = PSH + PS
C
      EN = EN + DTH
   35 CONTINUE
C
      EFF = - V * REAL(FTH) / REAL(PSH)
      PFC = REAL(PSH) / CABS(PSH)
C
      TEFF = - V * REAL(FTH) / REAL(PINH)
      TPFC = REAL(PINH) / CABS(PINH)
C
      FDR(II)  = REAL(FTH)
      FNDR(II) = REAL(FNH)
      PSDR(II) = REAL(PSH)
      PPDR(II) = REAL(PINH)
      EFSDR(II) = EFF
      EFPDR(II) = TEFF
      PFSDR(II) = PFC
      PFPDR(II) = TPFC
      SPRDR(II) = ABS(SPR)
C
      SPR = SPR + DSPR
   90 CONTINUE
```

```
C
C              THE WRITING STATEMENTS OF THE RESULTS
C
      WRITE (6,96)
   96 FORMAT (///5X,'SPR-LINE CURRENTS :'/)
      DO 97  I = 1,NDTP
      WRITE (6,98) SPRDR(I),(CIDR(J,I),J=1,3)
   97 CONTINUE
   98 FORMAT (1F10.4,' :   ',6E14.6)
C
      WRITE (6,101)
  101 FORMAT(///5X,'SPR-TANG. FORCE CHARACTERISTICS',/)
      DO 102 I = 1,NDTP
      WRITE (6,150) SPRDR(I),FDR(I)
  102 CONTINUE
C
      WRITE (6,103)
  103 FORMAT (///5X,'SPR-NORM. FORCE CHARACTERISTICS',/)
      DO 104 I = 1,NDTP
      WRITE(6,150) SPRDR(I),FNDR(I)
  104 CONTINUE
C
      WRITE (6,105)
  105 FORMAT (///5X,'SPR-SEC. POWER CHARACTERISTICS',/)
      DO 106 I = 1,NDTP
      WRITE (6,150) SPRDR(I),PSDR(I)
  106 CONTINUE
C
      WRITE (6,107)
  107 FORMAT (///5X,'SPR-PRIM. INP. POWER CHARACTERISTICS'/)
      DO 108 I = 1,NDTP
      WRITE (6,150) SPRDR(I),PPDR(I)
  108 CONTINUE
C
      WRITE (6,109)
  109 FORMAT (///5X,'SPR-SEC. EFFICIENSY CHARACTERICS',/)
      DO 110 I = 1,NDTP
      WRITE (6,150) SPRDR(I),EFSDR(I)
  110 CONTINUE
C
      WRITE (6,111)
  111 FORMAT (///5X,'SPR-PRIM. EFFICIENCY CHARACTERISTICS',/)
      DO 112 I = 1,NDTP
      WRITE (6,150) SPRDR(I),EFPDR(I)
  112 CONTINUE
C
      WRITE (6,113)
  113 FORMAT (///5X,'SPR-SEC. P.F. CHARACTERISTICS',/)
```

```
      DO 114 I = 1,NDTP
      WRITE (6,150) SPRDR(I),PFSDR(I)
 114  CONTINUE
C
      WRITE (6,115)
 115  FORMAT (///5X,'SPR-PRM. P.F. CHARACTERISTICS',/)
      DO 116 I = 1,NDTP
      WRITE (6,150) SPRDR(I),PFPDR(I)
 116  CONTINUE
C
 150  FORMAT (2F15.6)
C
 200  CONTINUE
C
      STOP
      END
C
C ****************************************************************
C         THE 3 MAIN SUBROUTINES : IMPEDN, CURRNT AND FRCENP
C ****************************************************************
C
      SUBROUTINE IMPEDN(EN,R,D,V,Z)
C
C  THIS SUBROUTINE DETERMINES THE 9 ENTRIES OF THE MATRIX [Z], GIVEN
C     BY THE EQN.  I * Z = VLTG, AT A CERTAIN SPEED V.
C
      REAL R(3),D(4)
      COMPLEX Z(3,3),Z0S,Z0H,ZM(3,3),Z0E,FCI(3),FCH(3),CMF,
     $        EKW,EKWM,C1,C2
C
      COMMON NRG,DP,BO,BS,BOS,BSS,TAUS,TAUSS,SLTF,W2,WI,WH,WE
     $,PRM0,PRMR,EM,P,Q,TAU,U,CNDPP,HZ,PI,SEG,SEGE,OMG,VS
      COMMON /IMNFRC/ PRMX,PRMY,Z0S,Z0H
      COMMON /MPIMFP/ SSPH,NSPH,DSPH
C
C     Primary region parameters and boundaries :
C
      PRM  = PRM0 * PRMR
      PRMX = PRM/(1.0+(PRMR-1.0)*BS/TAUS)
      PRMY = PRM*(1.0 + (1.0/PRMR - 1.0) * BS/TAUS)
      Z0S  = (0.0,1.0E+20)
      Z0H  = (0.0,0.01) * PRM0
C
C  Z0E : input impedance at the lower prim. interf. (sec. rgn.)
C  Z0H : input impedance at the lower prim. interf. (overhang rgn.)
C  Z0S : input impedance at the upper prim. interf. (back  rgn.)
C
```

```
      DO 30 J = 1,3
      DO 20 I = 1,3
      ZM(I,J) = (0.0,0.0)
   20 CONTINUE
   30 CONTINUE
C
          CTR  = - P/(2.0*TAU) * CNDPP*CNDPP
C
          RN   = SSPH
          N1   = NSPH
          JJ   = 1
      DO 40 I = 1,N1
C
C     Primary iron  region:
C
          CALL RGMTRX(RN,EN,D,V,Z0E)
C
          PENF = 1.0
          CALL FIELDC(RN,EN,PRMX,PRMY,Z0E,Z0S,PENF,FCI)
C
C     Overhang region with iron back (Z0S is very large) :
C
          OENF = 1.0
          CALL FIELDC(RN,EN,PRM0,PRM0,Z0H,Z0S,OENF,FCH)
          CALL WDGFAC(RN,EKW,EKWM)
C
      CMF = CTR * EKW * CONJG(EKW) * (WI*FCI(3) + WH*FCH(3))
C
C     THE INDUCED VOLTAGE REVERSES SIGN AS (V .GT. VS)
      IF (ABS(V).GT.ABS(VS)) CMF = - CMF
C
C    THE FOLLOWING STATEMENTS NEEDED FOR THE ACCURACY FOR SMALL RESIS
      IRN = RN
      IF (IRN.EQ.1) THEN
      C1 = (-0.500000, -0.866025)
      C2 = (-0.500000,  0.866025)
      ELSE
      C1  = CEXP ((0.0,-1.0)*2.0*PI*RN/3.0)
      C2  = CEXP ((0.0,-1.0)*4.0*PI*RN/3.0)
      END IF
C
C    Formation of the machine self and mutual impedances
C
      ZM(1,1) = ZM(1,1) + CMF
      ZM(1,2) = ZM(1,2) + CMF*C1
      ZM(1,3) = ZM(1,3) + CMF*C2
C
      ZM(2,1) = ZM(2,1) + CMF/C1
      ZM(2,2) = ZM(1,1)
      ZM(2,3) = ZM(2,3) + CMF*C1
```

```
C
      ZM(3,1) = ZM(3,1) + CMF/C2
      ZM(3,2) = ZM(3,2) + CMF/C1
      ZM(3,3) = ZM(1,1)
C
      RN = RN + DSPH
   40 CONTINUE
C
      DO 70 I = 1,3
      ZM(I,I) = ZM(I,I) + R(I)
   70 CONTINUE
C
C     Formatio of the Entries of the VLTG-CURR Matrix.
C
      Z(1,1) = ZM(1,1) - ZM(2,1)
      Z(1,2) = ZM(1,2) - ZM(2,2)
      Z(1,3) = ZM(1,3) - ZM(2,3)
C
      Z(2,1) = ZM(2,1) - ZM(3,1)
      Z(2,2) = ZM(2,2) - ZM(3,2)
      Z(2,3) = ZM(2,3) - ZM(3,3)
C
      Z(3,1) = (1.0,0.0)
      Z(3,2) = (1.0,0.0)
      Z(3,3) = (1.0,0.0)
C
      RETURN
      END
C
C ********************************************************************
C
      SUBROUTINE CURRNT(Z,VLTG,CI,JJ)
C
C     SUBROUTINE CURRENT:
C                        THIS SUBROUTINE SOLVES A 3*3 SYSTEM OF
C   MACHINE IMPEDANCE EQUATIONS. THE INPUT IS THE MACHINE IMPEDANCE
C   ARRAY Z(3,3) AND THE APPLIED VOLTAGE VLTG(3); AND THE OUTPUT
C   IS THE MACHINE PHASE/DELTA OR LINE/WYE CURRENTS.
C   JJ : A CONTROL INTEGER = 0, WHEN THE MATRIX RANK < 3.
C
      COMPLEX Z(3,3),VLTG(3),CI(3),DET
      INTEGER JJ
C
      JJ = 1
      DET = Z(1,1)*Z(2,2)*Z(3,3) + Z(1,2)*Z(2,3)*Z(3,1)
     $    + Z(1,3)*Z(2,1)*Z(3,2) - Z(3,1)*Z(2,2)*Z(1,3)
     $    - Z(3,2)*Z(2,3)*Z(1,1) - Z(3,3)*Z(2,1)*Z(1,2)
C
C   NEED TO CHEK THE MATRIX RANK IF DET = 0, THE RANK < 3.
C
```

```
      IF (CABS(DET).LE.7.0E-6) THEN
      JJ = 0
      WRITE (6,100)
      RETURN
      END IF
C
      CI(1) = VLTG(1) * ( Z(2,2)*Z(3,3) - Z(2,3)*Z(3,2) )
     $      + VLTG(2) * ( Z(1,3)*Z(3,2) - Z(1,2)*Z(3,3) )
     $      + VLTG(3) * ( Z(1,2)*Z(2,3) - Z(1,3)*Z(2,2) )
      CI(1) = CI(1)/DET
C
      CI(2) = VLTG(1) * ( Z(2,3)*Z(3,1) - Z(2,1)*Z(3,3) )
     $      + VLTG(2) * ( Z(1,1)*Z(3,3) - Z(1,3)*Z(3,1) )
     $      + VLTG(3) * ( Z(1,3)*Z(2,1) - Z(1,1)*Z(2,3) )
      CI(2) = CI(2)/DET
C
      CI(3) = VLTG(1) * ( Z(2,1)*Z(3,2) - Z(2,2)*Z(3,1) )
     $      + VLTG(2) * ( Z(1,2)*Z(3,1) - Z(1,1)*Z(3,2) )
     $      + VLTG(3) * ( Z(1,1)*Z(2,2) - Z(1,2)*Z(2,1) )
      CI(3) = CI(3)/DET
C
      RETURN
C
 100  FORMAT (/' SOLUTION NOT FEASIBLE. MATRIX RANK < 3',
     $' THE DETEMINANT OF THE IMPED. MAT. = ZERO'//)
      END
C
C ***************************************************************
C
      SUBROUTINE FRCENP(EN,V,D,CI,FT,FN,PW)
C
C THIS SUBROUTINE COMPUTES THE TANGENTIAL FORCE FT (&FX), THE
C NORMAL   FORCE, FN, AND THE SECONDARY INPUT POWER PW AT A CERTAIN
C SPEED V. THE INPUT ARE THE SPEED AND THE PHASE CURRENTS I(1),
C I(2) AND I(3),AS WELL AS THE REGION THICKNESSES D(1),...,D(4).
C
      COMPLEX CI(3),FT,FN,PW,Z0S,Z0H,EKW,EKWM,C1,C2,CJ,CNJ
     $       ,Z0E,FCI(3),FCH(3)
      REAL D(4)
C
      COMMON NRG,DP,BO,BS,BOS,BSS,TAUS,TAUSS,SLTF,W2,WI,WH,WE
     $,PRM0,PRMR,EM,P,Q,TAU,U,CNDPP,HZ,PI,SEG,SEGE,OMG,VS
      COMMON /IMNFRC/ PRMX,PRMY,Z0S,Z0H
      COMMON /MPIMFP/ SSPH,NSPH,DSPH
C
      OMGN = EN * OMG
C
      FT = (0.0,0.0)
      FN = (0.0,0.0)
      PW = (0.0,0.0)
```

```
C
            CTC = 1.0/(2.0*TAU)
            CTF = - 2.0 * TAU * P
C
          RN  = SSPH
          N1  = NSPH
       DO 40 I = 1,N1
C
C      Current calculations :
C
       CALL WDGFAC(RN,EKW,EKWM)
C
C  THE FOLLOWING STATEMENTS NEEDED FOR THE ACCURACY FOR SMALL RESIS.
       IRN = RN
       IF (IRN.EQ.1) THEN
       C1 = (-0.500000, -0.866025)
       C2 = (-0.500000,  0.866025)
       ELSE
       C1  = CEXP ((0.0,-1.0)*2.0*PI*RN/3.0)
       C2  = CEXP ((0.0,-1.0)*4.0*PI*RN/3.0)
       END IF
C
       CJ = CTC * CNDPP*EKW * (CI(1)+CI(2)*C1+CI(3)*C2)
       CNJ = CONJG(CJ)
C
C      The field coefficients of the iron region
C
       CALL RGMTRX(RN,EN,D,V,Z0E)
       PENF =1.0
       CALL FIELDC(RN,EN,PRMX,PRMY,Z0E,Z0S,PENF,FCI)
C
C      The field coefficients of the overhang region
C
       OENF = 1.0
       CALL FIELDC(RN,EN,PRM0,PRM0,Z0H,Z0S,OENF,FCH)
C
C       The Force and Power Calculations :
C
       FT = FT + CTF * (FCI(1)*WI + FCH(1)*WH) * CJ * CNJ
       FN = FN + CTF * PRM0 *(FCI(2)*WI + FCH(2)*WH) * CJ * CNJ
       PW = PW + CTF * (FCI(3)*WI + FCH(3)*WH) * CJ * CNJ
C
       RN = RN + DSPH
  40   CONTINUE
C
       RETURN
       END
```

```
C
C ******************************************************************
C   THE AUXILIARY SUBROUTINES :  RGNMTRX, FUNCTS, FIELDC AND WDGFAC
C ******************************************************************
C
      SUBROUTINE RGMTRX(RN,EN,D,V,Z0E)
C
C   This subroutine computes the four entries ENT(1), ENT(2), EN(3),
C   EN(4) as well as the equivalent region impedance Z0E OF the N
C   different regions at a certain speed V, wave number (sapce har-
C   monic order) RN and time harmonic order EN. The subroutine uses
C   the entries of E - H solution approach.
C
      REAL D(4),PRMX(4),PRMY(4),SEGZ(4)
      COMPLEX Z0E,GM(4),Z00,Z,Y,Z0(4),ZA,CCH,CSH,A(4),
     *        B(4),ENT(4),DT(4,4)
C
      DATA Z00/(0.0,1.0E+20)/
      COMMON NRG,DP,BO,BS,BOS,BSS,TAUS,TAUSS,SLTF,W2,WI,WH,WE
     $,PRM0,PRMR,EM,P,Q,TAU,U,CNDPP,HZ,PI,SEG,SEGE,OMG,VS
C
      PRM = PRM0 * PRMR
      PRMX(1) = PRM/(1.0+(PRMR-1.0)*BSS/TAUSS)
      PRMY(1) = PRM*(1.0 + (1.0/PRMR - 1.0) * BSS/TAUSS)
      PRMX(2) = PRM/(1.0+(PRMR-1.0)*BOS/TAUSS)
      PRMY(2) = PRM*(1.0 + (1.0/PRMR - 1.0) * BOS/TAUSS)
      PRMX(3) = PRM0
      PRMY(3) = PRM0
      PRMX(4) = PRM/(1.0+(PRMR-1.0)*BO/TAUS)
      PRMY(4) = PRM*(1.0 + (1.0/PRMR - 1.0) * BO/TAUS)
C
      SEGZ(1) = SEG*(BSS/TAUSS)*SLTF
      SEGZ(2) = 0.0
      SEGZ(3) = 0.0
      SEGZ(4) = 0.0
C
C       MODEL  :  III
C
      AREA = 0.05 * 0.02
      SEGR = SEG / SEGE
      ENRF = 1.0 + 2.0*D(1)*SEGR/(WI*AREA*(RN*PI/TAU)*(RN*PI/TAU))
      SEGZ(1) = SEGZ(1) / ENRF
C
C  Calculations of the propagation factors and the characteristic
C  impedances of the N regions.
C
      OMGN = EN * OMG
      SLIP = 1.0 + (RN*PI/TAU)*V/OMGN
      RNT = RN*PI/TAU
C
```

```
      DO 15 I = 1,NRG
C
      IF (I.LT.3) OMGR = OMGN * SLIP
      IF (I.GE.3) OMGR = OMGN
C
C  Where 3 is the air gap region (regions 3 or more are stationary)
C
      Z = (0.0,1.0) * OMGR * PRMX(I)
      Y = SEGZ(I) + RNT * RNT / ((0.0,1.0) * OMGR * PRMY(I))
      Z0(I) = CSQRT(Z/Y)
      GM(I) = CSQRT(Z*Y)
   15 CONTINUE
C
C     Formation of the entries of the four matrices
C
      DO 17 I = 1,NRG
      ZA = GM(I) * D(I)
      CALL FUNCTS(ZA,CCH,CSH)
      DT(I,1) = CCH
      IF (I.EQ.3) DT(I,1) = DT(I,1) / SLIP
      DT(I,2) = - Z0(I) * CSH
      DT(I,3) = - 1.0/Z0(I) * CSH
      IF (I.EQ.3) DT(I,3) = DT(I,3) / SLIP
      DT(I,4) = CCH
   17 CONTINUE
C
C     Calculation of the matrix product
C
      DO 20 J =1,4
      A(J) = DT(1,J)
   20 CONTINUE
C
      DO 50 I = 2,NRG
C
      ENT(1) = DT(I,1)*A(1) + DT(I,2)*A(3)
      ENT(2) = DT(I,1)*A(2) + DT(I,2)*A(4)
      ENT(3) = DT(I,3)*A(1) + DT(I,4)*A(3)
      ENT(4) = DT(I,3)*A(2) + DT(I,4)*A(4)
C
      DO 40 J =1,4
      A(J) = ENT(J)
   40 CONTINUE
C
   50 CONTINUE
C
      BETA = OMGN / RNT
      Z0E = ( SLIP*ENT(1) - ENT(2) / (BETA*Z00) ) /
     /      ( SLIP*BETA*ENT(3) - ENT(4) / Z00 )
C
      RETURN
      END
```

```
C
C ***************************************************************
C
      SUBROUTINE FUNCTS(Z,CCH,CSH)
C
C  THIS SUBROUTINES DETERMINES THE EXPRESSIONS OF COMPLES COSH AND
C  SINH.
      COMPLEX Z,CCH,CSH,EX
      EX = CEXP(Z)
      CCH = 0.5 * (EX + 1.0/EX)
      CSH = 0.5 * (EX - 1.0/EX)
      RETURN
      END
C
C ***************************************************************
C
      SUBROUTINE FIELDC(RN,EN,RMX,RMY,Z0E,Z0S,PENF,FC)
C
C   This subroutine is used to determine the FIELD COEFFICIENTS,
C   F(1), FC(2) and FC(3) in the primary region, which are given
C   by the expressions
C       Bav = FC(1)*Jlin,  Hav = FC(2)*Jlin   and   Eav = FC(3)*Jlin
C
      COMMON NRG,DP,BO,BS,BOS,BSS,TAUS,TAUSS,SLTF,W2,WI,WH,WE
     $,PRM0,PRMR,EM,P,Q,TAU,U,CNDPP,HZ,PI,SEG,SEGE,OMG,VS
C
      COMPLEX Z0E,Z0S,FC(3),ZP,Z0P,DLT,CNU,G1,G2
C
      OMGN = EN * OMG
      GMP = SQRT(RMX/RMY) * RN*PI/TAU
      GMD = GMP * DP
      ZP = (0.0,1.0) * RMX * RN*PI/TAU
      Z0P = (0.0,1.0) * SQRT(RMX*RMY)
      DLT = (COSH(GMD)/Z0P + SINH(GMD)/Z0S) /Z0E -
     $      (SINH(GMD)/Z0P + COSH(GMD)/Z0S) /Z0P
C
      SHR = SINH(GMD)/GMD
      CHR = (COSH(GMD) - 1.0) /GMD
      CNU = SHR + (Z0P/Z0S) * CHR
      G1 = CNU /(Z0P*DLT)
      G2 = -CNU /(Z0E*DLT)
C
      FC(1) = G1*SHR + G2*CHR + Z0P * ( (SHR-1.0)/GMD )
      FC(2) = - (G1*CHR + Z0P*(CHR/GMD) + G2*SHR) /Z0P
C
C
C   PENF, primary end factor, is used when the end effect of the
C   overhang winding is taken into consideration,
C   E = OMG B / (PENF * RN * PI / TAU).
C
```

```
      FC(3) = OMGN /(PENF*RN*PI/TAU) * FC(1)
C
      RETURN
      END
C
C ****************************************************************
C
      SUBROUTINE WDGFAC(RN,EKW,EKWM)
C
C   THIS SUBROUTINE, WINDING FACTOR, COMPUTES THE FOURIER TRANSFORM
C   THE FOURIER COEFFICIENT OF A DOUBLE LAYER SINGLE-PHASE WINDING,
C   AS WELL AS THE M-PHASE DOUBLE LAYER WINDING IN CASE OF BALANCED
C   OPERATIONS.
C     KB : TOOTH BREADTH FACTOR (REAL).
C     KC : COIL-PITCH FACTOR.
C     KD : PHASE-DISTRIBUTION FACTOR
C     KO : ODD-HARMONIC FACTOR.
C     KP : POLE-NUMBER FACTOR.
C     KM : PHASE-NUMBER FACTOR, FOR BALANCED M-PHASE OPERATIONS.
C    EKW : THE EQUIVALENT SINGLE-PHASE WINDING FACTOR.
C   EKWM : THE EQUIVALENT M-PHASE WINDING FACTOR (BALANCED OPERATION).
C
      REAL KB
      COMPLEX EKW,EKWM,KC,KD,KO,KP,KM
C
      COMMON NRG,DP,BO,BS,BOS,BSS,TAUS,TAUSS,SLTF,W2,WI,WH,WE
     $,PRM0,PRMR,EM,P,Q,TAU,U,CNDPP,HZ,PI,SEG,SEGE,OMG,VS
C
      TAUC = TAU - U*TAUS
      ALF = PI*TAUS/TAU
      IF (RN.EQ.1.0) RN = RN + 0.001
C
      KB = SIN(RN*PI*BS/(2.0*TAU))/(RN*PI*BS/(2.0*TAU))
      KC = ( 1.0 - CEXP((0.0,-1.0)*RN*PI*TAUC/TAU) ) / 2.0
      KD = (1.0 - CEXP((0.0,-1.0)*Q*RN*ALF))/
     /  (Q*(1.0 - CEXP((0.0,-1.0)*RN*ALF)))
      KO = 0.5*(1.0 - CEXP((0.0,-1.0)*RN*PI))
C
      KP = (1.0,0.0)
      KM = (1.0 - CEXP((0.0,-1.0)*PI*(RN-1.0)))/
     / (EM*(1.0 - CEXP((0.0,-1.0)*PI*(RN-1.0)/EM)))
C
      EKWM = EKW*KM
C
      RETURN
      END
C
C ****************************************************************
```